TU/e EINDHOVEN UNIVERSITY OF TECHNOLOGY

Microwave-matter effects in metal(oxide)-mediated chemistry and in drying

Citation for published version (APA):
Kruijs, van de, B. H. P. (2010). *Microwave-matter effects in metal(oxide)-mediated chemistry and in drying*. [Phd Thesis 1 (Research TU/e / Graduation TU/e), Chemical Engineering and Chemistry]. Technische Universiteit Eindhoven. https://doi.org/10.6100/IR658493

DOI:
10.6100/IR658493

Document status and date:
Published: 01/01/2010

Document Version:
Publisher's PDF, also known as Version of Record (includes final page, issue and volume numbers)

Please check the document version of this publication:

• A submitted manuscript is the version of the article upon submission and before peer-review. There can be important differences between the submitted version and the official published version of record. People interested in the research are advised to contact the author for the final version of the publication, or visit the DOI to the publisher's website.
• The final author version and the galley proof are versions of the publication after peer review.
• The final published version features the final layout of the paper including the volume, issue and page numbers.

Link to publication

General rights
Copyright and moral rights for the publications made accessible in the public portal are retained by the authors and/or other copyright owners and it is a condition of accessing publications that users recognise and abide by the legal requirements associated with these rights.

• Users may download and print one copy of any publication from the public portal for the purpose of private study or research.
• You may not further distribute the material or use it for any profit-making activity or commercial gain
• You may freely distribute the URL identifying the publication in the public portal.

If the publication is distributed under the terms of Article 25fa of the Dutch Copyright Act, indicated by the "Taverne" license above, please follow below link for the End User Agreement:

www.tue.nl/taverne

Take down policy
If you believe that this document breaches copyright please contact us at:

openaccess@tue.nl

providing details and we will investigate your claim.

Download date: 16. Nov. 2023

Microwave-matter effects in metal(oxide)-mediated chemistry and in drying

PROEFSCHRIFT

ter verkrijging van de graad van doctor aan de
Technische Universiteit Eindhoven, op gezag van de
Rector Magnificus, prof.dr.ir. C.J. van Duijn, voor een
commissie aangewezen door het College voor
Promoties in het openbaar te verdedigen
op maandag 15 maart 2010 om 16.00 uur

door

Bastiaan Helena Peter van de Kruijs

geboren te Weert

Dit proefschrift is goedgekeurd door de promotoren:

prof.dr. L.A. Hulshof
en
prof.dr. J. Meuldijk

Copromotor:
dr. J.A.J.M. Vekemans

The research described in this thesis was financially supported by Senter-Novem.
Project: FC SMART.

Druk: Universiteitsdrukkerij, Technische Universiteit Eindhoven
Cover Design: Verspaget & Bruinink
A catalogue record is available from the Eindhoven University of Technology Library

ISBN: 978-90-386-2178-4
Trefwoorden: microwave, microwave-assisted chemistry, microwave effect, heterogeneous systems, scaling-up, thermographic imaging, scanning electron microscopy, magnesium, Grignard, zinc, Reformatsky, copper, Ullmann, nylon-6, zirconia, amidation, drying.

Table of contents

Chapter 1
Microwave-assisted chemistry

1.1	*Introduction*	*- 4 -*
1.2	*Microwave radiation*	*- 4 -*
1.3	*Microwave-assisted chemistry*	*- 7 -*
1.4	*Aim of the thesis*	*- 13 -*
1.5	*Outline of the thesis*	*- 14 -*
1.6	*References*	*- 15 -*

Chapter 2
Influence of microwave irradiation on the reactivity of magnesium: application in the Grignard reagent synthesis

2.2	*Microwave – magnesium interactions*	*- 21 -*
2.3	*The influence of microwave irradiation on magnesium: electrical discharges*	*- 23 -*
2.4	*Application of microwave-induced electrical discharges in the Grignard reagent formation*	*- 27 -*
2.5	*Conclusion*	*- 33 -*
2.6	*Experimental section*	*- 34 -*
2.7	*References*	*- 37 -*

Chapter 3
Influence of microwave irradiation on the reactivity of zinc: application in the Reformatsky reagent synthesis

3.1	*Introduction*	*- 40 -*
3.2	*Microwave – zinc interactions*	*- 40 -*
3.3	*The influence of microwave irradiation on zinc: electrical discharges*	*- 42 -*
3.4	*Application of microwave-induced electrical discharges in the Reformatsky reagent formation*	*- 44 -*
3.5	*Conclusion*	*- 50 -*
3.6	*Experimental section*	*- 51 -*
3.7	*References*	*- 52 -*

Chapter 4
Influence of microwave radiation on the reactivity of copper: application in the Ullmann coupling
4.1 *Introduction* *- 56 -*
4.2 *Microwave – copper interactions* *- 56 -*
4.3 *Optimization of the thermal Ullmann coupling* *- 59 -*
4.4 *Microwave heating compared with conventional heating for the optimized Ullmann coupling* *- 69 -*
4.5 *Conclusion* *- 71 -*
4.6 *Experimental section* *- 71 -*
4.7 *References* *- 73 -*

Intermezzo
Comparison of the reactivity of magnesium, zinc and copper under microwave irradiation

Chapter 5
Heterogeneous zirconium oxide-catalyzed amidations
5.1 *Introduction* *- 78 -*
5.2 *Microwave – zirconium oxide interactions* *- 80 -*
5.3 *Determination of the zirconium oxide activity under influence of microwave irradiation* *- 81 -*
5.4 *Conclusion* *- 89 -*
5.5 *Experimental section* *- 89 -*
5.6 *References* *- 92 -*

Chapter 6
Comparison of conventionally and microwave-heated drying of non-natural amino acids
6.1 *Introduction* *- 96 -*
6.2 *Drying behavior and heating method* *- 98 -*
6.3 *Conclusion* *- 109 -*
6.4 *Experimental section* *- 109 -*
6.5 *References* *- 111 -*
Summary *- 115 -*
Samenvatting *- 117 -*
Curriculum Vitae *- 119 -*
List of publications *- 120 -*
Dankwoord *- 121 -*

Chapter 1

Microwave-assisted chemistry

Abstract

Microwave irradiation is a well-accepted heating technique for lab-scale organic synthesis. However, application for a large-scale operation is limited. To determine the applicability of microwave heating in industrial production of organic fine chemicals, the added value of this heating technique, compared to conventional heating, should be evaluated at accurately controlled conditions on lab-scale. This comparison may elucidate factors governing benefits of microwave heating, and, therefore, enable a well-founded choice either to apply microwave heating for process scaling-up or to utilize traditional heating methods.

1.1 Introduction

The property of microwave radiation to heat materials was first discovered by Percy LeBaron Spencer while investigating this irradiation for RADAR purposes at the Raytheon Corporation at the end of World War II.[1] Quickly the application of this type of heating in cooking food was envisaged, see Figure 1.1. One of the first foodstuffs to be heated by microwave irradiation was an egg, which promptly exploded in the face of one of the experimenters.

Figure 1.1: First table top microwave oven, the Radarange, introduced for household use in 1967.

This stresses the fact that, although microwave irradiation can be very useful, its application should be controlled properly to prevent dangerous situations. This also holds for other applications of microwave irradiation. One of these applications is the transfer of energy to reaction mixtures, *i.e.* microwave-assisted chemistry. The application of microwave radiation in chemistry has lead to better yields, improved selectivity, or enables conversions otherwise impossible.[2-5] These combined observations have been referred to as microwave effects. The mechanistic background of these "effects" has been a subject of debate over the last two decades.[6-12] Presently most claimed effects have been renounced by elaborate studies, revealing conclusions based on inaccurate temperature measurements.[13,14] Only a few examples of a microwave effect seem to hold and the matter of a true microwave effect still remains unresolved.[15]

1.2 Microwave radiation

Microwave radiation is electromagnetic radiation with a frequency range of 300 MHz to 300 GHz, corresponding to a wavelength in vacuum of 1 m to 1 mm respectively, see Figure 1.2. The radiation is used in communication,[16] remote sensing,[17-19] navigation,[20,21] power / heating[22] and spectroscopy.[23,24] The frequency of 2.45 GHz is most commonly used in heating applications, but is not limited to heating only. This frequency is also used in communication, such as Bluetooth, IEEE (institute of electrical and electronics engineers) 802.11b, 802.11g and 802.11n, direct-to-home satellite and cellular phones.

The energy of a microwave photon with a frequency of 2.45 GHz corresponds to 1.01×10^{-5} eV which is about 3 orders of magnitude lower than the bond energy of a covalent bond in a molecule, which range from 9.8 eV for nitrogen to 1.56 eV

for iodine. Even the energy of a hydrogen bond (in the range of 1-0.1 eV)[25] is much larger, see Figure 1.2.

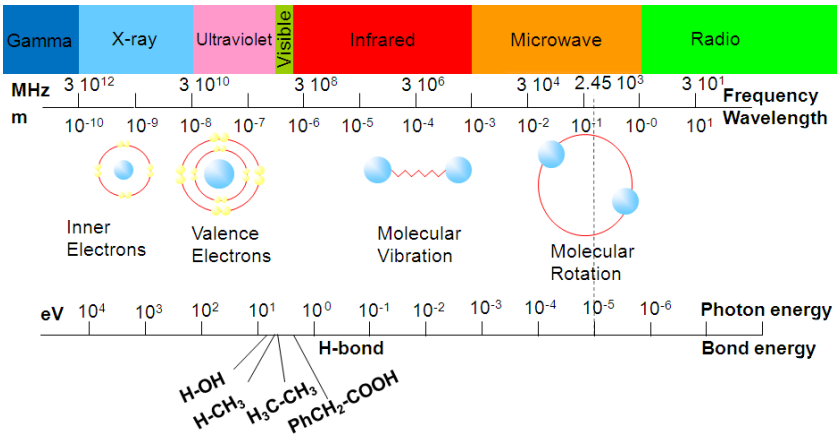

Figure 1.2: *Electromagnetic spectrum. Wavelength, frequency and corresponding energies.*

These differences between bond energies and photon energies indicate that direct absorption of a microwave photon cannot induce excitation of an electron in a chemical bond to a higher energy level and, therefore, cannot directly cause a reaction. However, the energy of a microwave photon can, in principle, excite the rotational state of molecules in the gas phase, which is the basis of microwave spectroscopy.[24] Most chemical reactions are performed in a condensed phase, *i.e.* liquid or solid. The rotational states are not quantified in condensed matter and absorption of a microwave photon may cause an excitation of a rotational state, but the energy is immediately distributed in other molecular movements, *i.e.* vibration and translation and thus heat. The interaction of microwave irradiation with dielectric materials is best described by classical Maxwell[26] type equations.[2]

Microwave-matter interaction

Microwave radiation is able to convey energy to certain matter, *i.e.* heating the substance. This conversion of electromagnetic energy into molecular motion, and by that into heat, can be described by different mechanisms. Basic understanding of the mechanisms involved in microwave heating is essential. The two main heating mechanisms in microwave chemistry are dipolar polarization and ionic conduction, see Figure 1.3.

Heating by dipolar polarization originates from the orientation of dipoles in the electromagnetic field. Dipoles tend to align in the direction of an external electric field. The degree of orientation is governed by the field strength and the static

dielectric constant. When an oscillating electric field is applied to a material, for instance microwave radiation, the dipoles are constantly trying to align with the changing electric field. The frequency of the field determines the way how the orientation of dipoles affects the material. With a very high frequency the dipoles cannot adapt to the electric field and orientation does not occur. With a low frequency the dipoles are in a constant equilibrium state with field, acting as dipoles in a static electric field. In between these frequencies the alignment of the dipoles, lagging behind the changing electric fields, causes molecular friction, which in turn is converted into heat.

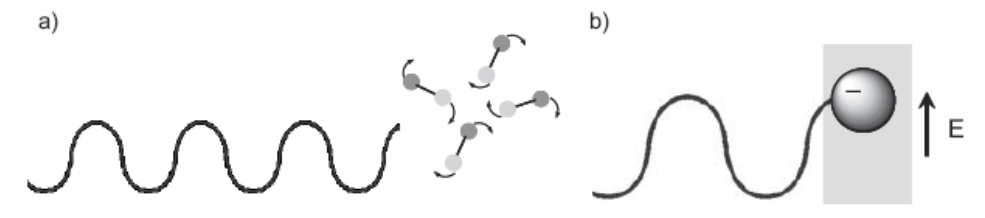

Figure 1.3: *a) Dipolar polarization and b) ionic conduction.*[3]

The mechanism of ionic conduction is similar to that of dipolar polarization. When charge carriers in a material are subjected to an electric field, they are subjected to a force. The alternation of the electric field causes the direction of the force to alternate equally. This alternation leads to molecular motion, and collision, and thus heat.

Loss tangent and penetration depth

The efficiency of converting electromagnetic radiation into heat is defined by the loss tangent. This quantity is the ratio of the imaginary (ε'') and real (ε') part of the complex dielectric constant, see Figure 1.4. This quantity is temperature dependent.

$$\tan\delta = \frac{\varepsilon''}{\varepsilon'} \qquad\qquad D_p = \frac{\lambda_0\sqrt{\varepsilon'}}{2\pi\varepsilon''}$$

Figure 1.4: *Left: loss tangent. Right: penetration depth.*

The absorbance of microwave radiation by a medium leads to decay of the electromagnetic wave in that medium, limiting the propagation of the waves. This penetration of radiation is quantified by the penetration depth, defined as the path length necessary to decrease the amplitude of the wave to a factor of 1/e (about 37 %) of the original value at the surface, see Figure 1.4.

High dielectric loss materials (tan $\delta > 0.1$) most commonly display a penetration depth in the range of centimeters. So the limited penetration depth is a key issue in reactor design. For materials with a low loss tangent the size of the reactor is not limited, but the microwave irradiation is unable to facilitate high heating rates. Altogether these features limit the industrial application of microwave heating.

Table 1.1: *Dielectric constant, dipole moment, dielectric loss and lost tangent of a selection of solvents at 25 °C and 2.45 GHz.*

Material	Dielectric constant	Dipole moment $\times 10^{30}$ (C m)	Dielectric loss	Loss tangent	Penetration depth (m)
Toluene	2.40	0.71	0.19	0.08	0.160
Chloroform	4.80	3.80	0.40	0.09	0.098
Acetone	21.40	9.00	1.20	0.05	0.078
DMF	38.32	3.24	6.17	0.16	0.020
Water	80.40	5.90	9.90	0.12	0.018
DMA	37.62	3.75	8.20	0.22	0.015
Methanol	33.70	5.50	22.20	0.66	0.005
Ethanol	25.70	5.80	24.20	0.94	0.004
Ethylene glycol	37.70	7.70	50.90	1.35	0.002

Metal-microwave interaction

When suspended metallic materials with sharp edges are present, microwave irradiation can lead to a dielectric breakdown of the medium in which these metallic materials are suspended.[27] These electrical discharges can cause damage to the reactor vessel and for processes where scaling-up was contemplated, conditions that facilitate arcing were, in general, to be avoided. Therefore, the beneficial effect of arcing on metal-mediated reactions is to the best of the authors knowledge not known.

1.3 Microwave-assisted chemistry

The first examples of microwave heating in chemical transformations were published in 1986. Several Diels-Alder reactions,[28] see Scheme 1.1, were investigated. The paper nicely demonstrates the struggle to make microwave irradiation suitable for organic chemistry. Also the acidic hydrolysis of benzamide into benzoic acid, see Scheme 1.2, the permanganate oxidation of toluene in basic solution giving benzoic acid, the esterification of benzoic acid with methanol, propanol and butanol, and the S_N2 reaction between sodium 4-cyanophenoxide and benzyl chloride, yielding 4-cyanophenyl benzyl ether were investigated.[29]

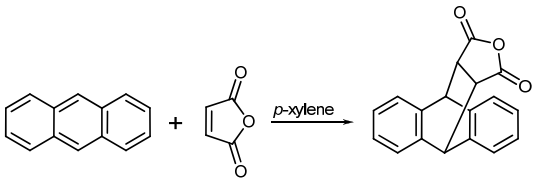

Scheme 1.1: *A Diels-Alder reaction of anthracene with maleic anhydride in p-xylene.*[28]

These preliminary studies on microwave heating employed sealed vessels. Reaction temperature was not monitored on-line and the reaction mixtures were heated to temperatures far above the boiling point at atmospheric pressure. This immediately explains the observed rate enhancements.

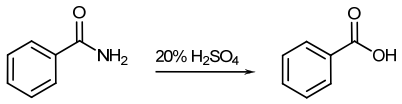

Scheme 1.2: *Hydrolysis of benzamide in aqueous sulfuric acid.*[29]

These explorative studies were performed in domestic microwave ovens. The use of microwave radiation as heating source for chemical reactions has increased dramatically since the explorative research mentioned earlier. This development facilitated the introduction of dedicated microwave equipment, see Figure 1.5.

Dedicated microwave equipment

A microwave generator is basically a thermionic diode (an anode combined with a directly heated cathode) that emits electromagnetic radiation.[30] Dedicated microwave equipment can be divided into mono-mode and multimode machines. In a mono-mode microwave oven the reaction vessels are placed inside a waveguide. Inside this waveguide, a standing wave is generated and the vial is placed in the maximum of the electromagnetic wave. This allows application of very high energy densities. The main drawback of mono-mode equipment is the relatively small sample size, making its application in larger scale synthesis cumbersome. Mono-mode equipment is extensively used in high-throughput experimentation[31,32] and rapid development of compound libraries which includes the optimization of reaction conditions.[33] CEM Corporation is market leader in this field (Figure 1.5). Other providers of laboratory dedicated microwave ovens are Biotage, Milestone and Anton-Paar.

(a) (b) (c) (d)

Figure 1.5: *Mono-mode microwave ovens from (a) CEM, (b) Biotage and multi-mode microwave ovens from (c) Milestone, (d) Anton Paar.*

In multimode equipment, the generated microwave radiation is guided through a waveguide into a cavity. A mode stirrer usually deflects the exiting waves in all directions. The waves deflect from the cavity walls and are scattered throughout the cavity. Ideally, this leads to a homogeneous energy distribution in the cavity. The size of the cavity is remarkably larger than that of mono-mode equipement. This makes the multimode microwave oven a much more versatile piece of equipment, with the possibility of applying a wider range of vessel sizes.

In all microwave ovens either normal glassware, quartz or Teflon (PTFE) reactors can be inserted into the cavity. Essential for dedicated microwave equipment is on the one hand stirring and on the other hand temperature control by an internal fiber-optic device, gas-pressure sensor or an infrared sensor.

Microwave effects

As mentioned in the introduction, microwave irradiation has been reported to increase yields, to change the selectivities or to enable conversion levels being impossible otherwise. Most commonly, microwave effects are divided in thermal and non-thermal effects.

Thermal microwave effects

Thermal microwave effects are defined as effects caused by the intrinsic difference of microwave heating, *i.e.* volumetric heating, compared to conventional heating. Microwave radiation is not hindered by heat-transfer resistances and is, therefore, able to heat reaction mixtures much more rapidly. The heating rate at the start of a reaction can have a dramatic influence on the selectivity.[34]

Microwave irradiation can cause superheating of solvents. The perceived boiling point can be increased dramatically by applying microwave irradiation as heating source.[35] This increase is caused mainly by the volumetric heating

character of microwave irradiation. When heating a solvent conventionally, it is in contact with a heating element, normally the reaction vessel wall. At this surface the temperature is the highest and when the boiling point is reached the bubble nucleation sites at the surface induce boiling.[36] Due to the lack of a hot surface during microwave heating boiling retardation can occur.[35] Usually this metastable state is not observed in reaction mixtures, especially not in heterogeneous reaction mixtures.

The irradiation of heterogeneous systems, solid-liquid and liquid-liquid, may lead to a preferential absorption of microwave energy by one of the components in the mixture. This may lead to large temperature gradients between phases. Melting ice in microwave oven demonstrates this phenomenon nicely. The loss tangent of ice is negligible while the loss tangent of water is substantial. Figure 1.6 shows thermographic images of melting ice in a microwave oven.

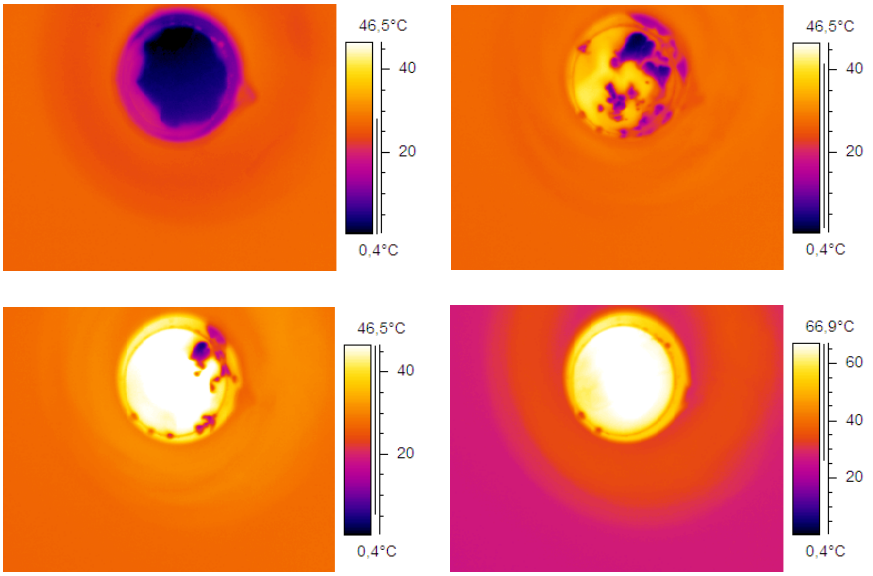

Figure 1.6: *Thermographic imaging of melting ice in a microwave oven at 200 W. Top left: cold sample. Top right: after 1 min of microwave irradiation. Bottom left: after 2 min of microwave irradiation. Bottom right: after the ice has melted completely.*

Initially, microwave radiation is absorbed by a small quantity of water. Water is heated and melts adjacent ice. Water is heated faster than it can transfer the heat to the ice, causing large temperature gradients, see Figure 1.6 (top right and bottom

left). After the ice has melted completely the microwave radiation is absorbed volumetrically, leading to a relatively homogeneous temperature distribution.

Selective heating may be beneficial for certain reactions,[37,38] especially when the reaction takes place at the interface of the phases, for instance in heterogeneous catalysis.[39] It must be stressed that, although high loss tangent molecules strongly interact with microwave radiation, the more polar molecules are not at a temperature higher than that of the bulk; *i.e.* there is not any localized superheating.[9]

Non-thermal microwave effects

The origin of non-thermal microwave effects is less straightforward. To explain observed differences in reaction performance, a collection of mechanisms / theories have been postulated.[2,6,8,9] These theories are based in the Gibbs free energy profile that is followed when reacting molecules proceed from the initial to the final state, see Figure 1.7 (left).[6] A change of the population of the initial and transient state by selective excitation of rotational states has been suggested. In addition, it is claimed that a increase of the Gibbs free energy of the initial state occurs in reactions with polar reaction mechanisms by microwave-induced desolvation and, as a consequence, decreasing in the activation Gibbs free energy, see Figure 1.7 (right).

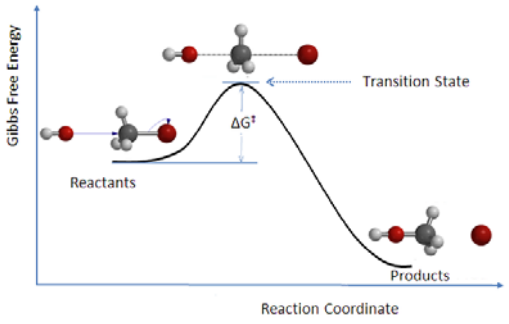

$$k = \frac{k_b \times T}{\hbar} \times e^{-\frac{\Delta G_a^{\ddagger}}{R \times T}} = \frac{k_b \times T}{\hbar} \times e^{\frac{\Delta S_a^{\ddagger}}{R}} \times e^{-\frac{\Delta H_a^{\ddagger}}{R \times T}}$$

k_b	=	*Boltzmann constant*
$\hbar$	=	*Planck's constant*
$\Delta G_a^{\ddagger}$	=	*Activation Gibbs energy*
$\Delta S_a^{\ddagger}$	=	*Activation Entropy*
$\Delta H_a^{\ddagger}$	=	*Activation Enthalpy*
T	=	*Temperature*

Figure 1.7: *Left: schematic energetic representation of a reaction. Right: the Eyring equation.*[40]

Electric fields can cause an alignment of dipoles. A change in reaction pathway due to this orientation has been suggested.[2] Also enzymes are claimed to be activated by microwave irradiation due to conformational changes in their polar structure under influence of this irradiation.[41] Although orientation of dipoles by the electric field is possible, the field strength is too weak to lead to induced organization.[42]

Although non-thermal microwave effects have been claimed in numerous articles, a recent evaluation by Kappe and coworkers rationalized the observed differences between microwave and conventional heating: *"(They) …can in fact be rationalized by inaccurate temperature measurements often using external IR temperature probes, rather than being the consequence of a genuine nonthermal effect. We, therefore, believe that the concept of non-thermal microwave effects has to be critically reexamined and that a considerable amount of research work will be required before a definitive answer about the existence or nonexistence of these effects can be given."*[14,15]

Microwave heating in a large-scale production environment

Microwave heating has been employed scarcely in a large-scale production environment.[43] The application of microwave heating in the production of bulk chemicals is non-existing due to the low added value of the products and the scale limitation due to the limited penetration depth of microwave radiation, see section 1.2. The potential for microwave heating is much greater in the production of fine chemicals. With the production of fine chemicals the energy consumption only plays a minor role in the manufacturing costs and the production scale is usually limited. Various companies though, confidentially produce perfumeries, specialty monomers and polymers in commercially available microwave continuous-flow and batch systems.[12] One example of an industrial-scale application of microwave radiation is the production of Laurydone, the esterification of (*S*)-pyroglutamic acid with *n*-decanol, see Figure 1.8, in a prototype microwave reactor produced by the French company Sairem.[44] The first steps in the design of industrial-scale microwave-assisted polymer production by the Japanese National Institute of Advanced Industrial Science and Technology have been reported.[45]

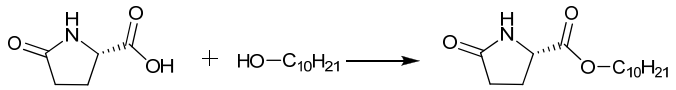

Figure 1.8: *The estrification of (S)-pyroglutamic acid with n-decanol.*

Microwave radiation is an established heating technique for drying on an industrial scale.[46-48] A variety of commercial equipment is available, see Figure 1.9. However, application of the microwave heating technique in drying of fine chemicals is limited up to now.

When scaling-up chemical reactions, the possibility of applying microwave radiation has been overlooked for the most part. Process scaling-up requires detailed information about reaction conditions and the beneficial results are, to

some extent, uncertain in microwave-assisted organic chemistry. This prompted us to investigate the difference between the performance of microwave heating and conventional heating, in terms of reaction rate and selectivity, for some promising reactions at well-defined reaction conditions.

Figure 1.9: *Commercial microwave-drying equipment. Left: μWaveVac 1290. Middle: μWaveVac 0209 Disk Dryer. Right: Vacuum μWave dryer.*

1.4 Aim of the thesis

The aim of this thesis was to evaluate microwave radiation as alternative heating source in industrial fine chemical applications with scaling-up as a final target. Although the application of microwave heating on an industrial scale is common in food processing, application in the chemical industry is very limited. Before an extensive study on the scalability of heating by microwave radiation can be conducted, an evaluation of this heating technique, more specifically of the added value of utilizing microwave radiation, on lab-scale is necessary. Previously reported rate enhancements with microwave heating demonstrate that heterogeneous reaction mixtures, especially solid-liquid systems, are promising to display beneficial microwave effects.[49,50]

One group of solid-liquid systems, used to a great extent in the fine chemicals industry, is the group of heterogeneous metal-mediated systems, for example the synthesis of Grignard reagents, Reformatsky reactions and Ullmann couplings. In these systems arcing under the influence of microwave radiation can occur. Special attention had to be devoted to the effect of microwave-induced arcing on these metal-mediated reaction systems.

Besides metals also metal oxides have been investigated. The influence of selective heating by microwave irradiation on the catalytic activity of a zirconia-based catalyst in the production of nylon-6 was investigated. Another widely used heterogeneous process is industrial drying but microwave drying of

pharmaceutical intermediates has received limited attention. The added value of applying microwave heating for this drying step has been explored.

1.5 Outline of the thesis

The differences between microwave heating and conventional heating, in terms of reaction rate, initiation time and selectivities of a variety of heterogeneous reactions have been investigated. Primarily, metal-mediated reactions were selected.

In Chapter 1 an overview of the state of the art of microwave irradiation in industry is given. A theoretical background on the heating method and its influence on reaction rates and selectivities are described.

In Chapters 2, 3 and 4 three metal-mediated reactions employing metals in their metallic state were studied, *e.g.* the formation of a Grignard reagent with magnesium, the Reformatsky reaction with zinc and the Ullmann coupling with copper, respectively. All three reactions involve the insertion of the metal into a carbon-halide bond. In these chapters a comprehensive study on the interaction of microwave radiation with the metal-solvent dispersions is described. Thermographic imaging, surface characterization by scanning electron microscopy (SEM) and X-ray photoelectron spectroscopy (XPS) were employed to elucidate the influence of microwave radiation on the metal surface. These observations were utilized to explain divergent effects on the reactivity of the metals with microwave radiation as heating source, and to compare them with the results of conventional heating.

In Chapter 2 the formation of Grignard reagents of a series of reactive and much less reactive substrates with conventional heating as well as microwave heating is reported in detail.

In Chapter 3 the Reformatsky reaction of α-bromo- and α-chloroesters with benzaldehyde is described. The influence of the degree of substitution in the esters on the reactivity towards zinc, *i.e.* the difference in reactivity of acetate, propionate and isobutyrate esters, is discussed.

The Ullmann coupling of 2-chloro-3-nitropyridine is presented in Chapter 4. The influence of the copper source on the reproducibility of the reaction and on the required stoichiometry of the copper in the reaction is reported. Also the influence of several polar aprotic solvents on the rate of reaction and selectivity is described.

The influence of microwave radiation on the catalytic activity of metal oxides has been investigated in view of the ZrO_2-catalyzed amidation of a nitrile with an amine. Chapter 5 deals with the influence of microwave irradiation on a prepared zirconiumoxide-based heterogeneous catalyst. The catalytic activity of the zirconia-based catalyst in the synthesis of nylon-6 from 6-aminocapronitrile with microwave irradiation is described and compared with conventional heating.

The drying behavior under microwave irradiation of (*S*)-*N*-acetylindoline-2-carboxylic acid, precipitated and non-precipitated and *N*-acetyl-(*S*)-phenylalanine, is presented in Chapter 6. The benefits of applying microwave irradiation in the drying process of these pharmaceutical intermediates instead of conventional heating was demonstrated in a straightforward setup.

1.6 References

(1) Spencer, P. L., Raytheon Mfg, patent number CAD489859, **1953**.
(2) Loupy, A. *Microwaves in Organic Synthesis*; WILEY VCH Verlag GmbH & Co **2002**.
(3) Kappe, C. O.; Stadler, A. *Microwaves in Organic and Medicinal Chemistry*; WILEY-VCH Verlag GmbH & Co, **2005**.
(4) Kappe, C. O.; Dallinger, D. *Mol. Diversity* **2009**, *13*, 71-193.
(5) Kappe, C. O. *Angew. Chem. Int. Ed.* **2004**, *43*, 6250-6284.
(6) Loupy, A.; Perreux, L.; Liagre, M.; Burle, K.; Moneuse, M. *Pure Appl. Chem.* **2001**, *73*, 161-166.
(7) Perreux, L.; Loupy, A. *Tetrahedron* **2001**, *57*, 9199-9223.
(8) De la Hoz, A.; Diaz-Ortiz, A.; Moreno, A. *Chem. Soc. Rev.* **2005**, *34*, 164-178.
(9) Schmink, J. R.; Leadbeater, N. E. *Org. Biomol. Chem.* **2009**, *7*, 3842-3846.
(10) Caddick, S.; Fitzmaurice, R. *Tetrahedron* **2009**, *65*, 3325-3355.
(11) Obermayer, D.; Gutmann, B.; Kappe, C. O. *Angew. Chem. Int. Ed.* **2009**, *48*, 8321-8324.
(12) Strauss, C. R. *Org. Process Res. Dev.* **2009**, *13*, 915-923.
(13) De Souza, R.; Antunes, O. A. C.; Kroutil, W.; Kappe, C. O. *J. Org. Chem.* **2009**, *74*, 6157-6162.
(14) Herrero, M. A.; Kremsner, J. M.; Kappe, C. O. *J. Org. Chem.* **2008**, *73*, 36-47.
(15) Razzaq, T.; Kremsner, J. M.; Kappe, C. O. *J. Org. Chem.* **2008**, *73*, 6321-6329.
(16) Kizer, G. M. *Microwave Communication*; Iowa State University Press, Ames, Iowa, **1990**.
(17) Vrieling, A. *CATENA* **2006**, *65*, 2-18.

(18) Evans, D. L.; Alpers, W.; Cazenave, A.; Elachi, C.; Farr, T.; Glackin, D.; Holt, B.; Jones, L.; Liu, W. T.; McCandless, W.; Menard, Y.; Moore, R.; Njoku, E. *Remote Sens. Environ.* **2005**, *94*, 384-404.
(19) Payan, S.; De La Noe, J.; Hauchecorne, A.; Camy-Peyret, C. *C.R. Phys.* **2005**, *6*, 825-835.
(20) Haynes, S. K.; Jackson, W. J. *Am. J. Phys.* **1946**, *14*, 143-164.
(21) Haynes, S. K.; Jackson, W. J. *Am. J. Phys.* **1946**, *14*, 403-431.
(22) Meredith, R. *Engineers Handbook of Industrial Microwave Heating*; The Institution of Electrical Engineers, **1998**.
(23) Meckenstock, R. *Rev. Sci. Instrum.* **2008**, *79*.
(24) Towness, C. H.; Schawlow, A. L. *Microwave Spectroscopy*; Dover Publications Inc. New York, **1975**.
(25) Smith, M. B.; March, J. *March's Advanced Organic Chemistry 5th ed.*; John Wiley & Sons, Inc. , **2001**.
(26) Maxwell, J. C. *A Treatise On Electricity and Magnetism*; Macmillan and Co. Oxford, **1873**.
(27) Whittaker, A. G.; Mingos, D. M. P. *J. Chem. Soc., Dalton Trans.* **2000**, 1521-1526.
(28) Giguere, R. J.; Bray, T. L.; Duncan, S. M.; Majetich, G. *Tetrahedron Lett.* **1986**, *27*, 4945-4948.
(29) Gedye, R.; Smith, F.; Westaway, K.; Ali, H.; Baldisera, L.; Laberge, L.; Rousell, J. *Tetrahedron Lett.* **1986**, *27*, 279-282.
(30) Kingston, H. M.; Haswell, S. J. *Microwave-enhanced chemistry: fundamentals, sample preparation, and applications*; ACS: Washington D.C, **1997**.
(31) Damm, M.; Kappe, C. O. *J. Comb. Chem.* **2009**, *11*, 460-468.
(32) Hoogenboom, R.; Schubert, U. S. *Rev. Sci. Instrum.* **2005**, *76*, 6-7.
(33) Schon, U.; Messinger, J.; Eichner, S.; Kirschning, A. *Tetrahedron Lett.* **2008**, *49*, 3204-3207.
(34) Yadav, G. D.; Motirale, B. G. *Ind. Eng. Chem. Res.* **2008**, *47*, 9081-9089.
(35) Baghurst, D. R.; Mingos, D. M. P. *J. Chem. Soc., Chem. Commun.* **1992**, 674-677.
(36) Oman, D. M.; Dugan, K. M.; Killian, J. L.; Ceekala, V.; Ferekides, C. S.; Morel, D. L. *Sol. Energy Mater. Sol. Cells* **1999**, *58*, 361-373.
(37) Pol, V. G.; Langzam, Y.; Zaban, A. *Langmuir* **2007**, *23*, 11211-11216.
(38) Rassaei, L.; Compton, R. G.; Marken, F. *J. Phys. Chem. C* **2009**, *113*, 3046-3049.
(39) Irfan, M.; Fuchs, M.; Glasnov, T. N.; Kappe, C. O. *Chem. Eur. J.* **2009**, *15*, 11608-11618 and references therein.
(40) Wynne;, W.; Eyring, H. *J. Chem. Phys.* **1935**, 492.

(41) Young, D. D.; Nichols, J.; Kelly, R. M.; Deiters, A. *J. Am. Chem. Soc.* **2008**, *130*, 10048-10049.
(42) Stuerga, D.; Gaillard, P. *Tetrahedron* **1996**, *52*, 5505-5510.
(43) Kremsner, J. M.; Stadler, A.; Kappe, C. O. *Microwave Methods in Organic Synthesis* **2006**, *266*, 233-278.
(44) Howarth, P.; Lockwood, M. *TCE* **2004**, June, 30.
(45) AIST *http://www.aist.go.jp/aist_e/latest_research/2009/20091216/20091216.html* **2009**.
(46) Esveld, E.; Chemat, F.; Van Haveren, J. *Chem. Eng. Technol.* **2000**, *23*, 279-283.
(47) Esveld, E.; Chemat, F.; Van Haveren, J. *Chem. Eng. Technol.* **2000**, *23*, 429-435.
(48) Puschner, H. A. *Elektrotech. Z. B* **1968**, *20*, 278-279.
(49) Dressen, M. H. C. L.; Van de Kruijs, B. H. P.; Meuldijk, J.; Vekemans, J. A. J. M.; Hulshof, L. A. *Org. Process Res. Dev.* **2007**, *11*, 865-869.
(50) Dressen, M. H. C. L. PhD-thesis, Eindhoven University of Technology, **2009**.

Chapter 2

Influence of microwave irradiation on the reactivity of magnesium: application in the Grignard reagent synthesis

Abstract

The influence of microwave irradiation on one of the most common and useful heterogeneous organometallic reactions, the Grignard reaction, was determined. The reaction involves the use of a heterogeneous metal, i.e. magnesium. Microwave irradiation influenced the metal in a variety of ways depending on the geometry of this metal. Irradiating large metal objects led to selective heating while irradiating small objects, such as powders, did not lead to significant interaction. Irradiating intermediately sized objects, for instance magnesium turnings (most commonly used in the Grignard reaction), caused dramatic electrical discharges. The influence of these discharges on the metal surface was determined by surface analysis utilizing scanning electron microscopy and X-ray photoelectron spectroscopy. It is shown that these discharges led to the removal of an inhibiting magnesium oxide / hydroxide layer, the formation of finely dispersed magnesium spheres and the formation of magnesium carbide species on the surface of the magnesium. Magnesium carbide was formed predominantly in the absence of a reactive halogenated compound. The influence of modifying the magnesium surface on the reactivity of the metal in the Grignard reagent formation was determined for a series of halo-compounds. Irradiating the reaction mixtures of non-reactive halogenated compounds (3-bromopyridine and n-octyl chloride) led to major magnesium carbide formation causing reduced reactivity of the metal and prolonged initiation times. In contrast, the initiation time was shortened upon irradiating the reaction mixtures of relatively reactive (2-bromothiophene, 2-bromopyridine, bromobenzene, iodobenzene and n-octyl bromide) and moderately reactive (2-chlorothiophene and 2-chloropyridine) halo-substrates.

2.1 Introduction

As pointed out in Chapter 1, previously reported rate enhancements with microwave heating teach that heterogeneous reaction mixtures are promising to display beneficial microwave effects. One of the most common and useful heterogeneous organometallic reactions is the Grignard reagent formation.[1] Numerous detailed studies on Grignard reagent formations have been previously reported.[2-5] Nevertheless, performing the reaction can be challenging, the results are often not reproducible, and may depend on the experimental skills of the chemist. The reproducibility of the initiation step can be improved by various techniques.[6-10]

The formation of Grignard reagents by microwave irradiation in sealed vessels at temperatures above the normal boiling points of the solvents has been reported.[11,12] In these reported experiments the pressure was higher than atmospheric, which is not advantageous when working on a larger scale. However, the microwave-heated formation of these reagents at atmospheric pressure and without using an initiator (*e.g.* iodine, 1,2-dibromoethane) appeared to be possible. Recently, this observation was reported as being unprecedented in literature.[13] During irradiation in an inert argon atmosphere violent blue arcing was observed (see Figure 2.1). The mechanism of this particular activation is, however, unknown which challenged us to gain more insight into these arcing phenomena. Especially the role of selective heating and the electrical discharges were studied in detail. Also the applicability of the activation method was screened for a series of substrates.

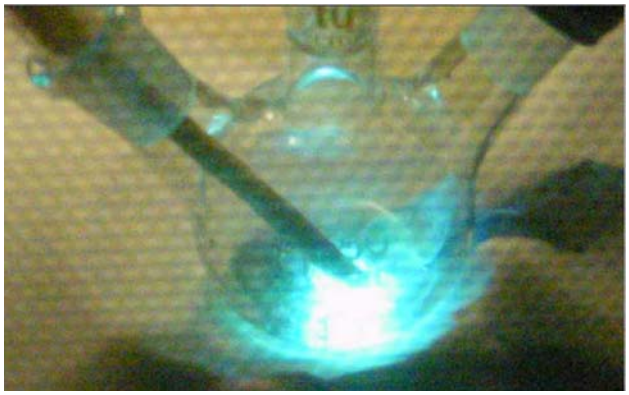

Figure 2.1: *Violent blue arcing induced by irradiating magnesium turnings with microwaves.*

2.2 Microwave – magnesium interactions

In the first place, to get insight into the interaction of magnesium with microwaves, heating experiments in the absence of all reagents except magnesium and solvent were conducted. Magnesium samples of different sizes were compared and the temperature-time history was recorded, see Figure 2.2.

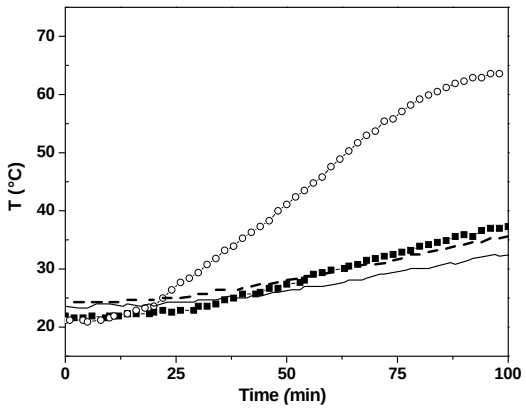

Figure 2.2: *Temperature-time history of solvent (20 mL) and magnesium samples of different sizes (0.2 g) under microwave irradiation (100 W). (▪): THF, (○): THF and a magnesium ribbon, (–): THF and magnesium turnings, (▬): THF and magnesium powder.*

The results in Figure 2.2 demonstrate that the size of the metal particles strongly influences the heating rate of the mixture. A magnesium ribbon submerged in THF showed rapid heating of the mixture resulting in boiling at the surface of the ribbon. The ribbon acts as an antenna for the radiation, causing the ribbon to heat by electrical conduction. Arcing was not observed. Magnesium turnings submerged in THF on the other hand showed a heating pattern similar to that of pure THF and substantial arcing. These particles are too small to act as an antenna. Also magnesium powder showed a temperature-time history similar to that of pure THF. In this case arcing was not observed. Hence, the appearance of the magnesium plays a dominant role in the interaction of magnesium with microwaves.

The similar temperature-time history observed for pure THF and the turnings in THF suggests that no significant heat transfer from the magnesium particles to the solvent occurs. However, the temperature around the arc impact area can increase dramatically, leading to melting of the magnesium and even in some cases

the glass from the vessel wall. These observations point to the absence of selective heating of the magnesium.

Thermographic imaging

To further detect any selective heating, thermographic imaging[14] was applied, see Figure 2.3. A camera was mounted above an open 6 cm diameter reaction tube to detect infrared radiation emitted from a sample. The image was recorded by transmission in an argon atmosphere. As expected, the recording of the microwave-irradiated magnesium turnings in THF did not show selective heating. The thermographic images of the irradiation of a magnesium ribbon are shown in Figures 2.4 and 2.5. Figure 2.4 depicts a magnesium ribbon submerged in THF showing the selective heating of the ribbon. Note that THF is not transparent for the wavelength used by this infrared camera and the heating ring shown in the picture is a result of natural convection. In this temperature range no boiling of the solvent occurs, thus eliminating the effect of preferred nucleation sites for boiling on the magnesium surface. Figure 2.5 shows a magnesium ribbon partly above the THF surface. Surprisingly, the part of the ribbon at the gas / THF surface displays no heating, as seen by the darker color in the middle of the vessel.

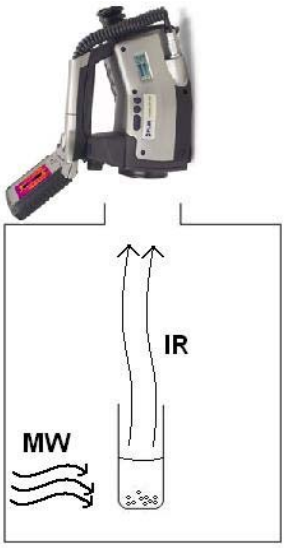

Figure 2.3: *Thermographic imaging setup. IR: infrared irradiation used for imaging.*

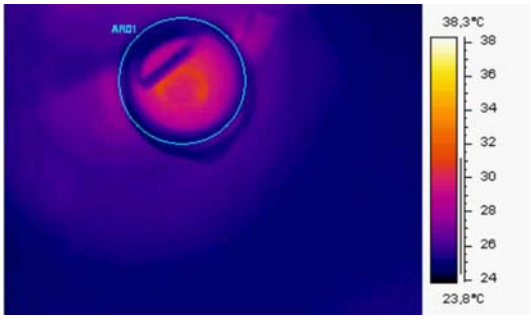

Figure 2.4: *Thermographic imaging: magnesium ribbon submerged in THF. The dark rod in the upper left corner of the vessel is a tube supplying argon above the solvent surface.*

It can be concluded that heating of the magnesium occurs in a layer at the magnesium / THF boundary and is only observed for relatively large metal objects (*i.e.* a ribbon). Therefore, selective heating is certainly not the origin of the decrease in initiation time for the reactions performed with magnesium turnings.

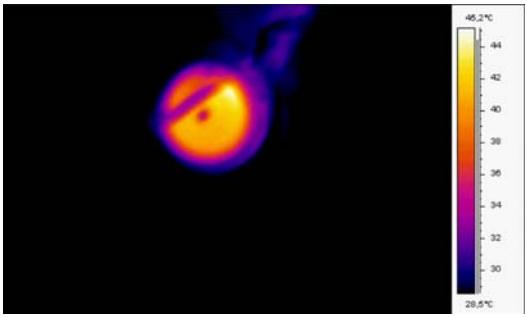

Figure 2.5: *Thermographic imaging: magnesium ribbon partially positioned above the gas / THF surface.*

2.3 The influence of microwave irradiation on magnesium: electrical discharges

The interaction of microwave irradiation with magnesium turnings used for Grignard reagent formation causes violent arcing. The possibility that these electrical discharges give rise to a large decrease in initiation and reaction time was further investigated using scanning electron microscopy (SEM) and X-ray photoelectron spectroscopy (XPS).

The arcing influences the surface of the magnesium dramatically. The impact area of the arcing is clearly visible in Figure 2.7 (right) and Figure 2.9 (left) already at low magnification. Figure 2.8 (right) shows that the impact of the arcs on the surface causes a distortion of the magnesium surface. Probably this distortion also influences the magnesium oxide / magnesium hydroxide layer. A magnesium oxide / magnesium hydroxide layer is always present on non-activated magnesium.[15] This layer prevents an immediate reaction with organic halides. The etching causes metallic magnesium (Mg^0) to be exposed to the reactant. During investigation of the arcing phenomenon it was also discovered that, when arcing is induced in the absence of a reactive organic halide, the solvent becomes turbid, see Figure 2.6. A black dispersion of small magnesium particles is produced. The shape of the particles in this dispersion is predominantly spherical, see Figure 2.9 (right). Presumably, the formation of these spherical magnesium particles is induced by the impact of high electrical currents at the magnesium surface.

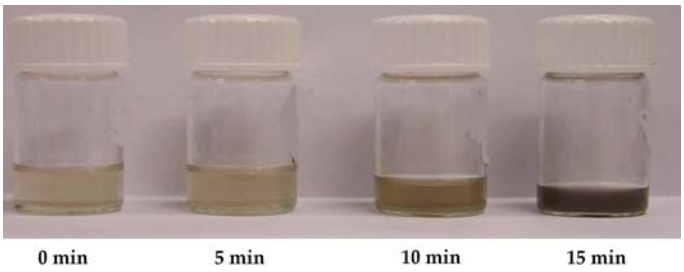

Figure 2.6: *The increase in turbidity of THF subjected to microwave irradiation in the presence of magnesium turnings. The pristine sample (left), after 5 min intervals of microwave exposure (progressively to the right).*

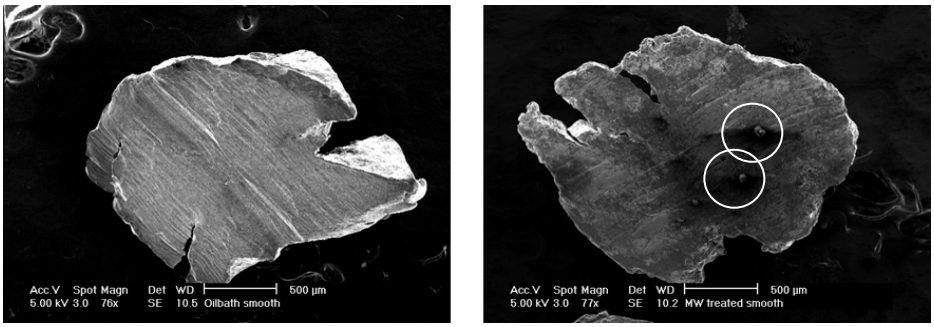

Figure 2.7: *SEM images of a magnesium turning subjected to refluxing THF. Left: oil-bath heating. Right: microwave heating. The circles indicate the impact area of the microwave-induced electrical discharges.*

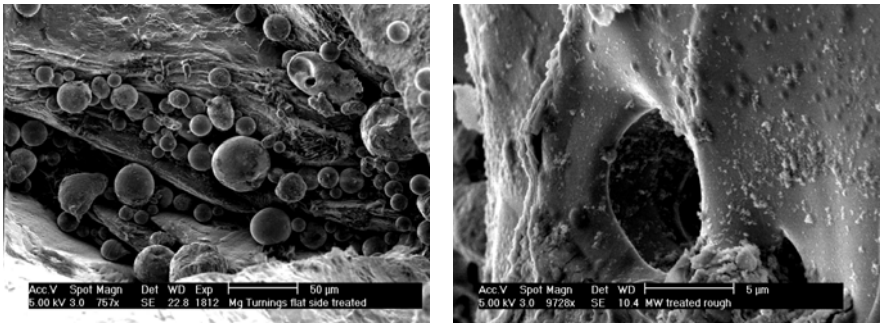

Figure 2.8: *SEM images of magnesium turnings after microwave irradiation. Left: spherical objects that remain in the cavities of the surface after removal of THF. Right: impact area of the arc showing disruption of the magnesium surface and formation of cavities.*

These currents give rise to extremely high local temperatures, which are not generated by the direct absorption of microwave energy, and melting of the magnesium occurs.

The molten magnesium is transferred to the solvent phase and is cooled almost instantaneously which leads to a preservation of the spherical geometry that is adopted in the molten state. The size of the produced particles varies between about 5 μm and 50 μm, see Figure 2.8 (left). The generation of this type of spherical debris by electrical discharges in electrical discharge machining (EDM)[16] is known but the usefulness in synthetic chemistry was never investigated.

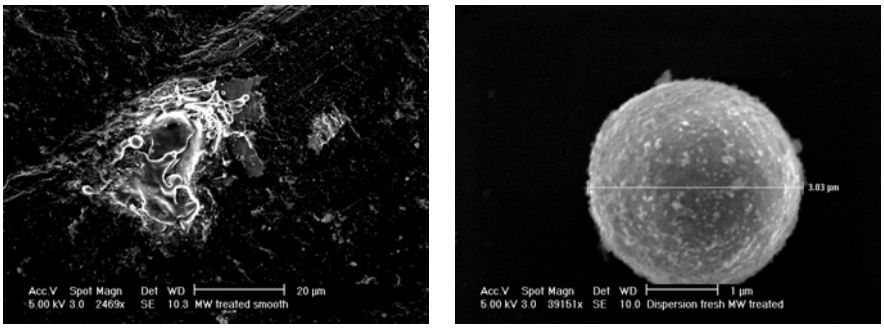

Figure 2.9: *SEM images of magnesium turnings after microwave irradiation. Left: impact area of an arc on the magnesium surface. Right: spherical magnesium particle produced by the electrical discharges.*

X-ray photoelectron spectroscopy

To determine the composition of the magnesium surface after exposure to microwave-induced electrical discharges, X-ray photoelectron spectroscopy measurements were conducted. The surface of magnesium turnings exposed to the electrical discharges in the presence of solvent alone was analyzed. The surface showed a large degree of carbide formation, as indicated by the shift of the binding energy of the 1s electrons of magnesium to lower energy.[17] This shift was not observed in untreated magnesium. Also the removal of the material by argon laser sputtering, which removes material at 1-2 nm / min, shows a decrease in magnesium carbide, see Figure 2.10.

Figure 2.11 shows the binding energies of the 1s electrons of the carbon species present at the magnesium surface after the microwave-induced electrical discharges. A small amount of CO_2 originating from exposure to air is present. The shift to a lower energy is also observed for the 1s electrons of carbon, indicative of carbide species.[17] These results indicate that magnesium carbide coats the magnesium surface, suggesting that arcing only facilitates side reactions with the

solvent. In the presence of reactive organic halides, the formation of arcing-induced magnesium carbide from the solvent is hampered severely, indicated by the absence of the shifted Mg 1s and carbon 1s electron binding energies.

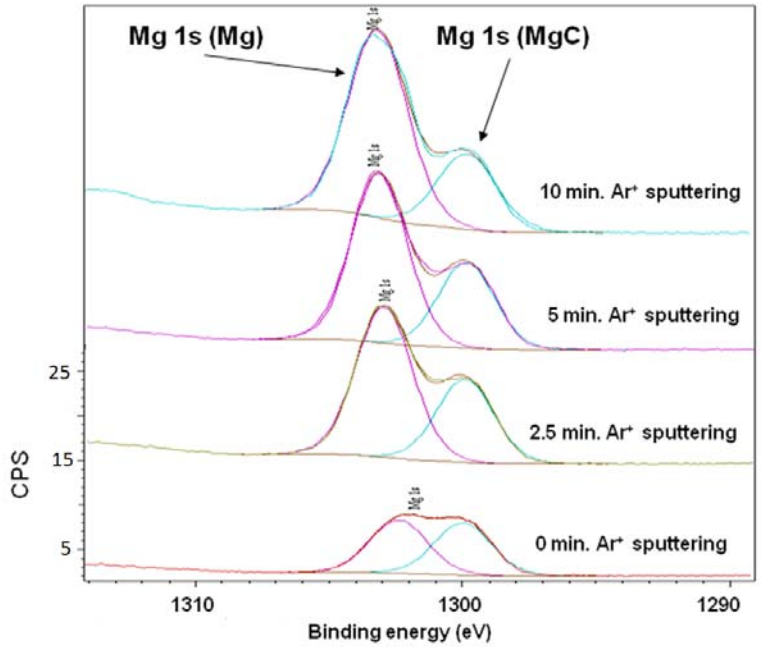

Figure 2.10: *Deconvoluted binding energies of the 1s electrons of magnesium and of magnesium carbide on the surface exposed to microwave-induced electrical discharges in the presence of solvent (THF) alone. Bottom graph: pristine surface; top graphs: surface after argon laser sputtering.*

The surface characterization described above, combined with the fast oxidation observed for the spherical particles after short exposure to air, stresses the reactive nature of the magnesium produced by microwave-induced electrical discharges. This reactive nature is mainly due to the high surface area to volume ratio and lack of inhibiting magnesium oxide / hydroxide layers.

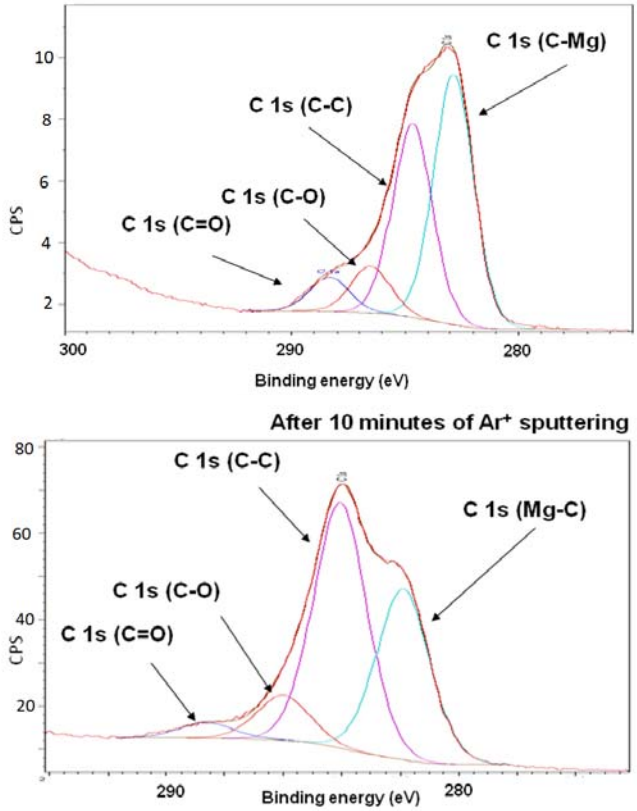

Figure 2.11: *Deconvoluted binding energies of the 1s electrons of carbon species at the magnesium surface exposed to microwave-induced electrical discharges in the presence of solvent (THF) alone. Top graph: pristine surface; bottom graph: surface after argon laser sputtering (10 min).*

2.4 *Application of microwave-induced electrical discharges in the Grignard reagent formation*

To demonstrate the applicability of microwave-induced electrical discharges for the Grignard reagent formation a series of halogenated compounds was tested. The time-conversion histories of the Grignard reagent formation was monitored by GC / MS analyses of small aliquots quenched by saturated ammonium chloride.

2-Bromothiophene and 2-chlorothiophene, precursors in the synthesis of α-terthienyl,[18] were selected for this study, see Scheme 2.1.

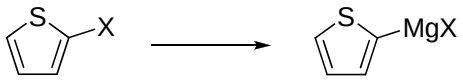

I = Br, II = Cl

Scheme 2.1: *Grignard reagent formation from 2-chlorothiophene and 2-bromothiophene.*

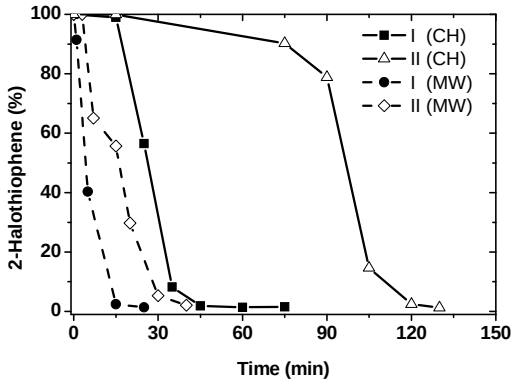

Figure 2.12: *Dimensionless concentration of 2-bromothiophene (I) and 2-chlorothiophene (II) as a function of time with either conventional heating (CH) or microwave heating (MW) in the presence of Mg turnings (C_0 = 1.4 mol/dm^3).*

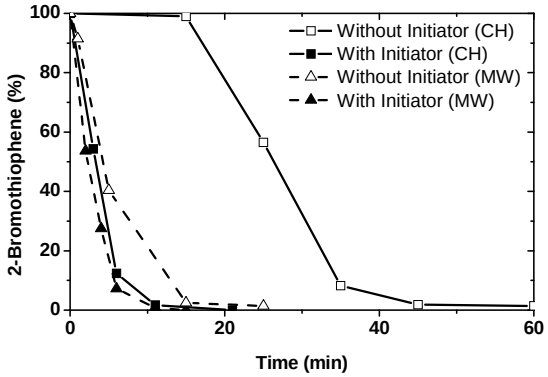

Figure 2.13: *Dimensionless concentration of 2-bromothiophene as a function of time with either conventional heating (CH) or microwave heating (MW) in the presence of Mg turnings with(out) initiator (C_0 = 1.4 mol/dm^3).*

As expected, 2-bromothiophene reacts faster than its chloro analogue under conventionally heated conditions. This was also observed in the microwave oven, see Figure 2.12. The intensity of arcing decreased after initiation of the reaction. The formation of Mg salts caused the liquid phase to interact with the microwaves more strongly. As a consequence, the absorption of microwaves by magnesium is simultaneously reduced.

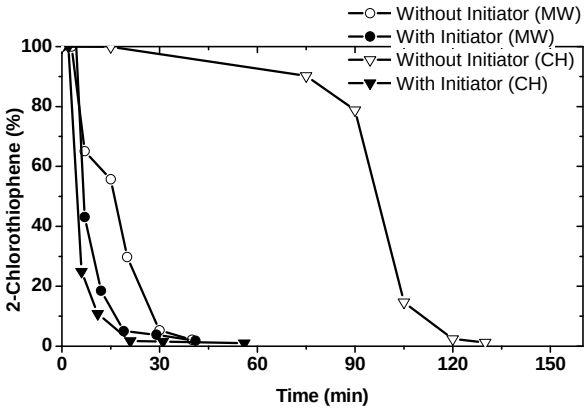

Figure 2.14: *Dimensionless concentration of 2-chlorothiophene as a function of time with either conventional heating (CH) or microwave heating (MW) in the presence of Mg turnings with(out) initiator (C_0 = 1.4 mol/dm^3).*

To acquire a proper insight into the positive effect of microwave heating on the rate of the Grignard reagent formation, the reaction was also studied in the presence of the initiator 1,2-dibromoethane. The latter is often used to initiate the Grignard reagent formation and could alter the initiation mechanism. Both thiophenes reacted in the presence of the initiator with similar initiation times for both heating methods, see Figures 2.13 and 2.14.

The positive effect on the conversion rates of both 2-halothiophenes, observed under microwave conditions, is desirable for practical purposes. However, the side effect of arcing limits its use upon scaling-up. Generating arcing in a large vessel on plant-scale is undesirable. The initiation can, however, be accomplished by irradiating a small part of the reaction mixture in a lab-scale microwave oven and transferring the resulting initiated mixture to a large vessel.

Table 2.1: *Grignard reagent synthesis of selected substrates under microwave irradiation and conventional heating (oil bath) and subsequent quenching reactions.*

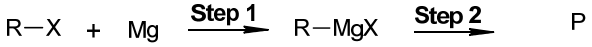

Entry	R	X	Conditions Step 1	Conditions Step 2	Product (P)
1		2-Br	A	C	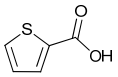
2		2-Br	B	C	
3		2-Cl	A	C	
4		2-Cl	B	C	
5		2-Br	A	D	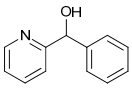
6		2-Br	B	D	
7		2-Cl	A	D	
8		2-Cl	B	D	
9		3-Br	A	D	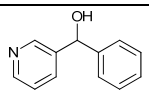
10		3-Br	B	D	
11		Br	A	E	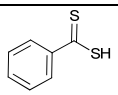
12		Br	B	C	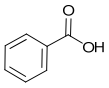
13		I	A	C	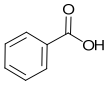
14		I	B	C	
15	*n*-C_8H_{17}	Br	A	C	*n*-C_8H_{17}COOH
16	*n*-C_8H_{17}	Br	B	C	*n*-C_8H_{17}COOH
17	*n*-C_8H_{17}	Cl	A	C	*n*-C_8H_{17}COOH
18	*n*-C_8H_{17}	Cl	B	C	*n*-C_8H_{17}COOH

A: oil-bath reflux (66 °C), B: microwave, reflux (66 °C), max power = 300 W, C: dry CO_2, -78 °C, D: benzaldehyde, oil-bath 66 °C, E: CS_2, room temperature.

The issue of arcing can be overcome by adjusting the geometry of the magnesium particles. Smaller particles and a solid ribbon with similar mass prevent arcing under microwave irradiation. Also arcing can be suppressed by choosing other parameters,[19,20] such as choice of solvent, applied microwave power, density of metal, rate of stirring and pressure. Although these adaptations diminish the arcing phenomenon, this feature seems necessary for microwave irradiation to show a beneficial effect on the Grignard reagent formation. To

further demonstrate general applicability, a series of halogenated compounds was tested under microwave irradiation and conventional heating, see Table 2.1. Especially the initiation time, which was influenced positively for the thiophenes, was compared, see Table 2.2. For the determination of the yield of the Grignard reagent a suitable consecutive reaction had to be performed. A series of quenching reactions was evaluated. The ease of purification and isolation of the product, the absence of byproducts, and quantitative yields made the reaction with carbon dioxide the best choice for analyzing reactive Grignard reagents. The analogous reaction with CS_2 was also almost completely selective and gave an approximately 100 % yield for the quenching reaction. Relatively non-reactive or insoluble Grignard reagents, *i.e.* Grignard reagents resulting from 3-halopyridine, can be reacted with benzaldehyde at reflux temperature leading to moderate yields and minor byproduct formation. The undesired formation of the ketone corresponding to the secondary alcohol together with equimolar amounts of benzyl alcohol is clearly a consecutive process that does not change the overall conclusions. Unstable Grignard reagents, resulting from 2-halopyridine derivatives, tend to polymerize into insoluble tars making the subsequent quenching reaction redundant.

Table 2.1 depicts a selection of substrates that were subjected to microwave-induced arcing and conventional heating to facilitate the synthesis of their corresponding Grignard reagents. Table 2.2 depicts the initiation and reaction times with corresponding yields for these reactions. The lower isolated yields under microwave irradiation are caused mainly by a difficult layer separation in the work-up procedure of the carboxylic acids due to residual magnesium carbide particles. The crude yields were similar for both heating methods. Further optimization of the work-up procedure may minimize these losses. The previously discussed 2-halothiophenes[13] are included in the table for reference purposes.

A large decrease in the initiation time, compared to conventional heating, was observed for 2-chlorothiophene and 2-bromothiophene (entries 1-4) when the reaction was performed with microwave-induced electrical discharges, as discussed in the previous section.

Surprisingly, the formation of the Grignard reagent from 3-bromothiophene and 3-chlorothiophene failed using both heating methods, stressing the non-reactive nature of the 3-position of thiophene. Whether the reluctance to form a Grignard reagent relies on the relatively high electron density at C-3 / C-4 or an unproductive interaction of magnesium surface with the sulphur in the 1 position is unknown.

Table 2.2: *Grignard reagent synthesis of selected substrates under microwave irradiation and conventional heating (oil bath) and subsequent quenching reactions.*

Entry	Initiation time Step 1 (min)[e]	Reaction time Step 1 (min)[f]	Yield (%)
1	20	45	86 [a]
2	0-1	15	73 [a]
3	75	120	82 [a]
4	5	40	73 [a]
5	0-1	10 [b]	trace [c]
6	0	10 [b]	trace [c]
7	125	200	trace [c]
8	75	110	trace [c]
9	30	180	37 (8) [d]
10	50	200	41 (19) [d]
11	0-1	10 [b]	88 [a]
12	0	10 [b]	87 [a]
13	0-1	10 [b]	30 [a]
14	0	10 [b]	30 [a]
15	0-1	10 [b]	87 [a]
16	0	10 [b]	70 [a]
17	80	150	85 [a]
18	-	-	-

[a] isolated yield, [b] addition time of the substrate, [c] tar formation, [d] between brackets: % of product representing ketone corresponding to the produced alcohol accompanied by equimolar amounts of benzyl alcohol [e] Time at which Grignard reagent starts to form, [f] time at complete conversion.

When heating the reaction mixture of the halopyridines (entries 5-10) the intensity of arcing under microwave irradiation was less pronounced. This is mainly due to the higher dielectric loss[21] of the pyridine derivatives, ensuring a higher absorption of the microwave irradiation by the solvent / reagent mixture. The higher absorption of the microwave irradiation by the solvent leads to a diminished charge accumulation at the magnesium surface. The lower intensity of arcing for these substrates gives rise to a smaller influence of microwave irradiation on the initiation time: 75 (entry 8) instead of 125 (entry 7) min for 2-chloropyridine. The formation of the Grignard reagent from 3-bromopyridine (entries 9 and 10) is retarded slightly under microwave irradiation indicating some competitive carbide formation.

The influence of magnesium carbide formation is seen most clearly from the Grignard reagent formation of *n*-octyl chloride (entries 17 and 18). Although this substrate is reactive under conventional heating conditions with an initiation time

of 80 min, the reaction does not occur with microwave irradiation. The formation of magnesium carbide species from the activated magnesium is believed to occur at a higher rate than the generation of Grignard reagent from *n*-octyl chloride leading to an inhibiting layer on the surface of the magnesium turnings. This layer causes the Grignard reagent formation to be inhibited completely for *n*-octyl chloride under microwave-induced electrical discharges. The formation of magnesium carbide is a competitive process, rendering the generation of Grignard reagents from very poorly reactive halides less probable. Short exposure to microwave irradiation and subsequent transferring the mixture to oil-bath heating (and therefore without additional electrical discharges) gave comparable results as for oil-bath heating only.

The results in Table 2.2 demonstrate that 2-bromopyridine (entries 5 and 6), bromobenzene (entries 11 and 12), iodobenzene (entries 13 and 14) and *n*-octyl bromide (entries 15 and 16) are very reactive towards magnesium. The lower yield, under both heating methods, for iodobenzene was caused mainly by the insolubility of the formed Grignard reagent and the formation of biphenyl. Due to the short initiation time of these substrates a clear difference between thermal activation and activation by electrical discharges is difficult to quantify. Note that for microwave irradiation the instantaneous initiation is consistent and for conventional heating a scatter was observed, meaning an increased reproducibility for these substrates with microwave irradiation. The very exothermic reaction of the active substrates with magnesium demands the drop-wise addition of these substrates. The addition time governs the overall reaction time, thus obscuring the influence of area enlargement of the magnesium by electrical discharges on the reaction rate. Although no quantitative distinction between conventional and microwave heating for the reactive species can be made, the comparable yields for both heating techniques make the application of microwave heating for the production of Grignard reagents for the active substrates feasible and increase the reproducibility. Therefore, it can be concluded that microwave heating leads to a higher reproducibility of the Grignard reaction than conventional heating.

2.5 Conclusion

The use of metals in combination with microwave heating can cause dramatic electrical discharges. The suppression of these discharges has been a point of interest[19,20] to expand the scope of microwave heating in organic syntheses. The deliberate generation of these discharges (with of course due caution) gives rise to effects that cannot be mimicked easily by other methods. One of these effects is the generation of highly active magnesium that can be used directly for the formation of Grignard reagents. Selective heating of the metal during microwave irradiation

does not occur with magnesium turnings and is obviously not the origin of the observed decrease in initiation time. The formation of highly active magnesium spheres and the etching of the magnesium surface resulting from the interaction of the microwaves with the metal explain the large decrease in initiation times for selected substrates. This novel and straightforward initiation method generates magnesium with a reactivity similar to that of Riekes[9,22] magnesium and eliminates the use of highly toxic and environmentally adverse initiators and, therefore, limits the formation of byproducts and the total production cost.

2.6 Experimental section

General:
All starting materials were obtained from commercial suppliers and used as received unless otherwise indicated. All moisture sensitive reactions were performed under an atmosphere of dry argon. Dry tetrahydrofuran distillation from Merck molecular sieves (4 Å). ^{1}H-NMR spectra were recorded on a Varian Mercury, 400 MHz for ^{1}H-NMR and 100 MHz for ^{13}C-NMR or on a Varian Gemini, 300 MHz for ^{1}H-NMR and 75 MHz for ^{13}C-NMR. Proton chemical shifts are reported in ppm downfield from tetramethylsilane (TMS) and carbon chemical shifts downfield from TMS using the resonance of the deuterated solvent as internal standard. Elemental analysis was performed on a Perkin Elmer 2400 series analyzer. GC/MS analysis was performed on Shimadzu GC-17A equipped with a GCMS-QP5000 and a Phenomenex Zebron ZB-35 column (30 m). Standard temperature profile: 1 min isothermal at 50 °C, ramped at 25 °C / min to 300 °C and 3 min hold time.

Microwave heating:
A commercially available, automated multimode microwave oven MicroSynth from Milestone s.r.l. (Italy) was used. This oven operates at 2.45 GHz and is temperature controlled by a fiber-optic sensor. To eliminate significant temperature distributions the temperature was monitored by insertion of the fiber-optic sensor in the reaction mixture while stirring properly. The maximum power input could be adjusted between 0 and 1000 Watt.

Thermographic imaging:
An infrared camera (FLIR Systems ThermaCAMTM P65) was placed outside the cavity of the microwave unit and was focused on an open vessel containing the THF / magnesium sample. The images were recorded real time via IEEE-1394 FireWire DV-output during irradiation. The mixture was covered with a blanket of

argon to ensure safety (no oxygen should be present during the electrical discharges).

Scanning electron microscopy (SEM):
SEM was performed on a Philips XL30 ESEM-FEG electron microscope in the high-vacuum mode. The acceleration voltage used was 5.0 kV. Samples were prepared by either placing a droplet of a suspension of the particles in THF on an aluminum stub followed by evaporation of the THF or by mounting the particles with carbon tape on an aluminum stub.
Note: The activated magnesium may be pyrophoric and create a flare which is hazardous to the eyes when exposed to air. Due caution should always be taken in the handling of activated magnesium.

X-ray photoelectron spectroscopy (XPS):
The XPS measurements were carried out with a Kratos AXIS Ultra spectrometer, equipped with a monochromatic Al Kα X-ray source and a delay-line detector (DLD). Spectra were obtained using the aluminium anode (Al Kα = 1486.6 eV) operating at 150W. For survey scans a constant pass energy of 160 eV was used and for region scans a constant pass energy of 80 eV. The background pressure was 2×10^{-9} mbar.

Grignard reagent formation of the reactive substrates under conventional heating (entries 1, 5, 11, 13, 15 in Table 2.1). Magnesium turnings (0.44 g, 18 mmol) were introduced in an oven-dried 25 mL three-neck round-bottomed flask. 2-Bromothiophene (2.28 g, 14 mmol was dissolved in dry THF (10 mL, distilled from mol sieves 3 Å). A volume of 1 mL of the 2-bromothiophene solution was added to the Mg in an argon atmosphere and the mixture was heated by a preheated oil-bath (T = 85 °C) to reflux. As soon as initiation took place, the oil-bath was lowered and the remaining solution was added drop-wise in 10 min to maintain a gentle reflux. Additional heating with an oil bath was applied for 30-60 min. The solution of Grignard reagent was separated from the remaining Mg with a syringe. The same procedure was used for 2-bromopyridine (2.21 g, 14 mmol), bromobenzene (2.20 g, 14 mmol), iodobenzene (2.86 g, 14 mmol) and *n*-octylbromide (2.7 g, 14 mmol).

Grignard reagent formation of the reactive substrates under microwave heating (entries 2, 6, 12, 14, 16 in Table 2.1). Magnesium turnings (0.44 g, 18 mmol) were introduced in an oven-dried 25 mL three-neck round-bottomed flask. 2-Bromothiophene (2.28 g, 14 mmol) was dissolved in dry THF (10 mL, distilled from

mol sieves 3 Å). A volume of 1 mL of the 2-bromothiophene solution was added to Mg in an argon atmosphere (Note: no oxygen, or fire supporting oxygen-rich compounds, should be present upon the occurrence of the electrical discharges) and irradiated with microwave energy (maximum power input 350 W) to reflux. As soon as initiation took place the remaining solution was added drop-wise in 10 min to maintain a gentle reflux (the microwave was in an OFF state during this period). Additional irradiation with microwave energy (maximum power input 200 W) was applied for 30-60 min. The solution of Grignard reagent was separated from the remaining Mg with a syringe. The same procedure was used for 2-bromopyridine (2.21 g, 14 mmol), bromobenzene (2.20 g, 14 mmol), iodobenzene (2.86 g, 14 mmol) and *n*-octylbromide (2.7 g, 14 mmol).

Grignard reagent formation of the relatively non-reactive substrates under conventional heating (entries 3, 7, 9, 17, in Table 2.1). Magnesium turnings (0.44 g, 18 mmol) and 2-chlorothiophene (1.66 g, 14 mmol), dissolved in dry THF (10 mL, distilled from mol sieves 3Å), were introduced in an oven-dried 25 mL three-neck round-bottomed flask under an argon atmosphere. The mixture was heated by a preheated oil bath (T = 85 °C) to reflux. Additional heating was applied for 30-200 min. The solution of Grignard reagent was separated from the remaining Mg with a syringe. The same procedure was used for 2-chloropyridine (1.87 g, 14 mmol), 3-bromopyridine (2.21 g, 14 mmol) and *n*-octylchloride (2.08 g, 14 mmol).

Grignard reagent formation of the relatively non-reactive substrates under microwave heating (entries 4, 8, 10, 18 in Table 2.1). Magnesium turnings (0.44 g, 18 mmol) and 2-chlorothiophene (1.66 g, 14 mmol), dissolved in dry THF (10 mL, distilled from mol sieves 3 Å), were introduced in an oven-dried 25 mL three-neck round-bottomed flask under an argon atmosphere. (Note: no oxygen, or fire supporting oxygen rich compounds, should be present upon the occurrence of the electrical discharges). The reaction mixture was heated by microwave irradiation (maximum power input 350 W) to reflux. Additional irradiation with microwaves (maximum power-input 200 W) was applied for 30-200 min. The solution of Grignard reagent was separated from the remaining Mg with a syringe. The same procedure was used for 2-chloropyridine (1.87 g, 14 mmol), 3-bromopyridine (2.21 g, 14 mmol) and *n*-octylchloride (2.08 g, 14 mmol).

Quenching the Grignard reagents with CO_2 (entries 1, 2, 3, 4, 12, 13, 14, 15, 16, 17, 18 in Table 2.1). The solution of the Grignard reagent was added drop-wise to an excess of freshly prepared dry, solid CO_2 (prepared by passing sublimated CO_2 over 3 stages of concentrated sulphuric acid and depositing it in a liquid nitrogen

cooled flask). After addition of the reagent another layer of dry CO_2 was deposited. The mixture was slowly heated to room temperature in 15 min, acidified with 10 wt% HCl (10 mL) and extracted with toluene (3 x 10 mL). The organic layer was dried with $MgSO_4$, filtered and evaporated. Optional purification method: the crude residue was dissolved in toluene (15 mL) and extracted with 1.0 M KOH (2 x 10 mL). The aqueous layer was acidified with conc. HCl and extracted with toluene. The toluene layer was dried with $MgSO_4$, filtered and evaporated yielding the pure product. Benzoic acid: ^{1}H-NMR (400 MHz, $CDCl_3$) δ: 7.49 (m, 2H), 7.63 (m, 1H), 8.14 (m, 2H), 11.72 (s, 1H); Nonanoic acid: ^{1}H-NMR (400 MHz, $CDCl_3$) δ: 0.88 (t, 3H), 1.25–1.30 (m, 12H), 1.63 (t, 2H), 10.63 (br s, 1H), 2-Thiophenecarboxylic acid: ^{1}H-NMR (400 MHz, $CDCl_3$) δ: 7.1 (dd, 1H), 7.90 (dd, 1H), 7.66 (dd, 1H), 9.76 (br s, 1H). See Table 2.2 for the yields.

Quenching the Grignard reagents with CS_2 (entry 11 in Table 2.1). The solution of the Grignard reagent was added drop-wise at room temperature to a flask containing a large excess of CS_2 dissolved in THF (10 mL, distilled from mol sieves 3 Å). The solution was stirred for 1 h and subsequently acidified with 10 wt% HCl (10 mL) and extracted with toluene (3 x 10 mL). The organic layer was dried with $MgSO_4$, filtered and evaporated. Benzodithio acid: ^{1}H-NMR (400 MHz, $CDCl_3$) δ: 6.38 (br s, 1H) 7.40 (t, 2H), 7.60 (t, 1H), 8.05 (d, 2H). See Table 2.2 for the yields.

Quenching the Grignard reagent with benzaldehyde (entries 5, 6, 7, 8, 9, 10 in Table 2.1). The solution of the Grignard reagent was added drop-wise to a flask containing a two-fold molar excess of benzaldehyde dissolved in THF (10 mL, distilled from mol sieves 3 Å) at reflux temperature (oil-bath heating). The solution was stirred for 1 h and subsequently acidified with saturated NH_4Cl (10 mL) and extracted with toluene (3 x 10 mL). The organic layer was dried with $MgSO_4$, filtered and evaporated. Phenyl (2-pyridinyl)methanol: ^{1}H-NMR (400 MHz, $CDCl_3$) δ: 4.69 (s, 1H,), 5.74 (s, 1H), 7.23-7.49 (m, 7H), 7.62 (td, 1H), 8.56 (d, 1H). Phenyl-(3-pyridyl)methanol: ^{1}H-NMR (400 MHz, $CDCl_3$) δ: 8.52 (d 1H), 8.37 (dd, 1H), 7.78 (dd, 1H) 7.20 (m, 5H), 7.15 (dd, 1H), 5.82 (s, 1H), 4.7 (s, 1H) 3.15-4.36 (br s, 1H). See Table 2.2 for the yields.

2.7 References

(1) Grignard, V. *Compt. rend.* **1900**, 1322-1324.
(2) Ashby, E. C.; Oswald, J. *J. Org. Chem.* **1988**, *53*, 6068-6076.
(3) Garst, J. E.; Soriaga, M. R. *Coord. Chem. Rev.* **2004**, *248*, 623-652.
(4) Hill, C. L.; Vandersande, J. B.; Whitesides, G. M. *J. Org. Chem.* **1980**, *45*, 1020-1028.
(5) Rachon, J.; Walborsky, H. M. *Tetrahedron Lett.* **1989**, *30*, 7345-7348.

(6) Baker, K. V.; Brown, J. M.; Hughes, N.; Skarnulis, A. J.; Sexton, A. *J. Org. Chem.* **1991**, *56*, 698-703.
(7) Luche, J. L.; Damiano, J. C. *J. Am. Chem. Soc.* **1980**, *102*, 7926-7927.
(8) Oppolzer, W.; Kundig, E. P.; Bishop, P. M.; Perret, C. *Tetrahedron Lett.* **1982**, *23*, 3901-3904.
(9) Rieke, R. D.; Bales, S. E. *J. Am. Chem. Soc.* **1974**, *96*, 1775-1781.
(10) Tilstam, U.; Weinmann, H. *Org. Process Res. Dev.* **2002**, *6*, 906-910.
(11) Gold, H.; Larhed, M.; Nilsson, P. *Synlett* **2005**, 1596-1600.
(12) Mutule, G.; Suna, E. *Tetrahedron* **2005**, *61*, 11168-11176.
(13) Dressen, M. H. C. L.; Van de Kruijs, B. H. P.; Meuldijk, J.; Vekemans, J. A. J. M.; Hulshof, L. A. *Org. Process Res. Dev.* **2007**, *11*, 865-869.
(14) Borrello, S. *Thermography, Kirk-Othmer Encyclopedia of Chemical Technology* **1998**.
(15) Abreu, J. B.; Soto, J. E.; Ashley-Facey, A.; Soriaga, M. P.; Garst, J. F.; Stickney, J. L. *J. Colloid Interface Sci.* **1998**, *206*, 247-251.
(16) Khanra, A. K.; Pathak, L. C.; Godkhindi, M. M. *J. Mater. Sci. - Mater. Electron.* **2007**, *42*, 872-877.
(17) Moulder, J. F.; Stickle, W. F.; Stobol, P. E.; Bomben, K. D. *Handbook of X-ray Photoelectron Spectroscopy*; Perkin Elmer, Eden Prairie,, **1992**.
(18) Smeets, B. J. J.; Meijer, R. H.; Meuldijk, J.; Vekemans, J.; Hulshof, L. A. *Org. Process Res. Dev.* **2003**, *7*, 10-16.
(19) Whittaker, A. G.; Mingos, D. M. P. *J. Chem. Soc., Dalton Trans.* **2000**, 1521-1526.
(20) Whittaker, A. G.; Mingos, D. M. P. *J. Chem. Soc., Dalton Trans.* **2002**, 3967-3970.
(21) *The dielectric loss of the halopyridines is unknown. Therefore, the estimation was done on the basis of unsubstituted pyridine which has a dielectric constant of 13.25 and a loss tangent of 0.107 (for values see R. S. Holland, C. P. Smyth, J. Chem. Phys.* ***1955****, 10, 1088). The dielectric loss of substituted pyridines is assumed to be higher. This assumption is based on the comparison of bromobenzene (dielectric constant: 5.08 and loss tangent: 0.149), chlorobenzene (dielectric constant: 5.5 and loss tangent: 1.016) and benzene (dielectric constant: 2.284 and loss tangent: ~0). For values see F.H. Branin Jr., C.P. Smyt, J. Chem. Phys.* ***1952****, 7, 1121.*
(22) Rieke, R. D. *Science* **1989**, *246*, 1260-1264.

Chapter 3

Influence of microwave irradiation on the reactivity of zinc: application in the Reformatsky reagent synthesis

Abstract

The influence of microwave irradiation on another heterogeneous organometallic reaction involving metallic zinc, the Reformatsky reagent preparation, has been studied and is shown to be governed by the geometry of zinc. Irradiation of liquid / Zn dispersions with zinc powder and mossy zinc led to similar reaction rates for conventional as well as microwave heating. No arcing was observed. On the other hand, irradiation of zinc granules, normally used in the Reformatsky reaction, led to violent electrical discharges. The effect of these discharges on the metal surface has been investigated with the aid of scanning electron microscopy and X-ray photoelectron spectroscopy. These microwave-induced electrical discharges caused major zinc carbide formation, irrespective of the presence of a species reactive towards zinc. The exothermic character of the Reformatsky reaction with α-bromoesters, making heating during the reaction redundant, and their high reactivity towards zinc, hampered any direct comparison between microwave and conventional heating for these substrates. On the other hand, a comparison between the reactivity of α-chloroesters was feasible. During their irradiation in the presence of zinc major zinc carbide formation was observed. The zinc carbide formation coated the zinc, which was responsible for inhibition of organozinc formation. Organozinc formation occurred when arcing decreased or even stopped. Only then the zinc surface became accessible for the substrate (i.e. α-haloesters). The zinc carbide formation during microwave-induced electrical discharges limited its application for the Reformatsky reaction to such an extent that conventional heating has to be preferred.

3.1 Introduction

The resemblance between zinc and magnesium relies on the position in the periodic table of Mendeleev. Both belong to group II, albeit that zinc has the $(3d)^{10}$ $(4s)^2$ electron configuration in its outer shell and magnesium has the $(3s)^2$ electron configuration in its outer shell.[1] Therefore, both metals react in a similar manner with carbonhalide substrates.

In Chapter 2 the influence of microwave heating on the Grignard reagent formation reaction was described. For this reaction involving metallic magnesium, microwave irradiation causes a decrease in initiation time for a series of substrates when compared to conventional heating. An analogous reaction involving the insertion of a metal, *i.e.* zinc instead of magnesium, in a carbon-halide bond, leads to the formation of Reformatsky reagents.

In 1887[2] Sergeius Reformatsky (1860-1934) first reported the reaction of an α-haloester with metallic zinc in the presence of a ketone yielding a β-hydroxyester. It is a versatile[3] carbon-carbon bond forming reaction differing from the Grignard reaction in the compatibility of an ester functionality and in the ability to perform both the formation and addition reaction of the organozinc species in one pot. The scope of the reaction has broadened to a number of electrophiles, including aldehydes, ketones, nitriles, phosphonates, amides and imides, yielding β-hydroxy- or α,β-unsaturated products. The reproducibility of the initiation step can be improved by various techniques.[4-11] The aim of our work was to investigate the potential application of microwave irradiation as a novel activation method.

3.2 Microwave – zinc interactions

To gain more insight into the influence of microwave irradiation on the reactivity of zinc, the interaction of microwaves with zinc-solvent mixtures, in the absence of other reagents, was investigated. The heating rate of zinc-solvent mixtures, with zinc of different shapes irradiated with microwaves was recorded, see Figure 3.2. The types of zinc used in these experiments, namely: mossy, granular and powder, are depicted in Figure 3.1. The combination of microwave and highly conducting materials, *i.e.* metals, can cause charge accumulation on the surface of these materials. Eventually the strong electric fields caused by these charges may lead to an electrical breakdown of the medium between the particles of this material. The breakdown manifests itself as a violent arc. The intensity of arcing is dependent on many factors[12,13] such as solvent, microwave power applied, density of metal, stirring speed and pressure.

Our study has demonstrated that the shape of the metal has a major influence on the intensity of arcing.

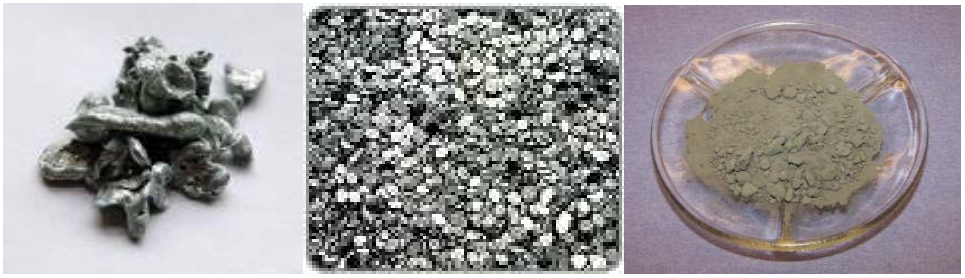

Figure 3.1: *Forms of zinc used in heating rate determination of zinc-solvent mixtures under microwave irradiation. Left: mossy zinc (technical zinc). Middle: granular zinc. Right: zinc powder.*

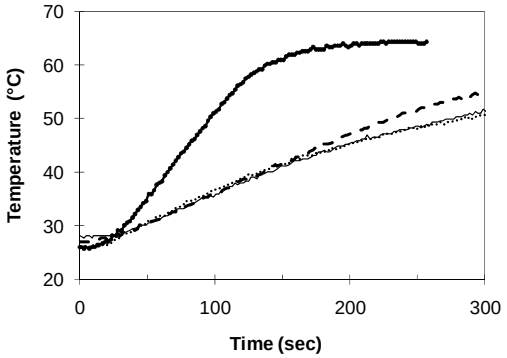

Figure 3.2: *Temperature-time history of solvent (20 g of THF) and zinc of different shapes (2.2 g) under microwave irradiation (dashed line: zinc powder, dotted line: pure THF, solid line: mossy zinc and remaining line: granular zinc).*

The heating rate of the mossy zinc and zinc powder is similar to that of pure tetrahydrofuran (THF). This indicates that the microwaves are not absorbed by zinc, and, therefore, selective heating of these forms of zinc is excluded. This is corroborated clearly by the absence of arcing while irradiating THF / zinc powder dispersions. The microwaves are unable to generate sufficient charges on the surface of the zinc powder to cause a sufficiently strong electric field strength for a dielectric breakdown of THF. The large particles of the mossy zinc show limited charge accumulation, mainly due to a distribution of the charges over the entire particle. Therefore, a minor intensity of arcing occurs during microwave irradiation. The porous particles resemble a Faraday cage, shielding the inside of the particle from the electromagnetic field, limiting their ability to act as an antenna, and therefore, limiting their heating by electrical conduction.

In contrast, the charge accumulation on the particles of the granular zinc is extremely strong. As a consequence, the irradiation of granular zinc leads to a high arcing activity. The energy that is released by these arcs strongly influences the heating rate of the zinc-solvent mixture. The increased heating rate of the granular zinc particles may also indicate that, although the arcing intensity is high, selective heating of these zinc granules, *i.e.* turnings, occurs.

3.3 *The influence of microwave irradiation on zinc: electrical discharges*

As pointed out in the former section, the interaction of microwaves with zinc turnings used for the Reformatsky reagent formation causes violent arcing. This phenomenon was further investigated using scanning electron microscopy (SEM) and X-ray photoelectron spectroscopy (XPS).

Arcing influences the surface of the zinc particles in a similar fashion as the surface of magnesium turnings exposed to microwave irradiation, see section 2.3. The impact area of one of these arcs is clearly visible in Figure 3.3 (left).

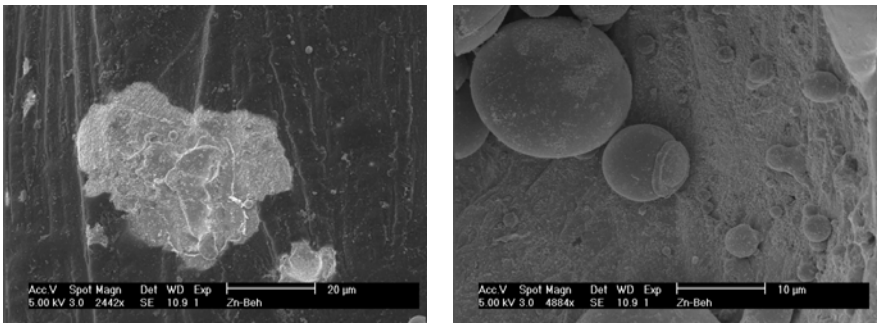

Figure 3.3: *SEM images of zinc turnings after microwave irradiation. Left: impact area of an arc on the zinc surface. Right: spherical zinc particle produced by the electrical discharges.*

During the investigation of the arcing phenomenon it was also discovered that, when arcing is induced the solvent becomes turbid. A black dispersion of small zinc-containing particles is formed. The shape of the particles in this dispersion is predominantly spherical, see Figure 3.3 (right) and Figure 3.4 (left).

The generation of these zinc particles by the electrical discharges is thought to be subject to the same mechanism as the generation of magnesium particles discussed in section 2.3. The charge accumulation between the zinc particles is

similar to the accumulation between the magnesium particles and the dielectric breakdown occurs at similar electric potential differences between charge acceptor and charge donor. Therefore, the energy that is released upon impact is also similar. Although the energy is similar, the generation of the particles derived from zinc is more abundant than for magnesium. This is expressed by the short time span after which a turbid solvent phase is formed under microwave-induced electrical discharges for zinc. This is caused predominantly by the considerably lower melting point of zinc compared to magnesium, 419 °C instead of 649 °C, and the similar energy consumption for melting the same volume of metal*.

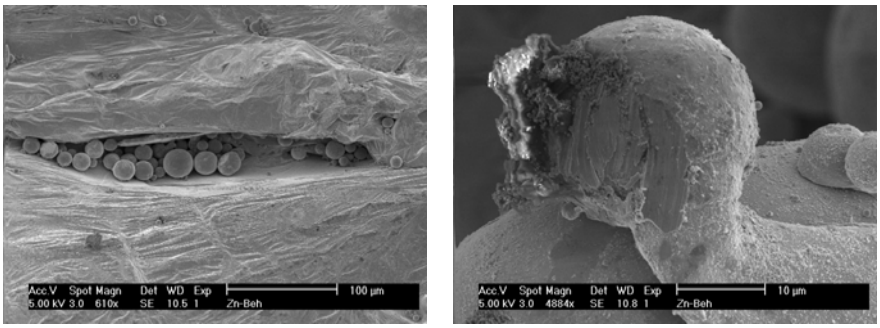

Figure 3.4: *SEM images of zinc turnings after microwave irradiation. Left: spherical objects that remain in the cavities of the surface after removal of THF. Right: impact area of the arc showing disruption of the zinc surface.*

X-ray photoelectron spectroscopy

To determine the composition of the zinc surface after exposure to microwave-induced electrical discharges, X-ray photoelectron spectroscopy measurements were conducted. The surface of zinc exposed to the electrical discharges in the presence of solvent alone was analyzed.

Unfortunately, the XPS spectra of the zinc were inconclusive. The shifts of the binding energies of the 1s electrons of carbon or 3p electrons of zinc in the zinc carbide species were not observed, suggesting the absence of this carbide species.

To confirm the absence of zinc carbide, zinc exposed to microwave-induced electrical discharges was treated with saturated ammonium chloride. Upon addition of an acid, the carbide species will be protonated, yielding acetylene for ZnC_2 or propyne for $Zn(C_3)$. The gas, liberated from the zinc, was analyzed by

* The heat of fusion of zinc (7.32 kJ/mol) is similar to that of magnesium (8.84 kJ/mol). The much lower molecular weight of magnesium (24.30 g/mol instead of 65.38 g/mol) and density (1.74 kg/dm^3 instead of 7.14 kg/dm^3) leads to a melting energy of 800 kJ/dm^3 for zinc and 633 kJ/m^3 for magnesium.

direct injection in a GC / MS. This gas was compared with the gas formed upon acidifying conventionally heated zinc, see Figure 3.5.

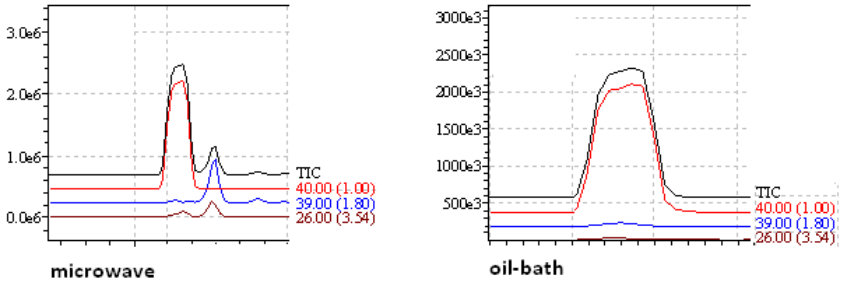

Figure 3.5: *Headspace GC / MS trace. Left: acidified microwave-treated zinc. Right: conventionally heated zinc. TIC: total ion counts, 40: ion counts with m/z = 40, 39: ion counts with m/z = 39, 26: ion counts with m/z = 26.*

The gas liberated from the microwave-irradiated zinc displayed fragments with m/z = 26, corresponding to the molecular ion of acetylene, upon acidification, which is not observed for the conventionally heated zinc. This observation indicates that carbide species of ZnC_2 are produced while irradiating zinc / solvent mixtures.

In both traces large amounts of ions with m/z of 40 were determined. Ions with m/z of 40 were also observed for pure air, indicating that these ions originate from argon in air. Unfortunately, the molecular ion of propyne originating from ZnC_3 upon acidification will have the same m/z-value. However, while recording a mass spectrum of propyne, also the fragment with m/z = 39 was abundantly present. This fragment was recorded for the gas, liberated from the microwave-irradiated zinc, and not for the conventionally heated zinc, indicating that also carbide species ZnC_3 are formed during microwave-induced electrical discharges.

Although the XPS measurements did not clearly indicate carbide species, headspace GC / MS analysis showed their formation during microwave irradiation of zinc in THF.

3.4 *Application of microwave-induced electrical discharges in the Reformatsky reagent formation*

To demonstrate the applicability of microwave heating in the Reformatsky reagent formation a series of halogenated compounds was tested.

Usually zinc is activated in a manner similar to that applied for magnesium in the Grignard reagent synthesis, *i.e.* by addition of either 1,2-dibromoethane or iodine or by applying ultrasound.[3] In contrast to the Grignard reagent formation,

the Reformatsky reaction is performed in the presence of the electrophile, *i.e.* in one pot. Eliminating the electrophile from the reaction mixture may result in a reaction of the Reformatsky reagent with its precursor. This can be partially circumvented when reacting sterically crowded esters, such as *t*-butyl-esters.[3]

The Reformatsky reaction does not go to completion when performed in dry THF, due to the formation of an insoluble film on the zinc surface during the reaction. Therefore, the reaction is performed preferentially in a solvent mixture of dry THF and toluene 1:1 (v/v).

α-Haloesters: conventional heating

At first, the reaction of ethyl α-bromoisobutyrate with 4-methoxy-phenylacetonitrile, the first step in the synthesis of the morphine analogue Bremazocine,[14] see Scheme 3.1(B_1), was chosen to investigate the influence of microwave irradiation on the reactivity of zinc.

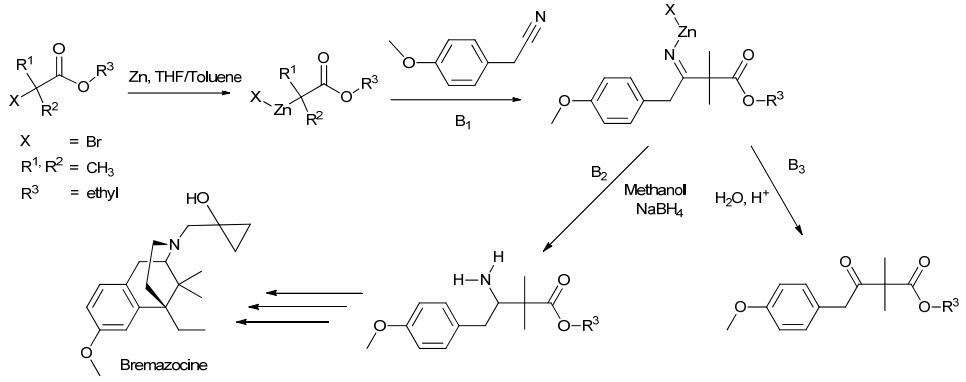

Scheme 3.1: *Reformatsky and consecutive reactions of α-halogenated esters. B_1: first step in the synthesis of Bremazocine, B_2: reduction of the enamine to the desired primary amine, B_3: hydrolysis of the enamine (for monitoring global kinetics).*

In this investigation, the reduction with sodium borohydride, see Scheme 3.1(B_2), was replaced by hydrolysis of the enamine into the resulting β-keto-ester, see Scheme 3.1(B_3). Preliminary results indicated that the undesired side reactions (condensation reaction of the 4-methoxyphenylacetonitrile) made direct investigation of the reaction kinetics of the formation of the Reformatsky reagent cumbersome. The condensation reaction of 4-methoxyphenylacetonitrile is caused by deprotonation of its acidic α-proton. Hence, a suitable electrophile lacking an acidic α-proton was selected, *i.e.* benzaldehyde. To further expand the scope of the

applicability of microwave heating, a selection of α-haloesters was investigated using benzaldehyde, see Scheme 3.2.

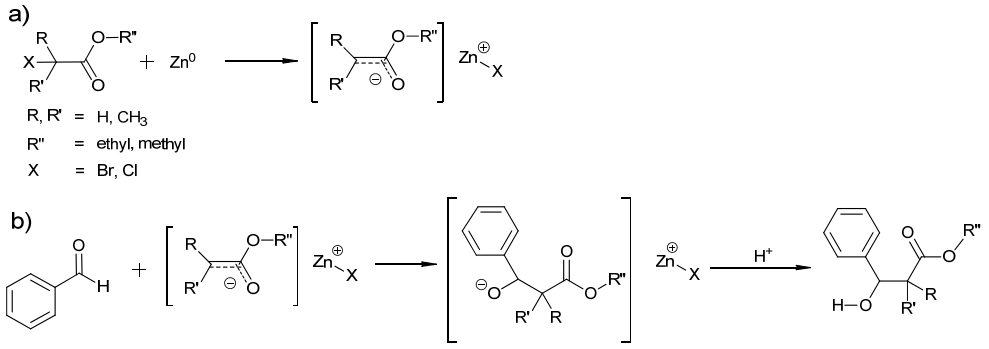

Scheme 3.2: *Reformatsky formation and consecutive reaction of α-haloesters: a) formation of the Reformatsky reagent, b) addition reaction of the Reformatsky reagent with benzaldehyde.*

All of these esters were commercially available, except ethyl 2-chloroisobutyrate. To evaluate the reactivity, ethyl 2-chloroisobutyrate had to be synthesized.

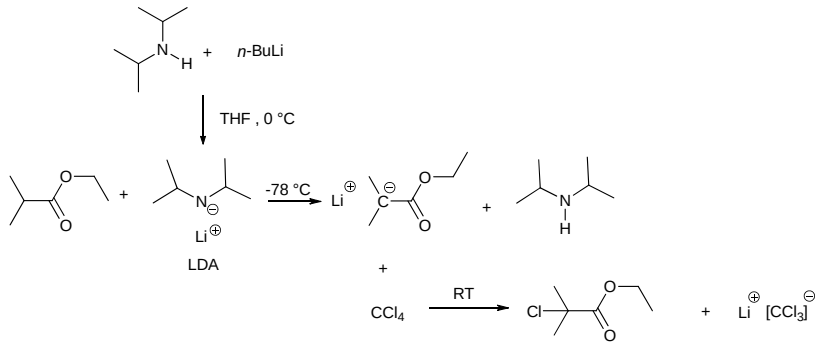

Scheme 3.3: *Synthesis of ethyl 2-chloroisobutyrate.*

The synthesis was accomplished by deprotonation of an isobutyrate ester with lithium diisopropyl amine (LDA) and subsequent addition of carbon tetrachloride to yield the desired chloroester in moderate yield, see Scheme 3.3.

Commercial LDA was available in a solvent mixture containing ethylbenzene which made the workup of the product more difficult, due to their closely related boiling points (149 °C for ethyl 2-chloroisobutyrate[15] and 136 °C for ethylbenzene).

Therefore, freshly prepared LDA was used in the synthesis of the 2-chloro-isobutyrate ester.

The initiation times of the reactions of zinc with the α-haloesters are collected in Table 3.1. As expected, the reactivity of the α-bromoesters towards zinc was high. The reaction time was governed mainly by the rate of addition of the ester, thus leading to a reaction under starving conditions. Addition of the solution of benzaldehyde and the α-bromoester to zinc proved to be necessary to control the rate of heat evolution of this fast, exothermic reaction.

Table 3.1: *Initiation times of reactions of α-haloesters with zinc in toluene-THF mixtures using conventional heating.*

R^1	R^2	R^3	X	Initiation time (min)	Yield (%)
H	H	CH_3CH_2	Br	0.5-1 [b]	82
H	H	CH_3CH_2	Cl	- [a]	0
CH_3	H	CH_3CH_2	Br	0.5-1 [b]	82
CH_3	H	CH_3CH_2	Cl	10-15	69
CH_3	CH_3	CH_3CH_2	Br	0-1 [b]	90
CH_3	CH_3	CH_3CH_2	Cl	5-10	84

[a] not determined, [b] initiation occurs during addition of the reactants.

On the other hand, α-chloroesters, although attractive due to their more beneficial environmental impact and economics, are known to be notoriously less reactive.[16] Slower reactions occurring with α-chloroesters allow the reaction mixture to be premixed enabling a straightforward investigation of their kinetics.

Unfortunately, ethyl α-chloroacetate proved to be not reactive at all towards zinc. Surprisingly, it was found that ethyl α-chloropropionate and ethyl α-chloroisobutyrate were reactive towards zinc. The reactivity of the carbon-chlorine bond is enhanced by heavier substitution of the carbon atom C-2.[17] The higher the degree of substitution, the more reactive the α-chloroester is towards zinc. However, no information on the influence of the substitution degree on the initiation time is available.

In the solid state the Reformatsky reagent constitutes a dimer with bridging zinc coordination, see Scheme 3.4 (left).[18] Heavier substitution of the carbon atom C-2 increases the nucleophilicity and, therefore, increases the reactivity of the

reagent towards an electrophile and decreases its stability. However, in a polar and coordinating solvent, for instance DMSO, the Reformatsky reagent primarily exists as monomeric species. This monomeric species is in equilibrium with its enol[19] and this equilibrium mainly lies on the enol side[20], see Scheme 3.4. In less polar solvents such as THF, this monomeric species is not observed,[21] but the dimeric species, similar to the crystal structure of the solid, also displays a keto-enol-tautomerization equilibrium that mainly lies on the enol side. The heavier substitution of the α-position increases the stability of the enol-tautomer, thus increasing the thermodynamic driving force for generation of the Reformatsky reagent. $\Delta_r G^{\ominus}$ becomes more negative, resulting in an acceleration of the reaction rate. Substitution of the α-position of the ester makes the carbon atom C-2 of the ester less electrophilic and more sterically crowded and, therefore, seemingly less reactive. On the other hand, the increase of stability of the Reformatsky reagent, which is improved by these electron-donating methyl groups, favors their formation. The latter seems to have predominance over the intrinsic reactivity of the ester towards zinc. The increase in reactivity with more methyl substituents at C-2 is also present in the bromoesters, but this increase is insignificant as a result of their inherently higher reactivity.

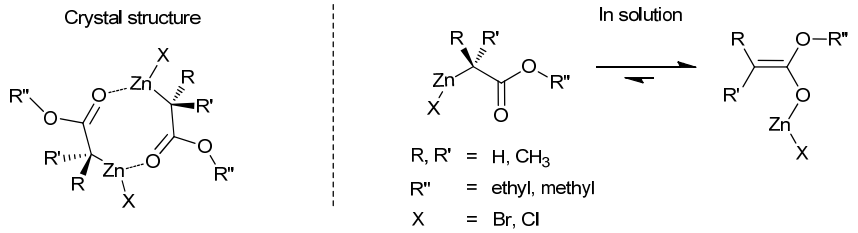

Scheme 3.4: *Structure of the Reformatsky reagent (coordinating THF molecules have been omitted for clarity). Left: crystal structure.*[18] *Right: keto-enol tautomerization in solution.*

α-Haloesters: comparing conventional and microwave heating

The extended addition time of mixtures of benzaldehyde and α-bromoesters to zinc to avoid thermal runaways, hampers any direct comparison of microwave with conventional heating in these cases. The exothermic character of the reaction even made actual microwave power input not necessary to maintain reflux. Only when the reaction had almost reached completion, the microwave oven started to irradiate the reaction mixture. Therefore, the experiments performed for the α-bromoesters with microwave irradiation showed conversion-time profiles identical to those observed for conventional heating.

With conventional heating, ethyl α-chloroacetate is not reactive towards zinc. Unfortunately, microwave heating was not sufficient to induce a reaction with this substrate. In addition, the reaction rates of the Reformatsky reaction with ethyl α-chloroisobutyrate were investigated with microwave and conventional heating. Both conversion-time histories clearly demonstrate that the oil-bath heated reaction follows apparent first order kinetics[†], see Figure 3.6 (right).

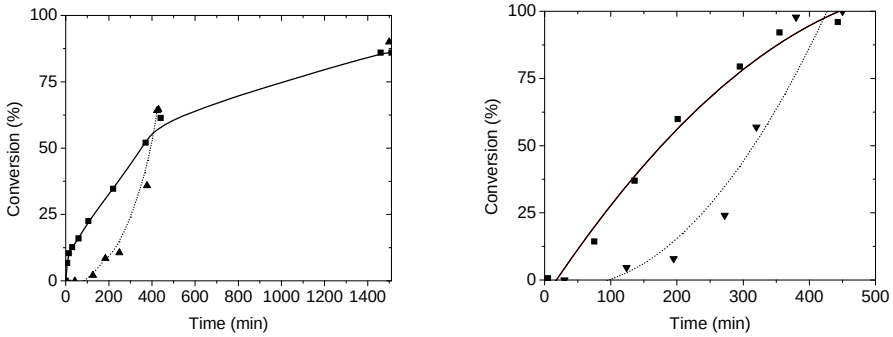

Figure 3.6: *Conversion-time histories of the Reformatsky reaction. Left: ethyl α-chloropropionate. Right: ethyl α-chloroisobutyrate with benzaldehyde (solid line: oil-bath heating, dashed line: microwave heating).*

The same experiment performed for both substrates under the influence of microwave irradiation showed violent arcing. Arcing produced finely dispersed, spherical and active micro-sized zinc particles. These particles showed a striking similarity with the finely dispersed magnesium particles that are produced when magnesium turnings are irradiated with microwaves, see section 2.3. The magnesium particles were shown to be very active towards organohalides in generating the Grignard reactants.

In contrast, the zinc particles resulting from continuous arcing do not seem to be very reactive towards α-chloroesters. The presence of these particles during the Reformatsky reaction with ethyl α-chloroisobutyrate negatively influences the conversion rate of this reaction. Inhibition occurs during the first 120 min, whereafter electrical discharging diminishes due to the need of a sufficient particle size of zinc for arcing to occur.[12,13] Indeed, these discharges cause the particles to break apart and the overall size of the particles is diminished in time, thus lowering the arcing frequency. From XPS measurements it was concluded that

[†] A plot of ln(1-x) versus time displayed a straight line with $R^2 = 0.992$ for ethyl α-chloroisobutyrate and $R^2 = 0.988$ for ethyl α-chloropropionate, indicating apparent first order kinetics for both substrates with conventional heating.

major zinc carbide formation occurs while irradiating zinc-solvent mixtures, see section 3.3. The turbidity observed in these experiments is also observed for the reaction mixtures with the α-haloesters. This indicates that, although a reactive compound is present, the formation of zinc carbide is favored over the actual Reformatsky reaction. Zinc carbide coats the zinc surface, similar to zinc oxide, and reduces the reactivity of zinc towards the α-haloester. When the arcing diminishes, also the carbide formation is slowing down. Eventually, after 30-45 min the Reformatsky reaction starts, and the zinc particles are partially consumed. During this consumption the zinc carbide is dislodged from the zinc surface. So, the zinc surface becomes available for the α-haloester. The process of zinc carbide dislodgement is slow and, therefore, the zinc exposure is limited, leading to a rather low reaction rate during the intermediate period. The continued consumption of zinc and the lower zinc carbide formation rate, caused by the lower arcing frequency, increases the accessibility of the zinc surface. The exposed zinc reacts readily, and the increased zinc surface leads to a rate enhancement in the formation of the Reformatsky reagent.

The lower substitution degree at the α-position of ethyl α-chloropropionate makes it less reactive towards zinc than ethyl α-chloroisobutyrate. This is expressed by the longer time necessary to obtain complete conversion with oil-bath heating, as shown in the time-conversion histories shown in Figure 3.6 (left). The same three stages in reaction rate as observed for ethyl α-chloroisobutyrate are detected for ethyl α-chloropropionate. The inhibition period is 15-30 min as a result of microwave-induced electrostatic discharges leading to zinc carbide coverage of the zinc surface. After an intermediate period, 300 min instead of 150 min, with a relatively low reaction rate, the electrical discharges greatly diminish and the high final reaction rate, caused by the increased specific surface, leads to a conversion of 65 % after 400 min. The total absence of electrical discharges after this period and the diminished zinc content cause the reaction to follow the same time-conversion profile as observed during the conventionally heated experiments for the remainder of the reaction.

3.5 Conclusion

The use of metals in combination with microwave heating may cause electrical discharges influencing the metal in a dramatic way. For zinc the discharges lead to major zinc carbide formation. Zinc carbide is generated irrespective of the presence of a reactive α-haloester. Moreover, the zinc carbide formation covers the zinc surface substantially. Therefore, the reaction of zinc with α-haloesters is inhibited almost completely. After the electrical discharges become less intensive or stop, the

zinc surface becomes accessible for the α-haloesters and the reaction starts to proceed. The dominant zinc carbide formation and the blocking of the zinc surface with microwave heating, limits its application for the Reformatsky reaction and renders microwave heating less efficient than conventional heating. This result is in contrast with the reaction of magnesium in the Grignard reagent formation, where microwaves lead to surface cleaning instead of contamination with non-reactive materials.

3.6 Experimental section

General:
See experimental section of Chapter 2.

Microwave heating:
See experimental section of Chapter 2.

Synthesis of 2-chloroisobutyrate: A solution of diisopropylamine (22.24 g, 0.2 mol) in 35 mL THF was introduced in a 250 mL flask and cooled to 0 °C with an ice-bath. A solution of *n*-butyl lithium (100 mL, 2.0 M in cyclohexane) was added drop-wise in 20 min. After an additional 15 min of stirring, the resulting solution was cooled with an acetone / dry-ice bath to -78 °C. Ethyl isobutyrate (21.12 g, 0.18 mol) was added drop-wise in 10 min and the solution was stirred for additional 20 minutes. A solution of carbon tetrachloride (30.76 g, 0.19 mol) in 20 mL THF was added drop-wise in 20 min, after 2/3 of the addition a solid was formed ($LiCCl_3$). The mixture was warmed to room temperature in 2 h and poured into 1.0 M HCl (200 mL) while stirring. The water layer was extracted with diethyl ether (2 x 100 mL) and the organic layer was washed with saturated $NaHCO_3$ (200 mL), water (200 mL) and dried with $MgSO_4$, filtered and solvent was evaporated yielding the crude product. The product was purified by vacuum distillation, the fraction collected at 45 °C at 4 kPa corresponded to 2-chloroisobutyrate. Yield: 12.0 g (62 %), bp = 149 °C. ^{1}H-NMR (400 MHz, $CDCl_3$) δ: 4.21. (q, *J*=7.13, 7.13, 7.16 Hz, 2H), 1.75 (s, 6H), 1.29 (t, *J*=7.11, 7.11 Hz, 3H).

Reformatsky reaction with α-bromoesters: Zinc turnings (1.44 g, 22 mmol) were introduced in an oven-dried 25 mL three-neck round-bottomed flask. Ethyl 2-bromoisobutyrate (1.95 g, 10 mmol) and benzaldehyde (2.23 g, 22 mmol) were dissolved in dry THF / toluene 1:1 (10 mL, distilled from mol sieves 3 Å). A volume of 1 mL of the ethyl 2-bromoisobutyrate solution was added to zinc in an argon atmosphere and the mixture was heated by a preheated oil-bath (T = 85 °C) to reflux. As soon as initiation took place, the oil-bath was lowered and the remaining

solution was added drop-wise in 10 min to maintain a gentle reflux. After the reaction had gone to completion, the solution was acidified with saturated NH_4Cl (10 mL) and extracted with toluene (3 x 10 mL). The organic layer was washed with $NaHSO_3$ (15%, 3 x 10 mL) and dried with $MgSO_4$, filtered and evaporated. The same procedure was employed for ethyl 2-bromoacetate (1.67 g, 10 mmol) and ethyl 2-bromopropionate (1.81 g, 10 mmol). In the microwave-heated experiments, the oil-bath was substituted with microwave heating (P_{max} = 150 W) with fiber-optic temperature control. Ethyl 3-hydroxy-3-phenylpropanoate (1.59 g, 82 %): ^{1}H-NMR (400 MHz, $CDCl_3$) δ: 7.37 (m, 5H), 5.14 (dd, 1H), 4.17 (q, 2H), 3.50 (br s, 1H), 2.73 (m, 2H), 1.26 (t, 3H). Ethyl 3-hydroxy-2-methyl-3-phenylpropanoate (1.68 g, 82 %): ^{1}H-NMR (400 MHz, $CDCl_3$) δ: 7.34 (m, 5H), 5.10 (d, 1H), 4.17 (q, 2H), 3.50 (br s, 1H), 2.81 (m, 1H), 1.26 (t, 3H) 1.14 and 1.01 (d. 3H). Ethyl 3-hydroxy-2,2-dimethyl-3-phenylpropanoate (2.0 g, 90 %): ^{1}H-NMR (400 MHz, $CDCl_3$) δ: 7.31 (m, 5H), 4.89 (s, 1H), 4.2 (q, 2H), 1.26 (t, 3H), 1.14 (s. 3H), 1.11 (s, 3H).

Reformatsky reaction with the *α*-chloroesters: Zinc turnings (1.44 g, 22 mmol), and a solution of either ethyl 2-chloroisobutyrate (1.51 g, 10 mmol) or ethyl 2-chloropropionate (1.36 g, 10 mmol) and benzaldehyde (2.23 g, 22 mmol) in dry THF / toluene 1:1 (10 mL, distilled from mol sieves 3 Å) were introduced in an oven-dried 25 mL three-neck round-bottomed flask. The mixture was heated by microwave heating (P_{max} = 150 W) with fiber-optic temperature control to reflux. After the reaction had gone to completion the solution was acidified with saturated NH_4Cl (10 mL) and extracted with toluene (3 x 10 mL). The organic layer was extracted with $NaHSO_3$ (15 %, 3 x 10 mL) and dried with $MgSO_4$, filtered and evaporated. The same procedure was employed for the conventionally heated experiments, substituting microwave heating by a preheated oil-bath (T = 85 °C). Ethyl 3-hydroxy-2-methyl-3-phenylpropanoate (1.43 g, 69 %): ^{1}H-NMR (400 MHz, $CDCl_3$) δ: 7.34 (m, 5H), 5.10 (d, 1H), 4.17 (q, 2H), 3.50 (br s, 1H), 2.81 (m, 1H), 1.26 (t, 3H) 1.14 and 1.01 (d. 3H). Ethyl 3-hydroxy-2,2-dimethyl-3-phenylpropanoate (1.86 g, 84 %): ^{1}H-NMR (400 MHz, $CDCl_3$) δ: 7.31 (m, 5H), 4.89 (s, 1H), 4.2 (q, 2H), 1.26 (t, 3H), 1.14 (s. 3H), 1.11 (s, 3H).

3.7 References

(1) Kappe, C. O.; Dallinger, D. *Mol. Diversity* **2009**, *13*, 71-193.
(2) Reformatskii, S. *Ber. Dtsch. Chem. Ges.* **1887**, 1210.
(3) Ocampo, R.; Dolbier, W. R. *Tetrahedron* **2004**, *60*, 9325-9374.
(4) Baker, K. V.; Brown, J. M.; Hughes, N.; Skarnulis, A. J.; Sexton, A. *J. Org. Chem.* **1991**, *56*, 698-703.
(5) Luche, J. L.; Damiano, J. C. *J. Am. Chem. Soc.* **1980**, *102*, 7926-7927.

(6) Oppolzer, W.; Kundig, E. P.; Bishop, P. M.; Perret, C. *Tetrahedron Lett.* **1982**, *23*, 3901-3904.
(7) Picotin, G.; Miginiac, P. *J. Org. Chem.* **1987**, *52*, 4796-4798.
(8) Rieke, R. D.; Bales, S. E. *J. Am. Chem. Soc.* **1974**, *96*, 1775-1781.
(9) Rollin, Y.; Gebehenne, C.; Derien, S.; Dunach, E.; Perichon, J. *J. Organomet. Chem.* **1993**, *461*, 9-13.
(10) Smith, C. R. *Synlett* **2009**, 1522-1523.
(11) Tilstam, U.; Weinmann, H. *Org. Process Res. Dev.* **2002**, *6*, 906-910.
(12) Whittaker, A. G.; Mingos, D. M. P. *J. Chem. Soc., Dalton Trans.* **2000**, 1521-1526.
(13) Whittaker, A. G.; Mingos, D. M. P. *J. Chem. Soc., Dalton Trans.* **2002**, 3967-3970.
(14) Dortch-Carnes, J.; Potter, D. E. *CNS Drug Rev.* **2005**, *11*, 195-212.
(15) Balbiano *Ber. Dtsch. Chem. Ges.* **1878**, *11*, 1693.
(16) Oroshnik, W.; Spoerri, P. E. *J. Am. Chem. Soc.* **1945**, *67*, 721-723.
(17) Hussey, A. S.; Newman, M. S. *J. Am. Chem. Soc.* **1948**, *70*, 3024-3026.
(18) Miki, S.; Nakamoto, K.; Kawakami, J. I.; Handa, S.; Nuwa, S. *Synthesis* **2008**, 409-412.
(19) Furstner, A. *Synthesis* **1989**, 571-590.
(20) Vaughan, W. R.; Knoess, H. P. *J. Org. Chem.* **1970**, *35*, 2394-2395.
(21) Dekker, J.; Budzelaar, P. H. M.; Boersma, J.; Vanderkerk, G. J. M.; Spek, A. L. *Organometallics* **1984**, *3*, 1403-1407.

Chapter 4

Influence of microwave radiation on the reactivity of copper: application in the Ullmann coupling

Abstract

The influence of microwave irradiation on a heterogeneous organometallic reaction involving metallic copper, the Ullmann coupling, has been studied. Microwaves did not seem to interact with the copper directly, limiting the impact of this heating mode on this type of reaction. To investigate whether microwave irradiation actually influences the reactivity of copper, evaluation of the Ullmann coupling of 2-chloro-3-nitropyridine utilizing copper-bronze in dimethylformamide (DMF) was selected. The stoichiometry of copper in the reaction was determined to be significantly less than 1 molar equivalent due to the dismutation of copper(I) chloride into metallic copper and copper(II) chloride. Therefore, the reaction performed with 1 molar equivalent relative to 2-chloro-3-nitropyridine displayed reaction rates comparable to those observed in reactions utilizing a molar excess. When copper-bronze is the copper source the reproducibility of the reaction was poor, making a comparison of the heating techniques cumbersome. The reproducibility could be improved by activation of the copper-bronze. Replacing the copper source by copper powder strongly improved the reproducibility. To expand the temperature range and to improve the reproducibility, alternative solvents for the coupling reaction were screened, such as dimethylacetamide (DMA) and N-methyl-2-pyrrolidone (NMP). However, switching solvents to NMP or DMA diminished reaction rates, gave lower yields of the target product and substantial amounts of 2,2'-oxybis(3-nitropyridine) as byproduct. This result made DMF the preferred solvent for this Ullmann coupling. Comparison of microwave with conventional heating for the reactions performed at optimized conditions (in DMF at 110 °C), as well as under less ideal conditions (in DMA and NMP at various temperatures) revealed identical time-conversion histories, yields and selectivities.

4.1 Introduction

In Chapters 2 and 3 the influence of microwave heating on the formation of Grignard reagents and the Reformatsky reaction was discussed. The Grignard and Reformatsky reactions use metallic magnesium and metallic zinc, respectively. Microwave irradiation caused a decrease of the initiation time for the formation of the Grignard reagent and an increase of the initiation time for that of the Reformatsky reagent. A reaction also involving the insertion of a metal atom - copper instead of magnesium or zinc - in a carbon-halide bond is the Ullmann coupling. The Ullmann coupling which ultimately results in the formation of a carbon-carbon bond was first published in 1901[1] by Fritz Ullmann (1875-1939).[2] The reaction utilizes metallic copper to form symmetrical biaryl products. Although at first the reaction was performed neat, requiring harsh reaction conditions and was suitable only for sufficiently activated compounds. The application of the solvent dimethylformamide (DMF) allowed milder conditions and the use of less activated compounds, which broadened the scope of the reaction.[3-6]

The Ullmann coupling has been studied extensively[7] and the rate of the reaction can be increased by various methods, including ultrasonic irradiation.[8] The utilization of microwave irradiation is focused mainly on the Ullmann substitution with hetero-atoms, generating ethers,[9,10] amines,[11,12] or thioethers.[13,14] Microwave-induced activation of the original Ullmann C-C coupling has not attracted attention. Therefore, to broaden the scope of heterogeneous metal-mediated reactions with microwave heating the Ullmann C-C coupling was investigated.

4.2 Microwave – copper interactions

To gain more insight into the influence of microwave irradiation on the reactivity of copper, the interaction of microwaves with copper-solvent mixtures, in the absence of other reagents, was investigated. In dimethylacetamide (DMA) the heating rates of copper samples of different sizes were compared and the temperature-time histories were recorded. The temperature-time histories demonstrated to be identical in all combinations (copper powder, copper-bronze and copper turnings) and power settings (50, 100, 200 and 500 W) tested. These results indicate that no selective heating of copper occurs.

In contrast to zinc and magnesium (see Chapters 3 and 2, respectively), irradiation of copper-solvent mixtures did not lead to electrical discharges. Absence of arcing can be rationalized by the high loss tangent of the solvent, see

Table 4.2, causing an efficient absorption of microwaves by the solvent. This high absorption shields the metal from the microwaves, preventing sufficient charge accumulation on the copper surface to facilitate dielectric breakdown of the medium. Also the higher electrical conductivity of copper (59.6 x 10^6 S/m) compared to magnesium (22.4 x 10^6 S/m) or zinc (16.9 x 10^6 S/m), facilitates the distribution of accumulated charges over the entire particle, limiting the electrical field strength between the particles. Therefore, electrical discharges are not induced by irradiating copper particles, of any size, in DMA.

X-ray photoelectron spectroscopy

To determine the composition of the copper surface after exposure to microwave irradiation, X-ray photoelectron spectroscopy (XPS) measurements were performed. The surface of the copper turnings exposed to the microwaves and conventional heating in the presence of only solvent was analyzed. During microwave irradiation of zinc-solvent mixtures and magnesium-solvent mixtures, zinc carbide and magnesium carbide species were observed throughout the surface, see sections 2.3 and 3.3. The carbide species were caused by electrical discharges. The binding energies of the copper 2p electrons are depicted in Figure 4.1. The XPS spectrum clearly indicates that only a trace amount of copper oxide is present on the surface.

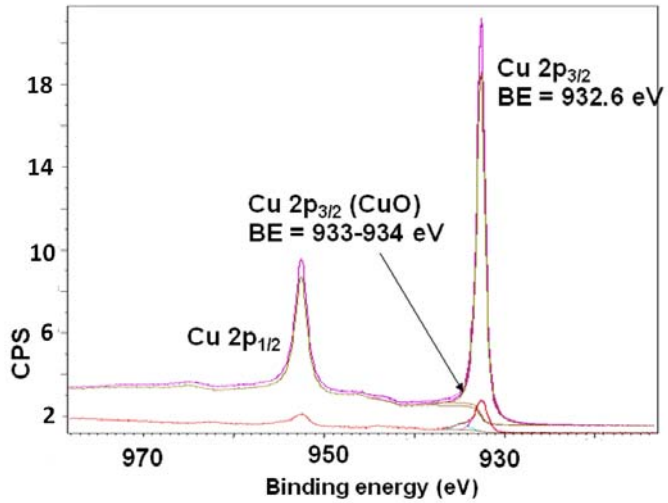

Figure 4.1: *Deconvoluted binding energies of the 2p electrons of copper on the surface exposed to microwave irradiation in the presence of solvent (DMA) only. (numbers in the spectrum stand for binding energies of the 2p electrons in copper).*

Copper carbide species would induce a shift of the binding energies to significantly lower values.[15,16] The binding energies of the 1s electrons of carbon on the copper surface are depicted in Figure 4.2. The results in Figure 4.2 also demonstrate that no copper carbide species are formed upon microwave irradiation.

Although no copper carbide species are formed in DMA, traces of carbon species were present on the copper surface, see Figure 4.2. Carbon mainly originates from chemisorption of residual solvent and CO_2 from air.

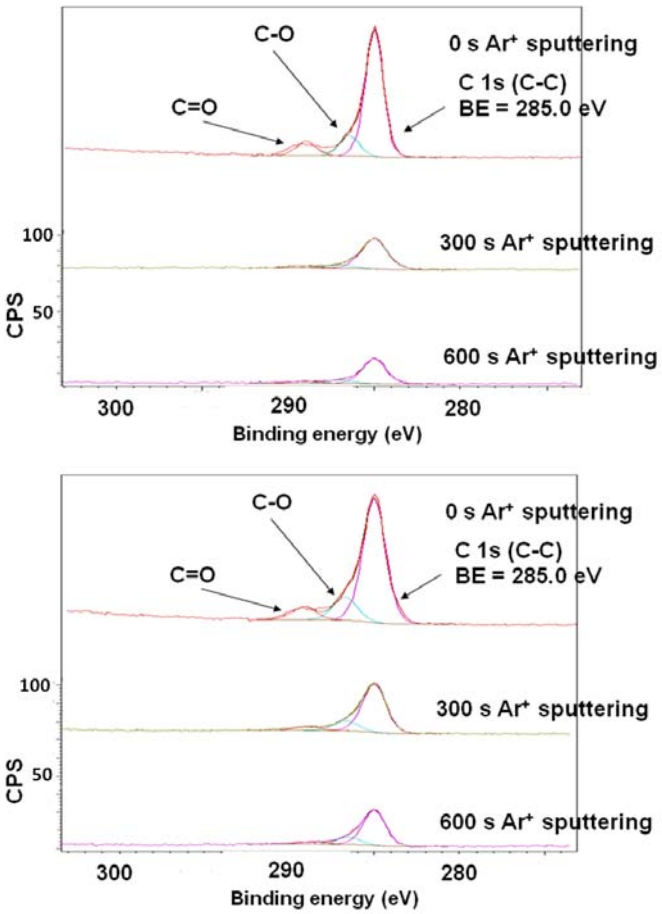

Figure 4.2: *Deconvoluted binding energies of the 1s electrons of the carbon species on the copper surface after heating in DMA. Top: conventional heating. Bottom: microwave heating.*

The absence of a shift of the carbon 1s electrons to lower values is indicative for carbon not being directly bound to a metal. The absence of a shift was also observed for copper turnings subjected to either microwave or conventional heating indicating that significant amounts of copper carbide species were not formed either.

Electrical discharges were not induced in copper-DMA mixtures, showing that significant amounts of the metal carbide species were not formed by direct metal-microwave interaction but instead by electrical discharges.

4.3 Optimization of the thermal Ullmann coupling

To get more insight into the effect of microwave irradiation on the Ullmann coupling, the reaction of 2-chloro-3-nitropyridine to 3,3′-dinitro-2,2′-bipyridine using copper-bronze was investigated, see Scheme 4.1.

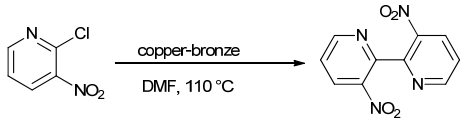

Scheme 4.1: *Ullmann coupling of 2-chloro-3-nitropyridine to 3,3′-dinitro-2,2′-bipyridine.*

Upon reduction 3,3′-dinitro-2,2′-bipyridine becomes a key building block for the construction of C_3-symmetrical discotic liquid crystals, see Figure 4.3.[17-20] These structures were studied elaborately to elucidate factors governing helical ordering above the molecular level. With achiral lipophilic tails two types of helical aggregates are formed place in apolar solvents like heptane.[21]

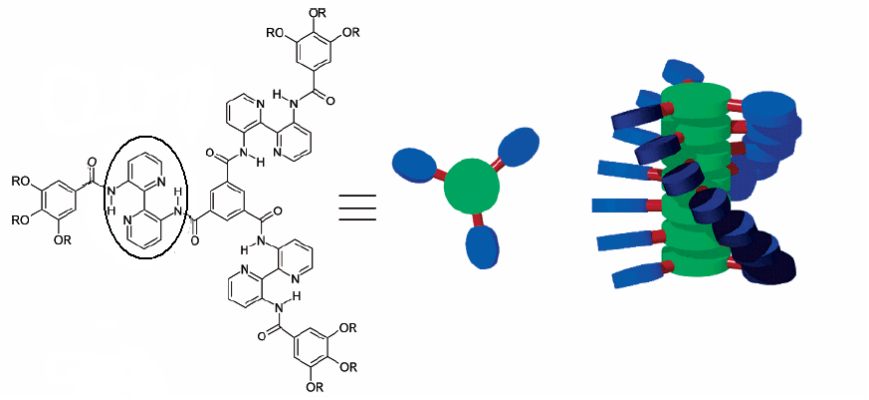

Figure 4.3: *C_3-symmetrical discotic liquid crystalline material. The circle showing the diamino-bipyridine moiety.*

With chiral tails, however, stacks of one helical sense are formed. These systems are subject to the sergeants and soldiers principle[20] and the majority rules effect.[17] Also helical aggregation was observed in water and other polar solvents when polar oligo-ethyleneoxide tails were present.[22]

Stoichiometry of copper in the Ullmann coupling

Commonly, the Ullmann coupling is performed with an excess of copper relative to the organic reactant.[23] The proposed reaction mechanisms for this type of coupling, such as with 2-chloro-3-nitropyridine, involve the oxidation of Cu(0) to Cu(I) with concomitant formation of a Cu-aryl species. This copper-aryl compound reacts either with a second 2-chloro-3-nitropyridine species to a Cu(III)-complex or this copper-aryl compound attacks a second 2-chloro-3-pyridine species in a nucleophilic aromatic substitution of the addition / elimination type in which copper remains in the Cu(I) state. In the mechanism in which a Cu(III)-complex is involved, this complex undergoes a reductive elimination of the bipyridine affording Cu(I) chloride. Both mechanisms dictate a 1:1 molar ratio of copper to 2-chloro-3-nitropyridine, see Scheme 4.2. Although Cu(III)-species have been proven to exist,[24,25] the copper-assisted nucleophilic substitution pathway is more likely.

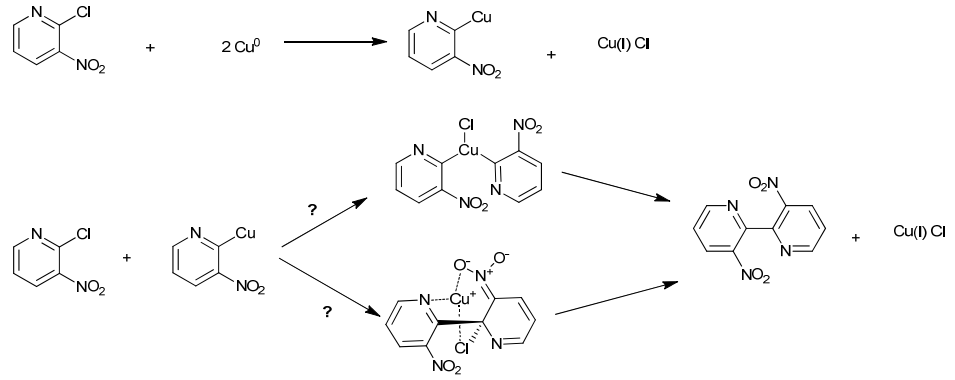

Scheme 4.2: *Proposed reaction mechanisms of the Ullmann coupling of 2-chloro-3-nitropyridine to 3,3′-dinitro-2,2′-bipyridine.[26] Top: Cu(III) complex. Bottom: nucleophilic aromatic substitution of the addition / elimination type. The complex is stabilized by the nitro-substituents.*

To investigate whether one of the mechanisms given in Scheme 4.2 is obeyed, the smallest amount of copper required for complete conversion in this Ullmann

coupling was determined. To that end, the reaction was carried out with 1.0, 0.85, 0.74 and 0.58 molar equivalents of copper relative to 2-chloro-3-nitropyridine. From Table 4.1 and Figure 4.4 it follows that at least 0.85 molar equivalents of copper were required.

Table 4.1: *Molar equivalents of copper in the conversion of 2-chloro-3-nitropyridine and calculation of the minimal molar equivalents of copper for the Ullmann coupling in DMF.*

Molar equivalent copper [a] (n)	Conversion [b] (X)	n / X
0.58	0.69	0.84
0.74	0.85	0.85
0.85	1.0	0.85
1.0	1.0	n/a

[a] based on copper amount in copper-bronze
[b] conversion based on 2-chloro-3-nitropyridine

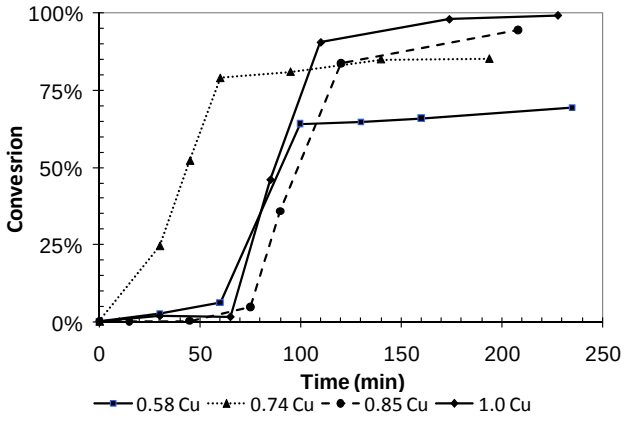

Figure 4.4: *Time-conversion histories of the Ullmann coupling of 2-chloro-3-nitropyridine with varying molar equivalents of copper.*

Regeneration of Cu^0 from Cu(I), see Scheme 4.3, formed during the synthesis rationalizes the discrepancy between the observed amount of copper for complete conversion and the amount expected from the reactions given in Scheme 4.2.

Complete conversion can be obtained with 0.85 molar equivalents of copper. Performing the reaction with this stoichiometry leads to remarkably diminished reaction rates above 80 % conversion.

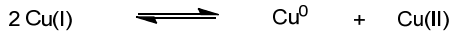

Scheme 4.3: *Dismutation of copper(I) into copper(II) and copper(0).*

This suggests that the regeneration of Cu(0) from Cu(I) is a slower process compared to the reaction steps involved in the actual Ullmann coupling. To simplify comparison of the different heating methods, a molar ratio of copper to 2-chloro-3-nitropyridine of 1:1 was selected, which causes the rates to remain high throughout the reactions.

Influence of the copper source on the Ullmann coupling

The reproducibility of the Ullmann coupling of 2-chloro-3-nitropyridine to 3,3'-dinitro-2,2'-bipyridine appeared to be an important issue to compare conventional heating with microwave heating reliably. Unfortunately, the irreproducibility of the initiation times when utilizing copper-bronze (90 % copper, 74 μm) made a reliable comparison of both heating methods impossible. Also the purity of the starting material and the water content of the solvent dramatically influenced the initiation time of the reaction. Therefore, these factors were kept constant, by using the same batch of starting materials. Nevertheless, the initiation time still varied considerably. To improve the reproducibility of the initiation times, copper-bronze was activated according to a reported procedure.[27] Also copper powder instead of copper-bronze was used to unravel the influence of the copper source on the course of the reaction, see Figure 4.5.

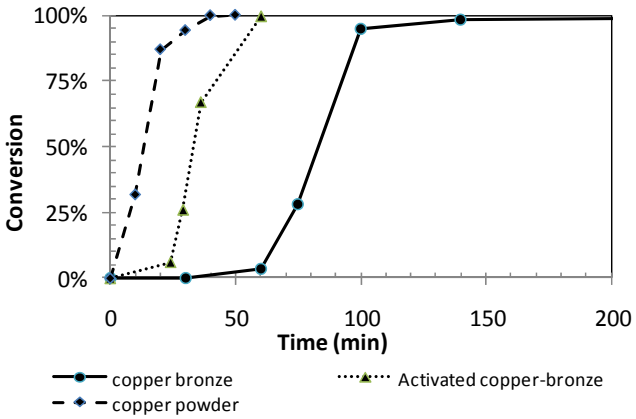

Figure 4.5: *Time-conversion histories of the Ullmann coupling with conventional heating using copper powder, activated, and non-activated copper-bronze.*

Without activation of copper-bronze the reaction showed a relatively long initiation time of 70 min. This initiation time varied significantly from experiment to experiment. The initiation time could be shortened to 20-30 min by activation of copper-bronze. Although the reproducibility of the initiation time improved with activated copper-bronze compared to unmodified copper-bronze, it still varied significantly. Each batch of activated copper-bronze showed differences in activity and hence in initiation times of the reaction.

Surprisingly, performing the reaction with non-treated copper powder (Cu 99 %, 45 micron, Acros Organics product nr. 190575000) in the Ullmann coupling resulted in an initiation time of less than 5 min. This period is remarkably shorter than the initiation time for both copper-bronze qualities used. Also the reproducibility of the initiation time while employing pure copper improved. The reaction rates after initiation were similar for all copper sources. So for the pure copper (45μm), reaction times to approach complete conversion were lower than those for copper-bronze. This improvement made comparison of the reaction rates with microwave and conventional heating more reliable.

Influence of solvent on the Ullmann coupling

The copper source influenced the initiation time of the Ullmann coupling. Another factor governing the initiation time, the reaction rate as well as the yield of the reaction was the solvent. Historically, the Ullmann coupling was performed neat at temperatures above 200 °C.[1,23] The introduction of DMF as solvent enabled the use of less harsh reaction conditions.[28] The amide functionality stabilizes the intermediate copper complexes formed by coordination of the carbonyl oxygen to the copper ion.[29] Stabilization of the copper complexes increases the thermodynamic driving force of their formation and as a consequence enables the use of lower temperatures for the Ullmann coupling. DMF has been employed widely as solvent for this type of reaction. Unfortunately, DMF decomposes into carbon monoxide and dimethylamine above 110 °C, thus limiting the applicable temperature range for this solvent. In addition, DMF and its decomposition products are extremely harmful, hampering application of this solvent in an industrial environment. The use of other, more stable and less harmful, solvents in the Ullmann coupling is less widespread.[7] Both DMA and *N*-methyl-2-pyrrolidone (NMP) share the amide functionality with DMF, see Table 4.2. However, contrary to DMF, the solvents DMA (bp = 165 °C) and NMP (bp = 206 °C) are stable at elevated temperatures and are less harmful. These features make DMA and NMP promising solvents as a substitute for DMF in the Ullmann coupling.

Rate-limiting step

Predicting the influence of the three solvents on the reactivity in the Ullmann coupling of 2-chloro-3-nitropyridine without knowing the rate-limiting step is challenging. Unfortunately, the rate-determining step of the Ullmann coupling of 2-chloro-3-nitropyridine is unknown. On the other hand, the rate-limiting steps in the Ullmann coupling of 2-chloropyridine and 2-chloro-3,5-dinitropyridine are known.

The Ullmann coupling of 2-chloropyridine requires very harsh reaction conditions, indicating that the first step, the formation of 2-cupro-pyridine, is rate determining.[28] Assuming that the first step in the Ullmann coupling of 2-chloro-3-nitropyridine, *i.e.* the formation of 2-cupro-3-nitropyridine, is the rate-determining step and that the transition state of this reaction step resembles the product, the thermodynamic driving force for the formation of the 2-cupro-3-nitropyridine will increase upon stabilization of the 2-cupro-3-nitropyridine. This stabilization would lead to an enhanced reaction rate.

The Ullmann coupling of 2-chloro-3,5-dinitropyridine does not proceed, however, and although 2-cupro-3,5-dinitropyridine is formed, the extreme stability of 2-cupro-3,5-dinitropyridine prevents further reaction, indicating that the second step is rate determining.[46] Assuming the second step of the Ullmann coupling of 2-chloro-3-nitropyridine, *i.e.* the reaction of 2-cupro-3-nitropyridine with 2-chloro-3-nitropyridine, is the rate-determining step, destabilization of 2-cupro-3-nitropyridine would lead to a higher reaction rate. The structural similarity between 2-chloro-3-nitropyridine and 2-chloro-3,5-dinitropyridine suggests that the second step may be the rate-limiting step in the former case.

Influence of the solvent on the stability of 2-cupro-3-nitropyridine

A selection of the characteristic properties of DMF, DMA and NMP is collected in Table 4.2. The surface tension of the three solvents is similar. The comparable values of the surface tension of DMF, DMA and NMP exclude any difference in reactivity in the solvents due to wetting effects of heterogeneous copper.[30]

All three solvents display similar dielectric constants and dipole moments, leading to similar electron densities on oxygen. However, the donor number (see Table 4.2) of DMF is slightly lower than that of DMA and NMP, suggesting that the bond strength of DMF with copper in the 2-cupro-3-nitropyridine is slightly lower compared to that of DMA and NMP. This lower bond strength leads to less stabilization of 2-cupro-3-nitropyridine in DMF as compared to DMA or NMP.

The difference in coordination strength to the copper ion is also governed by steric factors. As such, the three solvents surround uncoordinated copper ions in an octahedral shape, albeit that the surrounding by NMP and DMA is more sterically hindered causing a distortion of the octahedral symmetry.[31] This distortion does not occur in DMF. Although the coordination of DMF, NMP and DMA is similar in shape, the more sterically demanding DMA and NMP cause a longer copper-oxygen bond.[32] As a consequence, the bond strength between either DMA or NMP and the uncoordinated copper ions is smaller than that between DMF and the uncoordinated copper ions. However, in the intermediate copper complex only one solvent molecule can be accommodated. The smaller size of DMF as compared to DMA and NMP enables formation of a more dynamic, more reversible and, therefore, more reactive intermediate.

Table 4.2: *Selection of characteristic physical and chemical properties of the solvents investigated in the Ullmann coupling of 2-chloro-3-nitropyridine: dimethylformamide (DMF), dimethylacetamide (DMA) and N-methyl-2-pyrrolidone (NMP).*

	DMF 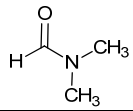	DMA 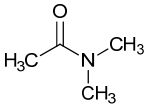	NMP 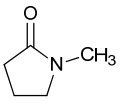
Bp (°C)	153 [a]	167	206
Dielectric constant [b]	37.6 [33]	38.3 [33]	32.6 [34]
Loss tangent [b]	0.161 [35]	0.218 [36]	-
Dipole moment	3.24 [34]	3.75 [34]	4.09 [34]
Donor number (DN) (kcal/mol) [c]	26.6 [32]	27.8 [32]	27.3 [37]
Coordination number [d]	6 [38]	6 [38]	6 [38]
Shape of copper-I coordination	octahedral [31]	distorted octahedral [31]	distorted octahedral [31]
Surface tension (10^{-3} N/m) [e]	36.76 [33,39]	32.34 [33]	40.25 [39]

[a] DMF decomposes at temperatures above 110 °C, [b] at 2 x 10^6 Hz, [c] A donor number is defined as the negative enthalpy value for the 1:1 adduct formation between a Lewis base and the standard Lewis acid $SbCl_5$ (antimony pentachloride), in dilute solution in the noncoordinating solvent 1,2-dichloroethane with a zero DN,[40,41] [d] Ligand coordination in pure solvent, [e] air / solvent at 20 °C.

DMF stabilizes 2-cupro-3-nitropyridine to a lesser extent than NMP or DMA and may lead to a more dynamic intermediate. Therefore, the reaction rate is expected to be higher in DMF, assuming the second step is rate-determining.

Comparing the reaction rates in DMF, DMA and NMP

Figure 4.6 (left) shows the results of the coupling performed in NMP. Performing the Ullmann coupling in NMP at the same temperature as the original coupling in DMF, *i.e.* 110 °C, demonstrated a decrease in reactivity. The decrease in reactivity indicates that indeed the second step in the Ullmann coupling of 2-chloro-3-nitropyridine is rate-determining. The reaction in NMP needed a longer initiation time compared to the reaction in DMF, 40 instead of 5 min, see Figures 4.6 and 4.5. Also the reaction rate in NMP after initiation was lower leading to complete conversion in 60 min. Increasing the temperature to 135 °C shortened the initiation time and accelerated the reaction, leading to complete conversion in 50 min. Further increasing the temperature to 160 °C only slightly influenced the initiation time and reaction rate. This observation indicates that the reaction rate becomes limited by mass transfer to the metal surface for temperatures equal or above 160 °C.

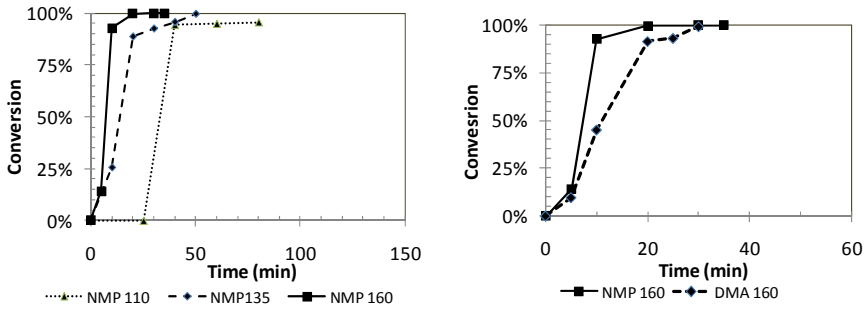

Figure 4.6: *Time-conversion histories of the Ullmann coupling of 2-chloro-3-nitropyridine and copper powder. Left: NMP at varying temperatures. Right: DMA and NMP at 160* °C.

To investigate the usefulness of DMA as a solvent for the Ullmann coupling, the reaction was also performed in this solvent. The time-conversion histories of the coupling performed in DMA at 160 °C were compared with those in NMP at the same temperature, see Figure 4.6 (right). The initiation time proved to be similar for both solvents. The reaction rate after initiation was somewhat lower for DMA as compared to NMP. This is in correspondence with the comparable properties of these solvents.

Switching the solvent has a profound effect on the Ullmann coupling of 2-chloro-3-nitropyridine. Not only a lower reaction rate at comparable temperatures, but also the isolated yield is lower for NMP than that for DMF, see Table 4.3. The yield decreased from 72 % to 61 % when changing the solvent from DMF to NMP

at 110 °C. Increasing the temperature to circumvent the lower reaction rate in NMP, decreased the yield further to 60 % at 135 °C and 41 % at 160 °C. The yield in DMA at 160 °C is higher than in NMP. The decrease of the yield at higher temperatures is mainly caused by tar formation resulting from the starting material and / or the product.

Surprisingly, the selectivity of the reaction is also influenced by the solvent. In DMF, solely the desired product was isolated. In NMP and DMA, besides the desired product, a byproduct was isolated.

Table 4.3: *Isolated yields, and byproduct formation of the Ullmann coupling of 2-chloro-3-nitropyridine with copper powder at complete conversion.*

Solvent	Temperature (°C)	Average yield (%)	Byproduct (mol%)
DMF	110	72	0
DMA	160	56	2.2
NMP	110	61	0.5
NMP	135	60	1.9
NMP	160	41	3.1

The precipitation procedure caused an enrichment of the desired product. Initially, the byproduct in the reaction mixture was assayed 2-3 times larger. The byproduct formation was thought to be governed by the water content of the solvent.

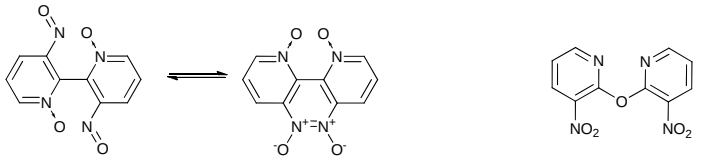

Scheme 4.4: *Presumed byproducts of the Ullmann coupling of 2-chloro-3-nitropyridine. Left: 3,3'-dinitroso-2,2'-bipyridine-1,1'-dioxide. Right: 2,2'-oxybis(3-nitropyridine).*

Initially, it was concluded that the byproduct was formed by a shift of the oxygen from the nitro group to the nitrogen of the pyridine ring in the biaryl-copper complex, yielding 3,3'-dinitroso-2,2'-bipyridine-1,1'-dioxide, see Scheme 4.4. Another option was the nucleophilic aromatic substitution of the addition / elimination type of the chloride in the 2-chloro-3-nitropyridine by water yielding 2-

hydroxy-3-nitropyridine. This alcohol and 2-chloro-3-nitropyridine can - in principle - undergo the subsequent copper(I)-catalyzed Ullmann ether[42,43] coupling yielding 2,2'-oxybis(3-nitropyridine), see Scheme 4.5. Further analysis of the byproduct by ^{1}H-NMR, ^{13}C-NMR and electron impact mass spectrometry did not elucidate the structure completely. The NMR-spectra point to a symmetrical molecule similar in structure to the desired product with chemical shifts that could correspond to both products. The main fragment observed (m/z 216) in the mass spectrum could correspond with the fragmentation of both possible byproduct molecules, *i.e.* the loss of a nitroso group from 3,3′-dinitroso-2,2′-bipyridine-1,1′-dioxide or the loss of a nitro group[44,45] from 2,2'-oxybis(3-nitropyridine).* The presence of an absorption peak in the wave-number region between 1290-1211 cm^{-1} in the ATR-IR spectrum indicated the presence of an ether functionality. Elemental analysis indicated that the deduced oxygen content was > 30 % while 26 % had been expected for the nitroso compound, confirming that the byproduct formed was indeed the ether.

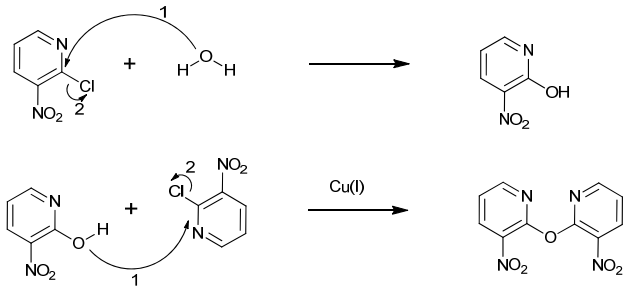

Scheme 4.5: *Mechanism of the byproduct formation during the Ullmann coupling of 2-chloro-3-nitropyridine (1 and 2 refer to the sequence of events).*

Deliberate contamination of the solvent with 1 molar equivalent of water relative to 2-chloro-3-nitropyridine increased the formation of 2-hydroxy-3-nitropyridine in DMA and NMP during the Ullmann ether coupling. Also the formation of some 3-nitropyridine by protonation of the copper-aryl complex by water was observed. Unexpectedly, addition of water to the reaction mixtures in DMF did not lead to the formation of the alcohol, but only resulted in a lower yield due to the formation of 3-nitropyridine. This observation indicates that the Ullmann coupling in DMF is not as sensitive to water as that performed in DMA or

* The molecular ion is not observed for the used ionization technique. This is also observed for 3,3′-dinitro-2,2′-bipyridine. The electron-poor aromatic ring does not allow the extraction of an electron leading to the molecular ion. The largest mass observed corresponds to the fragment formed by the loss of a nitro group (m/z = 200).

NMP. Addition of water to a solution of 2-chloro-3-nitropyridine in DMA or NMP at elevated temperature exclusively resulted in the formation of the alcohol. The regular Ullmann coupling initiates only after addition of copper powder and, thereafter, formation of the ether may occur. The formation of the ether lags behind the normal Ullmann coupling, indicating the necessity of copper(I) salts as catalyst for the ether synthesis.[42]

Nevertheless, DMA and NMP are useful solvents in the Ullmann coupling of 2-chloro-3-nitropyridine. However, the absence of byproduct formation in the presence of trace amounts of water, relatively high reaction rates and higher yield, make DMF a more suitable solvent for the Ullmann coupling of 2-chloro-3-nitropyridine.

4.4 *Microwave heating compared with conventional heating for the optimized Ullmann coupling*

The reproducible nature of the optimized Ullmann coupling of 2-chloro-3-nitropyridine made a reliable investigation of the influence of microwave irradiation on the reaction rate and yield feasible. The reaction was carried out under comparable experimental conditions, *i.e.* same flask, magnetic stirrer bar, solvent grade, starting materials grade, and temperature insert.

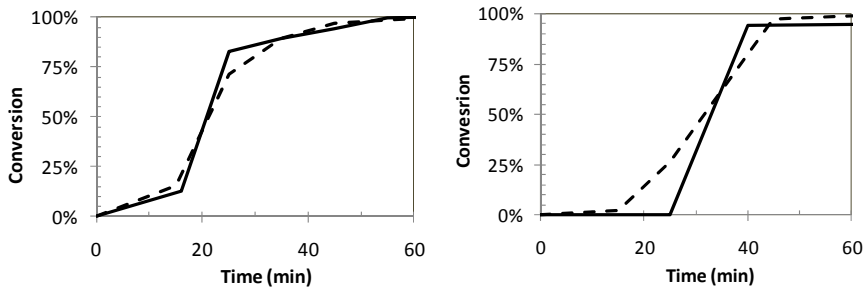

Figure 4.7: *Time-conversion histories of the Ullmann coupling of 2-chloro-3-nitropyridine and copper powder at 110 °C. Solid line: conventional heating; dashed line: microwave heating. Left: DMF; right: NMP.*

The time-conversion histories of the reactions performed were measured in DMF and NMP, see Figure 4.7. The initiation time and reaction rate in DMF are not significantly different for both heating methods. Also the yields of the microwave-heated reaction were similar to those of the conventionally heated experiments.

The lower rates of the Ullmann coupling in NMP at 110 °C, as compared to DMF, made an investigation of microwave activation for NMP more promising. Representative time-conversion histories in NMP also proved to be similar under both heating methods, see Figure 4.7 (right). Upon applying microwave irradiation the yield did not increase, compared to conventional heating. The selectivity of the reaction was identical for both heating methods.

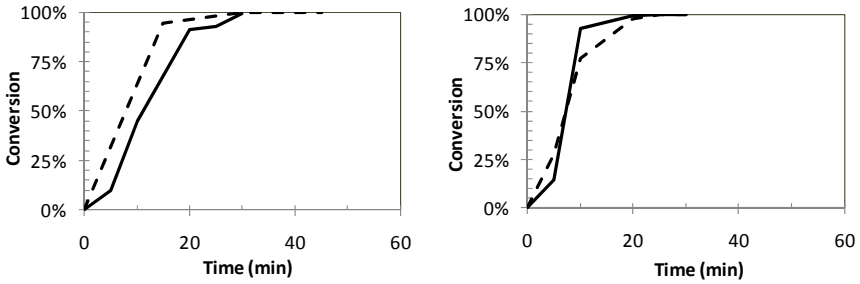

Figure 4.8: *Time-conversion histories of the Ullmann coupling of 2-chloro-3-nitropyridine and copper powder at 160 °C. Solid line: conventional heating; dashed line: microwave heating. Left DMA; right: NMP.*

Increasing the temperature to 160 °C for the reaction in NMP led to an increase of the reaction rate and a decrease of the initiation time for conventional heating. Under microwave heating comparable results were obtained, see Figure 4.8 (right). The yield remained similar and the selectivity did not improve.

To further expand the comparison of microwave heating and conventional heating, the Ullmann coupling in DMA at 160 °C was investigated. Again the time-conversion histories showed similar initiation times and reaction rates for both heating methods, see Figure 4.8 (left). The selectivity of the reaction was identical for both heating methods.

For all the investigated reaction conditions for the Ullmann coupling of 2-chloro-3-nitropyridine similar results were obtained for microwave with conventional heating. The high loss tangent of the solvents used, caused limited penetration depth, see section 1.2. The microwaves are absorbed in only a small part of the reaction mixture. So, only a small part of the reaction mixture is exposed to high-intensity microwave irradiation. Stirring distributes the heat, generated by the irradiation, in a similar manner as conventional heating. The absence of an effect of microwave irradiation and the non-appearance of arcing may suggest that the arcing seems to be vital in generating an effect of microwave heating in these types of systems.

4.5 Conclusion

The use of metals in combination with microwave heating may cause dramatic electrical discharges. These discharges were not observed for the reaction mixtures applied in the reductive Ullmann coupling of 2-chloro-3-nitropyridine.

The use of pure copper instead of copper-bronze as copper source for the Ullmann coupling of 2-chloro-3-nitropyridine led to an increase in reproducibility of the reaction and a higher yield of pure product.

Replacing the traditional solvent dimethylformamide (DMF) by dimethyl-acetamide (DMA) or *N*-methyl-2-pyrrolidone (NMP) for the coupling resulted in lower yields and required higher temperatures for similar reaction rates as found in DMF. Also the presence of water induced a loss of selectivity of the reaction. The formation of 2-hydroxy-3-nitropyridine and subsequent Ullmann ether coupling to 2,2'-oxybis(3-nitropyridine) were observed in DMA and NMP only. Lower reaction temperatures and higher yields make DMF the preferred solvent for the Ullmann coupling of 2-chloro-3-nitropyridine.

Comparison of microwave with conventional heating for the optimized Ullmann coupling of 2-chloro-3-nitropyridine, *i.e.* in DMF with copper powder at 110 °C, resulted in identical time-conversion histories and yields for both heating methods. Also in less ideal conditions, *i.e.* using copper-bronze powder, activated copper-bronze powder, copper powder and in DMA and NMP, the Ullmann coupling to 3,3'-dinitro-2,2'-bipyridine gave identical time-conversion histories and yields for both heating methods. The identical results under microwave and conventional heating are in contrast with the results obtained for the Grignard reaction (Chapter 2) and the Reformatsky reaction (Chapter 3). Our results for the Grignard reaction, the Reformatsky reaction and the copper-mediated Ullmann coupling point to arcing being essential for generating a microwave effect in these types of systems.

4.6 Experimental section

General:

See experimental section of Chapter 2. Dimethylacetamide (Across Organic, < 0,1 % H_2O), dimethylformamide (Biosolve extra dry, 0-0.01 % H_2O), *N*-methyl-2-pyrrolidone (Acros Organic, < 0.05 % H_2O), copper bronze (Sigma Aldrich, 90 % copper, 10 % tin, 200 Mesh., product nr: 520365), 2-chloro-3-nitropyrdine (Acros Organic, 99 %) and copper powder (Acros Organic, 45 micron, Cu 99 %) were used as received unless otherwise indicated.

Microwave heating:
See experimental section of Chapter 2.

Activation of the copper-bronze:[27] Copper-bronze (10 g) was treated with a solution of iodine (2 %) in acetone (100 mL) for 5-10 min. The solid was then collected in a Büchner funnel, removed from the filter, washed by stirring with 50 mL of concentrated HCl in acetone (1:1, v/v), and filtered again. The residue was washed with acetone (3 x 15 mL) and dried under vacuum to yield 8.2 g of activated copper-bronze.

3,3′-Dinitro-2,2′-bipyridine: 2-Chloro-3-nitropyridine (5.0 g, 31.5 mmol) was dissolved in DMF (25 mL). The reaction mixture was heated to 110 °C and freshly prepared activated copper bronze (2.2 g, 31.5 mol copper) was added (t=0). The reaction mixture was stirred until the reaction had gone to completion, after which the hot mixture was filtered over diatomaceous earth and washed with hot DMF. The conversion was determined with TLC (eluent: ethyl acetate:toluene 1:1) and ^{1}H-NMR. The filtrate was then poured into 5 % ammonia (95 mL) under vigorous stirring and the precipitate was collected and washed with 5 % ammonia until the filtrate was colorless. Overnight storage in a vacuum drying oven at 60 °C, afforded 3,3′-dinitro-2,2′-bipyridine as a yellow-brown solid (2.8 g, 72 %). ^{1}H-NMR (400 MHz, $(CD_3)_2CO$) δ: 8.91 (dd, *J*=1.44 and 4.76 Hz, 2H), 8.69 (dd, *J*=1.45 and 8.35 Hz, 2H) 7.87 (dd, *J*=4.77 and 8.35 Hz, 2H). Elemental analysis (%) for $C_{10}H_6N_4O_4$ (246.18): calcd C 48.79, H 2.46, N 22.76; found C 48.78, H 2.43, N 22.80. $(M\text{-}NO_2)^+$ m/z = 200. Melting point 208-212 °C.
The same procedure for non-activated copper-bronze (2.2 g, 31.5 mmol copper) or copper powder (2.0 g, 31.5 mmol) was used for the experiments indicated in the text. For the microwave-heated experiments, the oil-bath heating was substituted for temperature-controlled microwave heating (P_{max} = 200 W).

3,3′-Dinitro-2,2′-bipyridine and 2,2'-oxybis(3-nitropyridine): 2-Chloro-3-nitropyridine (5.0 g, 31.5 mmol) was dissolved in DMA (25 mL). The reaction mixture was heated by microwave irradiation (P_{max} =200 W) to 160 °C and copper (2.0 g, 31.5 mol) was added (t=0). The reaction mixture was heated and stirred until the reaction had gone to completion, after which the hot mixture was filtered over diatomaceous earth and washed with hot DMA. The conversion was determined with TLC and ^{1}H-NMR. The filtrate was then poured into 5 % ammonia (95 mL) under vigorous stirring and the precipitate was collected and washed with 5 % ammonia until the filtrate was colorless. Overnight storage in a vacuum drying oven at 60 °C, afforded a mixture of 3,3′-dinitro-2,2′-bipyridine (2.17 g, 52 %) and

2,2'-oxybis(3-nitropyridine) (0.09 g, 2.2 %) as a yellow-brown solid. Additional 2,2'-oxybis(3-nitropyridine) was obtained by extraction of the residual ammonia with ethyl acetate. The organic layer was evaporated and 2,2'-oxybis(3-nitropyridine) was purified using column chromatography (eluent: acetonitrile / chloroform 1:25 / v:v, R_f = 0.33). Yield 0.18 g (4.4 %). 2,2'-oxybis(3-nitropyridine): ^{1}H-NMR (400 MHz, $(CD_3)_2CO$) δ: 8.70 (dd, *J*=1.61 and 8.03, 2H), 8.58 (dd, *J*=1.60, 4.78 Hz, 2H), 7.64 (dd, *J*=4.81 and 8.03 Hz, 2H). Elemental analysis (%) for $C_{10}H_6N_4O_5$ (262.18): calcd: C 45.81, H 2.31; N 21.37; found: C 45.76, H 2.15, N 21.33. $(M\text{-}NO_2)^+$ m/z = 216. Melting point 165-166 °C.

The same procedure was used for NMP at the temperatures indicated in the text. For the conventionally heated experiments, temperature-controlled microwave heating (P_{max} = 200 W) was substituted by oil-bath heating.

4.7 References

(1) Ullmann, F.; Bielecki, J. *Ber. Dtsch. Chem. Ges.* **1901**, *34*, 2174–2185.
(2) Meyer, K. H. *Helv. Chim. Acta* **1940**, *23*, 93-100.
(3) Kornblum, N.; Kendall, D. L. *J. Am. Chem. Soc.* **1952**, *74*, 5782.
(4) Iqbal, K.; Wilson, R. C. *J. Chem. Soc. C* **1967**, 1690-1691.
(5) Bacon, R. G. R.; Hill, H. A. O. *Q. Rev. Chem. Soc.* **1965**, *19*, 95-96.
(6) Grigg, R.; Johnson, A. W.; Wasley, J. W. F. *J. Chem. Soc.* **1963**, 359-360.
(7) Hassan, J.; Sevignon, M.; Gozzi, C.; Schulz, E.; Lemaire, M. *Chem. Rev.* **2002**, *102*, 1359-1469.
(8) Lindlay, J.; Mason, T. J.; Lorimer, J. P. *Ultrasonics* **1987**, 45-48.
(9) Lipshutz, B. H.; Unger, J. B.; Taft, B. R. *Org. Lett.* **2007**, *9*, 1089-1092.
(10) Kidwai, M.; Mishra, N. K.; Bansal, V.; Kumar, A.; Mozumdar, S. *Tetrahedron Lett.* **2007**, *48*, 8883-8887.
(11) Veverkova, E.; Toma, S. *Chem. Pap.* **2008**, *62*, 334-338.
(12) Pellon, R. F.; Martin, A.; Docampo, M. L.; Mesa, M. *Synth. Commun.* **2006**, *36*, 1715-1719.
(13) Bagley, M. C.; Dix, M. C.; Fusillo, V. *Tetrahedron Lett.* **2009**, *50*, 3661-3664.
(14) Bagley, M. C.; Davis, T.; Dix, M. C.; Fusillo, V.; Pigeaux, M.; Rokicki, M. J.; Kipling, D. *J. Org. Chem.* **2009**, *74*, 8336-8342.
(15) Luthin, J.; Linsmeier, C. *Surf. Sci.* **2000**, *454*, 78-82.
(16) Moulder, J. F.; Stickle, W. F.; Stobol, P. E.; Bomben, K. D. *Handbook of X-ray Photoelectron Spectroscopy*; Perkin Elmer, Eden Prairie, **1992**.
(17) Van Gestel, J.; Palmans, A. R. A.; Titulaer, B.; Vekemans, J.; Meijer, E. W. *J. Am. Chem. Soc.* **2005**, *127*, 5490-5494.
(18) Van Gorp, J. J.; Vekemans, J.; Meijer, E. W. *J. Am. Chem. Soc.* **2002**, *124*, 14759-14769.
(19) Palmans, A. R. A.; Vekemans, J.; Hikmet, R. A.; Fischer, H.; Meijer, E. W. *Adv. Mater.* **1998**, *10*, 873-876.

(20) Palmans, A. R. A.; Vekemans, J.; Havinga, E. E.; Meijer, E. W. *Angew. Chem. Int. Ed.* **1997**, *36*, 2648-2651.
(21) Palmans, A. R. A.; Vekemans, J.; Fischer, H.; Hikmet, R. A.; Meijer, E. W. *Chem. Eur. J.* **1997**, *3*, 300-307.
(22) Brunsveld, L.; Zhang, H.; Glasbeek, M.; Vekemans, J.; Meijer, E. W. *J. Am. Chem. Soc.* **2000**, *122*, 6175-6182.
(23) Fuson, R. C.; Cleveland, A. E. *Org. Synth.* **1955**, *3*, 339.
(24) Bertz, S. H.; Cope, S.; Murphy, M.; Ogle, C. A.; Taylor, B. J. *J. Am. Chem. Soc.* **2007**, *129*, 7208-7209.
(25) Huffman, L. M.; Stahl, S. S. *J. Am. Chem. Soc.* **2008**, *130*, 9196-+.
(26) Cepanec, I. *Synthesis of Biaryls*; Elsevier Science & Technology Oxford, 2004.
(27) Kleiderer, E. C.; Adams, R. *J. Am. Chem. Soc.* **1933**, 4219-4225.
(28) Fanta, P. E. *Synthesis* **1974**, 9-21.
(29) Ozutsumi, K.; Ishiguro, S.; Ohtake, H. *Bull. Chem. Soc. Jpn.* **1988**, *61*, 945-951.
(30) Stepanek, F.; Marek, M.; Hanika, J.; Adler, P. M. *Catal. Today* **2001**, *66*, 249-254.
(31) Ishiguro, S.; Umebayashi, Y.; Fujii, K.; Kanzaki, R. *Pure Appl. Chem.* **2006**, *78*, 1595-1609.
(32) Fujii, K.; Endoh, T.; Yokoi, M.; Umebayashi, Y.; Ishiguro, S. I. *Thermochim. Acta* **2005**, *431*, 29-32.
(33) Wang, G. D.; Cole, R. B. *Org. Mass Spectrom.* **1994**, *29*, 419-427.
(34) Laurence, C.; Nicolet, P.; Dalati, M. T.; Abboud, J. L. M.; Notario, R. *J. Phys. Chem.* **1994**, *98*, 5807-5816.
(35) Kaval, N.; Bisztray, K.; Dehaen, W.; Kappe, C. O.; Van der Eycken, E. *Mol. Diversity* **2003**, *7*, 125-133.
(36) Patil, N. G., *Loss tangent data; Eindhoven University of Technology* **2009**.
(37) Varadarajan, T. K.; Ramakrishna, T. V.; Kalidas, C. *J. Chem. Eng. Data* **1998**, *43*, 527-531.
(38) Ohtaki, H. *Monatsh. Chem.* **2001**, *132*, 1237-1268.
(39) Kahl, H.; Wadewitz, T.; Winkelmann, J. *J. Chem. Eng. Data* **2003**, *48*, 580-586.
(40) Gutmann, V. *Z. Chem.* **1980**, *20*, 37-37.
(41) Gutmann, V. *Coord. Chem. Rev.* **1976**, *18*, 225-255.
(42) Monnier, F.; Taillefer, M. *Angew. Chem. Int. Ed.* **2009**, *48*, 6954-6971.
(43) Goldberg, I. *Ber. Dtsch. Chem. Ges.* **1906**, *39*, 1691-1692.
(44) Larkins, J. T.; Saalfeld, F. E.; Kaplan, L. *Org. Mass Spectrom.* **1969**, *2*, 213-214.
(45) Tyrkov, A. G.; Solov'ev, N. A.; Ladyzhnikova, T. D.; Altukhov, K. V. *Russ. J. Org. Chem.* **2004**, *40*, 1151-1155.
(46) Personal communication with J.A.J.M. Vekemans.

Intermezzo

Comparison of the reactivity of magnesium, zinc and copper under microwave irradiation

As shown in the previous chapters, the Grignard reagent formation (Chapter 2), the Reformatsky reaction (Chapter 3) and Ullmann coupling (Chapter 4) are very similar in the type of modification. These reactions utilize heterogeneous metals in their pure form, which are inserted in a carbon-halogen bond during the reaction, and the initiation time is variable. Although the reactions share striking similarities, the outcomes of microwave irradiation, on the other hand, do not.

These differences are expressed during investigation of the Reformatsky and Grignard reagent formation which, in contrast to the Ullmann coupling with copper(0), are influenced significantly by microwave irradiation. In both systems microwave heating leads to violent electrical discharges. These discharges were observed for turnings only while during irradiation of magnesium and zinc powder these discharges were not observed. The duration of the initiation period for the Reformatsky reaction is increased greatly, while this initiation time is decreased substantially for the Grignard reagent formation. To rationalize these observations a comparison of zinc and magnesium microwave interactions has been made.

Selective heating of the magnesium and zinc turnings does not occur. On the other hand, large magnesium objects, such as ribbons, display selective heating. The final reaction rate of the Grignard reagent formation is not influenced by microwave irradiation. Once the Reformatsky reaction is initiated, the reaction rate becomes higher than under conventional heating, leading to overall comparable yields.

In contrast to magnesium, zinc is not covered totally with an oxide layer. Arcing causes the dislodgement of molten metal from the surface. This metal solidifies into spheres with a clean (*i.e.* oxide-free) surface. The generation of zinc particles is much faster under comparable power / volume ratios compared to the generation of magnesium particles. This is due to the lower melting temperature of zinc. The oxide-free surface of zinc is similar in reactivity to that of the turnings, while the reactivity of the oxide-free surface of magnesium is considerably higher. In both systems metal carbides are formed during the electrical discharges. The

carbide formation can be competitive to the desired reaction pathway, depending on the reactivity of the substrate. Therefore, the reactivity of the magnesium during electrical discharges is increased dramatically while the reactivity of zinc is diminished. During these discharges the majority of zinc is dispersed as spheres. When initiation finally takes place an autocatalytic effect occurs. The zinc surface becomes more reactive in the presence of a Reformatsky reagent. The high fraction of small spherical zinc particles leads to a very high surface to volume ratio of zinc, leading to an increase in final reaction rate. The fast reaction after initiation combined with a lower arcing frequency suggests that arcing, or the zinc spheres produced by it, interferes with the normal reaction pathway for the Reformatsky reaction.

This interference is not observed for the Grignard reagent synthesis. The spheres are consumed immediately by a reactive halo-compound and after initiation the arcing diminishes greatly by the strong coupling of the formed salts with the microwaves. As a consequence, the influence of microwave irradiation on the final reaction rate is negligible.

Arcing is not observed for copper solvent mixtures. The total absence of arcing while irradiating copper-solvent mixtures is caused by the high dielectric constant and loss tangent of the used solvents, *i.e.* dimethylformamide (DMF), dimethylacetamide (DMA), *N*-methyl-2-pyrrolidone (NMP). This shields the copper from the microwaves, which are absorbed by these solvents. The high conductivity of copper distributes accumulated charges over the entire surface, thus limiting the electric field strength between particles upon microwave irradiation. The lack of electrical discharges leads to identical time-conversion histories under microwave irradiation and conventional heating, stressing the requirement of electrical discharges for generating an effect, either beneficial or detrimental, under microwave irradiation for these types of systems.

Chapter 5

Heterogeneous zirconium oxide-catalyzed amidations

Abstract

The influence of microwave irradiation on a freshly prepared zirconium-based heterogeneous catalyst for the amidation from a nitrile and an amine was determined. Microwave irradiation heats the catalyst very efficiently, leading to selective heating that enhances the catalytic activity, compared to conventional heating. This effect disappeared when $Zr(OH)_4$ was used instead of ZrO_2, indicating a microwave-induced shift in the hydrolysis equilibrium, i.e. the distribution of ZrO_2, $ZrO(OH)_2$ and $Zr(OH)_4$, of the zirconium-based catalyst. The catalyst efficiently catalyzes the amidation from valeronitrile with n-hexylamine with conventional and microwave heating. $Zr(OH)_4$ was also used for the polymerization of 6-aminocapronitrile in a sealed vessel with conventional and microwave heating. With both heating methods a relatively low molecular weight polymer with an M_n of 4000 g/mol was obtained, due to an equilibrium between oligomers and monomer governed by the presence of water and ammonia. This low molecular-weight polymer was subjected to a post-polymerization step under microwave irradiation, removing ammonia and / or water. The removal of ammonia alone had a modest effect, yielding a polymer with M_n of 6000 g/mol. The active removal of the water and ammonia by microwave irradiation shifts M_n to 10000 g/mol. To further increase the molecular weight the process pressure was lowered, thus facilitating the removal of the last traces of water. Unfortunately, the reduction of the process pressure to 5 kPa resulted in the generation of volatile ϵ-caprolactam at the applied temperature, dramatically decreasing the yield of the polymer and causing a drop in the molecular weight. However, a mild pressure of 50 kPa with an argon flow for the removal of water resulted in a high yield of polymer with M_n of 65000 g/mol which is substantially higher than achieved with conventional heating. The microwave-assisted polymerization of ϵ-caprolactam was efficiently catalyzed by the zirconia-based catalyst yielding a polymer with M_n of 8160 g/mol after 20 minutes.

5.1 Introduction

In the previous Chapters the interaction of microwave irradiation with metals (Chapter 2: magnesium, Chapter 3: zinc and Chapter 4: copper) in their metallic state was investigated. The impact of microwaves on the reactivity of these metals was completely different. As compared to conventional heating the application of microwave heating increased the reactivity of magnesium in the Grignard reagent formation. For copper in the Ullmann coupling there was no significant difference between both heating methods. For the reactivity of zinc in the Reformatsky reaction an even lower reactivity was observed for microwave heating than for conventional heating. Although the use of metals in their zero-valent state for synthetic purposes is wide-ranging, the oxidation state of metals used in synthetic organic chemistry is not limited to zero. Metal oxides are extensively used as heterogeneous catalyst carriers[1,2] and as heterogeneous catalysts themselves[3-5]. The activity of TiO_2 [6], amorphous SiO_2 / Al_2O_3 [7], Nb_2O_5 [8,9] and ZrO_2 [10] has been studied for a wide variety of reactions.

ZrO_2 was selected to investigate the influence of microwave irradiation on the catalytic activity of one of the metal oxides. Microwave irradiation is used frequently for the preparation of these metal oxide catalysts.[11-14] The use of microwave irradiation to activate a zirconium-based catalyst has been reported in a few articles.[15-17] Our work focused on the application of Zr-based catalysts for a novel route towards the production of nylon-6.[18,19]

Nylon-6, classical chemical route

Poly-ε-caprolactam (nylon-6) was invented by Paul Schlack at IG Farben[20] in 1938 and patented in 1943, and was first introduced in the market under the brand name Perlon.

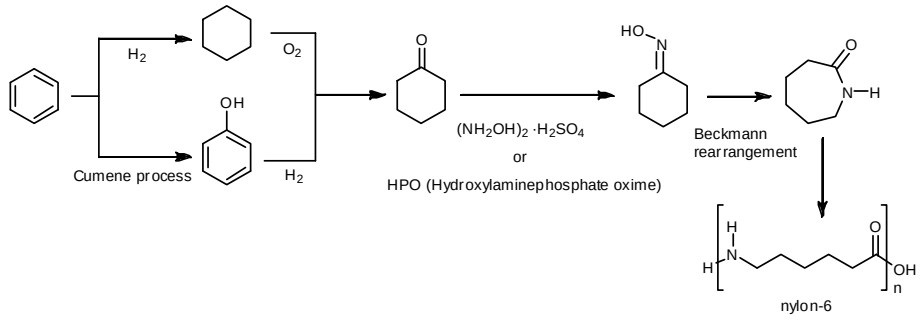

Scheme 5.1: *Commercial route to nylon-6 starting from benzene.*

Nylon-6 is a commodity polymeric material with an annual production of 670 x 10^6 kg in Western Europe alone.[21] This production scale makes a small reduction of

the production costs economically relevant. Nylon-6 is produced commercially by ring opening polymerization of ε-caprolactam, which in turn is produced industrially from benzene, see Scheme 5.1. This process has been studied intensively and has been optimized.[21]

Nylon-6, an alternative chemical route

One way of reducing the energy consumption as well as the overall production costs is short-cutting the chemical route by using an alternative starting material. A promising starting material is butadiene, which is industrially converted into 6-aminocapronitrile, see Scheme 5.2.[22]

The conversion of 6-aminocapronitrile into nylon-6 does not occur without the use of a catalyst. ZrO_2 is a very promising catalyst that is thought to catalyze the hydrolysis of the nitrile and subsequent the amidation.[18,19] TiO_2 has been reported as a good catalyst.[23] The influence of microwave heating on the ZrO_2-catalyzed production of nylon-6 from 6-aminocapronitrile is still unknown.

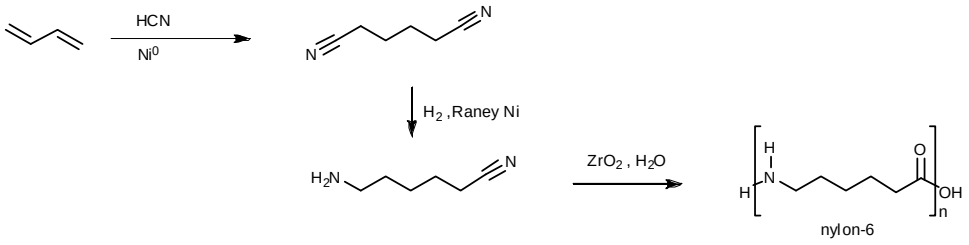

Scheme 5.2: *Alternative route to nylon-6 starting from butadiene.*

Selective heating of the catalyst may lead to higher activities and enhanced selectivities. Application of microwave irradiation in the production of polymers in the melt has high potential.[24,25] The increase in viscosity during the polymerization process may hamper the heat transfer from the reactor wall to the reaction medium. The volumetric heating nature of dielectric heating is not restricted by this limitation. Although the absence of heat-transfer limitations with this type of heating makes it a very suitable heating technique for viscous systems, the limited penetration depth does limit the overall reactor size, consequently making large-scale production less straightforward.

5.2 Microwave – zirconium oxide interactions

The way microwaves interact with a dispersed component in a reaction mixture, in this case the zirconium-based catalyst, may be significant with regard to the outcome of the reaction. The main reason that microwave irradiation may lead to different reaction rates, products and selectivities than with conventional heating is selective heating. This occurs when the preferred absorption of microwaves by the dispersed component leads to substantial temperature differences between the dispersed and continuous phase. To test whether selective heating occurs and could lead to an increase in catalyst activity, heating experiments of a representative reaction mixture under various power settings were performed, see Figure 5.1. For that purpose, the reaction mixture of a model reaction, *i.e.* the reaction of valeronitrile with *n*-hexylamine (see scheme 5.2 in section 5.3), was selected. The reaction mixtures were heated in the multimode microwave oven either in the presence or in the absence of $Zr(OH)_4$ catalyst. The heating rate of the reaction mixture with 50 W of microwave energy was similar in both cases. Upon increasing the power, the differences between the heating rates in the absence and presence of the catalyst were more pronounced. In the presence of $Zr(OH)_4$ heating is much more rapid than without $Zr(OH)_4$. The results collected in Figure 5.1 suggest that $Zr(OH)_4$ is selectively heated by microwave irradiation.

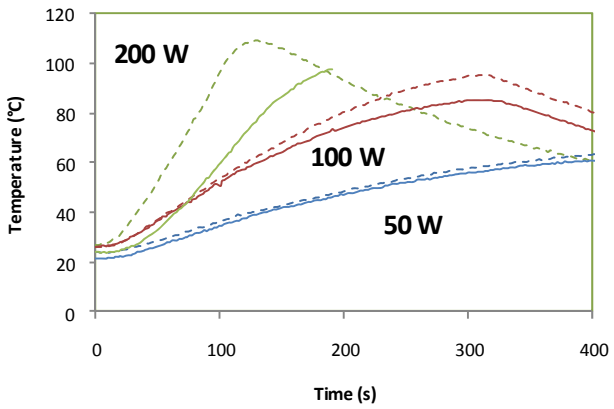

Figure 5.1: *Temperature-time histories of mixtures of valeronitrile (8.7 g), n-hexylamine (7.1 g) under different power settings. Solid lines: without $Zr(OH)_4$. Dashed lines: with $Zr(OH)_4$ (2 g).*

$Zr(OH)_4$ clearly facilitates heating under microwave irradiation. The high microwave absorption of the catalyst was supported by thermographic imaging*, see Figure 5.2. The catalyst was heated to more than 70 °C within one min of 100 W microwave irradiation. This selective heating may lead to a higher activity of the catalyst under microwave irradiation as compared to conventional heating.

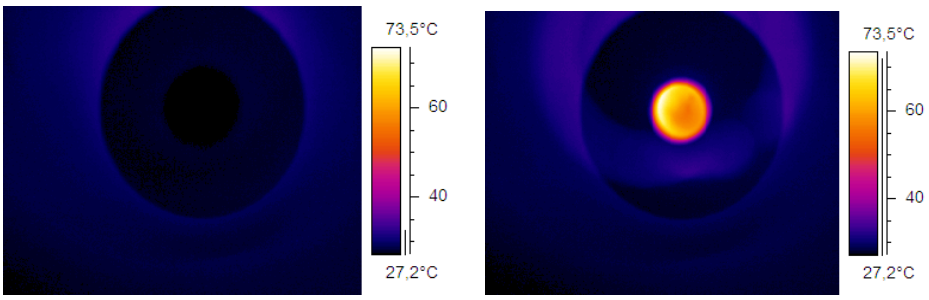

Figure 5.2: *Thermographic imaging of neat $Zr(OH)_4$ (2 g). Left: cold sample. Right: after 1 min of microwave irradiation (100 W).*

5.3 Determination of the zirconium-oxide activity under influence of microwave irradiation

The ZrO_2-catalyst was prepared by calcination of $Zr(OH)_4$. One batch was calcinated dynamically in a synthetic airstream for 3 hours at 300 °C. For a uniform calcination process a radially well-distributed air-flow through the packed bed of catalyst was necessary. A proper stacking of the catalyst particles was obtained by compressing $Zr(OH)_4$ in tablets and crushing these tablets. The crushed tablets were sieved on a 125-250 mesh sieve stack. Another batch was calcinated statically, *i.e.* was placed in an oven at a temperature of 300 °C. The specific areas of the catalyst particles were determined by BET-surface analysis, see Table 5.1 and experimental.

Table 5.1: *Surface area and porosity of the zirconium catalyst.*

	BET-surface area (m^2/g)	Pore diameter (nm)
Statically calcinated	155	5.3
Dynamically calcinated	226	4.1
Dynamically calcinated (lit.)[18,19,26]	288	4.9

* See section 2.1 for the setup used.

Figure 5.3: *Autoclaves used for the zirconium-catalyzed amidation. Left: the conventionally heated reactor, stainless steel.*[26] *Right: microwave reactor, modified PTFE / PEEK.*

The static calcination of $Zr(OH)_4$ resulted in a lower surface area and larger average pore diameter than achieved by the dynamic calcination of $Zr(OH)_4$. The dynamic procedure showed a similar area and pore size as the previously reported catalyst.[18,19] Preliminary experimental results for the ZrO_2-catalyzed amidation from valeronitrile with *n*-hexylamine pointed to similar activities and selectivities for the amide for both dynamic and static calcinated catalysts. This observation is rationalized by the dynamic nature of the ZrO_2-$Zr(OH)_4$-surface under the reaction conditions. At 230 °C in the presence of water, chemisorption of water on the ZrO_2-surface regenerates $Zr(OH)_4$. This reversible process leads to a modified surface. Gratifyingly, this modification causes similar catalyst surfaces for both grades of catalyst and, therefore, similar performances of the catalyst in terms of activity and selectivity. In all described reactions the dynamically calcinated grade of $Zr(OH)_4$ was utilized, unless indicated otherwise. The pore diameter was similar for both grades.

Table 5.2: *Dimensions of the autoclaves used for comparing microwave heating (MW) with conventional heating (CH).*

	Diameter (cm)	Height (cm)	Contact area (cm^2)	Volume (cm^3)	Filling ratio (%)
MW	3.5	9	9.6	86.6	27
CH	1.1	7.3	0.95	6.9	34

The reactions of valeronitrile with *n*-hexylamine and the polymerization of 6-aminocapronitrile were performed in the presence of water at 230 °C. During the reaction NH_3 is formed. In a closed system the pressure quickly rose to 3 MPa. These conditions require an autoclave setup. Figure 5.3 and Table 5.2 show the

relevant dimensions of the reaction vessels used during the experiments. Although the reactor for the conventionally heated experiment was much smaller, the loading of the reactors was chosen in such a way that the gas / liquid contact area and filling ratios were similar for both heating methods.

Amidation from valeronitrile and *n*-hexylamine

Initially, a model reaction, the amidation from valeronitrile and *n*-hexylamine, was investigated. Since in this reaction no polymerization can take place it is suitable to monitor the influence of microwave heating on the activity of the ZrO_2-catalyst towards amidation, see Scheme 5.3.

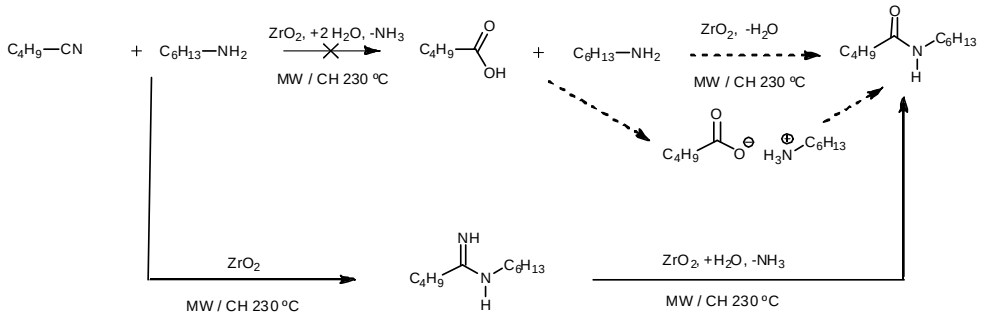

Scheme 5.3: *Model reaction for the determination of catalyst activity: The different pathways of the zirconia-catalyzed amidation from valeronitrile and n-hexylamine.*

To prove whether ZrO_2 actually catalyzes the hydrolysis of valeronitrile, the nitrile was first treated with both water and the catalyst at a temperature of 230 °C. Surprisingly, even after prolonged heating, valeronitrile did not show significant hydrolysis, indicating that the reaction pathway does not follow nitrile hydrolysis and subsequent amidation. However, the reaction to the desired amide proceeds in the presence of *n*-hexylamine. These observations strongly indicate that the pathway involves addition of *n*-hexylamine to valeronitrile yielding *N*-hexyl pentane-amidine followed by *in-situ* hydrolysis to *N*-hexyl pentanamide. During this transformation NH_3 is formed. The reaction was performed in a sealed vessel causing the pressure to build up. The ammonia formed can react in several ways, see Scheme 5.4. NH_3 acts as a nucleophile and reacts with valeronitrile yielding pentane-amidine which is hydrolyzed subsequently to the primary amide (pentanamide). Alternatively, pentanamide as well as *n*-hexylamine may also be formed by transamidation of *N*-hexyl pentanamide and ammonia. Removal of NH_3 will accelerate the reaction and will lead to a higher valeronitrile conversion, see

Figure 5.4. However, the cooling and heating cycles, required for removal of NH_3 safely, are undesirable. On larger scale this may be overcome by a proper equipment solution, see Meuldijk *et al.*[27]

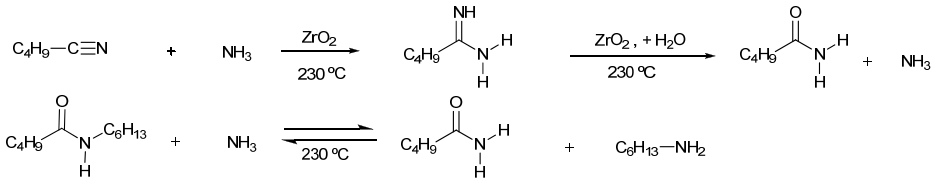

Scheme 5.4: *Reactions leading to pentanamide and n-hexylamine caused by the presence of ammonia in the reaction mixture.*

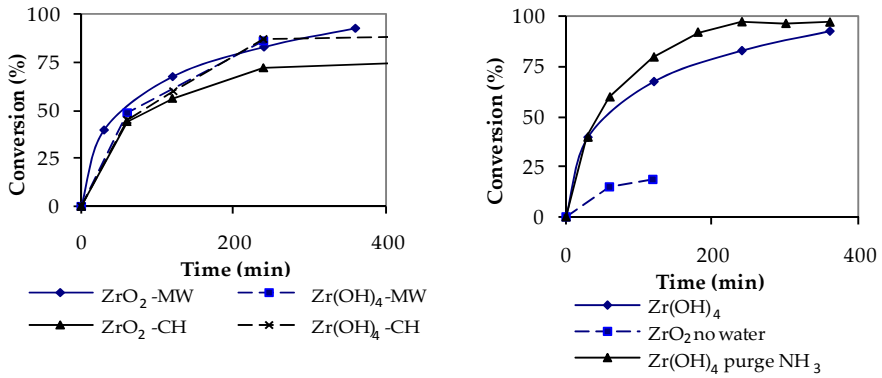

Figure 5.4: *Time-conversion histories of the amidation from valeronitrile and n-hexylamine. Left: various ZrO_2 and $Zr(OH)_4$ grades under microwave and conventional heating. Right: the influence of NH_3 removal on the conversion rate under microwave irradiation.*

The high temperature and the required presence of water in the reactor raised the question whether calcination of $Zr(OH)_4$ is essential before use. The dynamic character of the water chemisorption on the ZrO_2 surface at these temperatures could lead to an *in-situ* generation of $Zr(OH)_4$, thus blurring the distinction between both zirconium species in the reaction mixture. Therefore, determining which is actually the active catalytic species, ZrO_2 or $Zr(OH)_4$, is difficult. The dynamic nature of the zirconium species was tested by starting with $Zr(OH)_4$. The catalytic activity of this form of zirconium outperformed the non-hydrated ZrO_2-catalyst, making the cumbersome calcination step obsolete. The difference between

microwave and conventional heating using $Zr(OH)_4$ diminished, compared to using ZrO_2, indicating an influence of microwave irradiation on the conversion of ZrO_2 into $Zr(OH)_4$ and vice versa, see Scheme 5.5. This can be rationalized by the observation that both ZrO_2 and $Zr(OH)_4$ heat very rapidly with microwave irradiation. The enhanced reaction rate with ZrO_2 under microwave irradiation, compared to conventional heating, and the disappearance of this effect with $Zr(OH)_4$ as catalyst is a strong indication that $Zr(OH)_4$, or $ZrO(OH)_2$, are the active species. This is confirmed by the low conversion of the reaction when performed with ZrO_2 in the absence of additional water, see Figure 5.4 (right).

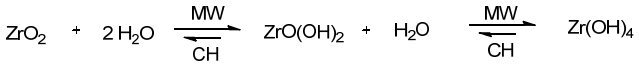

Scheme 5.5: *Influence of microwave irradiation on the reversible reaction between ZrO_2 and $Zr(OH)_4$.*

The synthesis of nylon-6 from 6-aminocapronitrile

Until now the influence of selective heating of the catalyst, presumably leading to a higher activity, was only observed for the model reaction. Therefore, the synthesis of nylon-6 starting from 6-aminocapronitrile was also performed using $Zr(OH)_4$ as catalyst, see Scheme 5.6.

The polymerization of 6-aminocapronitrile, pathway a, may proceed via numerous intermediates. A selection of anticipated pathways is illustrated in Scheme 5.6. One pathway to polymerization is the zirconia-catalyzed intramolecular addition of the amine to nitrile, generating azepan-2-imine, pathway b. The imine may then be hydrolyzed into ϵ-caprolactam which is able to polymerize under influence of heat and / or the zirconium-based catalyst. This polymerization route yields nylon-6 with terminal amide groups. These end groups can in principle be hydrolyzed into the corresponding carboxylic acid. The intermolecular addition to a nitrile can also occur, pathway c. Subsequent hydrolysis and repeated addition of another amine molecule would generate nylon-6 with terminal nitrile groups. In the previous section it was shown that hydrolysis of these nitrile end-groups to the primary amide or the carboxylic acid does not occur.

Polymer scission during the reaction may also occur either by reaction with ammonia, generated by the polymerization process, or by reaction with water, present for the hydrolysis, yielding oligomers with terminal primary amide or terminal carboxylic acids groups, respectively. These oligomers may further polycondensate into higher molecular weight nylon-6.

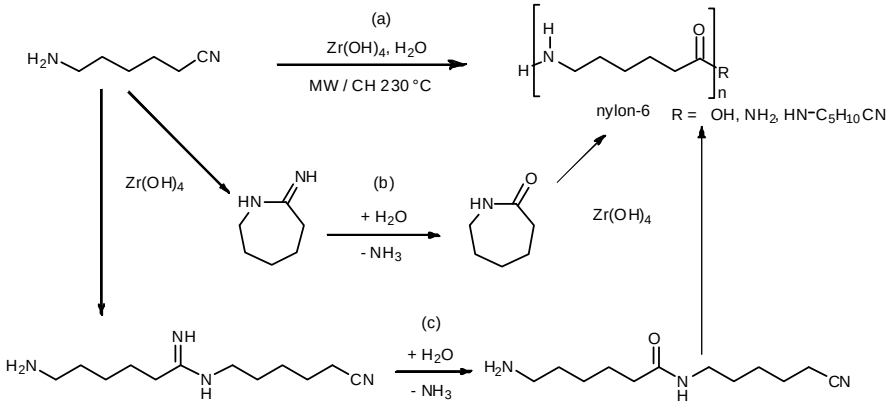

Scheme 5.6: *Postulated reaction pathways for the conversion of 6-aminocapronitrile into nylon-6.*

The produced polymer was analyzed using FT-IR. A typical adsorption band for a nitrile end group (2300 and 2200 cm^{-1}) was not present in the IR-spectra, clearly indicating an absence of nitrile end-groups in the solid. Maldi-TOF analysis of the oligomers showed that the end-groups are primary amide and carboxylic acid functions. These results suggest that the intermolecular addition, pathway c, plays a minor role in the polymerization process.

The results of the polymerization of 6-aminocapronitrile are collected in Table 5.3 for conventional heating and in Table 5.4 for microwave irradiation. The molecular weight distribution data of the nylon-6 samples, as given in the tables, indicate that the reaction goes to equilibrium within one hour, yielding a polymer with M_n (number average molecular weight) of 4000-4500 g/mol applying conventional heating. The polydispersity index (PDI, M_w / M_n) was in the range of 1.3-1.4 for all equilibrium situations. This is lower than the expected final PDI of 2 for polycondensation reactions.[28] This deviation is caused by the work-up procedure of the polymer. During the precipitation step, low molecular-weight fractions stay dissolved in the water, thus shifting M_n to higher values but having limited influence on the M_w. The reaction was performed in a closed vessel. This condition caused ammonia, which is generated during the reaction, and water, which is necessary for the hydrolysis of the amidine, to be trapped, resulting in an equilibrium between oligomers, 6-aminocaproamide and 6-aminocapronic acid. The removal of ammonia, see Table 5.3, shifts this equilibrium towards higher molecular-weight material, in analogy with the model reaction described in the previous section. Unfortunately, the effect of ammonia removal is modest, increasing M_n to 5000 g/mol after three consecutive heating and ammonia removal

steps. This modest effect and the cooling and heating cycles, that are required for safe NH_3 removal, are undesirable, limiting the value of this way of operation.

Table 5.3: *Molecular weight of nylon-6 samples prepared under conventional heating conditions. distribution (M_n: number average molecular weight, M_w: mass average molecular weight).*

Time (min)	M_n (g/mol)	M_w (g/mol)	M_w/M_n	Remark
60	4202	5163	1.266	Closed[a]
120	4315	5983	1.344	Closed[a]
240	4445	5172	1.388	Closed[a]
60 + 60	4276	5845	1.366	NH_3 purging after 1 h.[b]
60 + 60 + 60	4929	7083	1.437	NH_3 purging after 1 h.[b]

[a] Closed vessel, 230 °C, [b] Vessel was cooled to room temperature and opened for the removal of NH_3 after 1 h reaction. After NH_3 removal the reaction vessel was reclosed and heated again to the reaction temperature.

Table 5.4: *Molecular weight distribution of nylon-6 samples prepared under microwave heating conditions.*

Time (min)	M_n (g/mol)	M_w (g/mol)	M_w/M_n	Remark
30	3819	4365	1.41	Closed[a]
60	4600	6048	1.31	Closed[a]
240	3543	4855	1.37	Closed[a]
30 + 20[b]	6183	12360	1.99	Closed[a] + Reflux[c]
60 + 10[b]	6625	12455	1.88	Closed[a] + Reflux[c]
30 + 40[b]	10234	20061	1.96	Closed[a] + Dean Stark[d]
30 + 10[b]	7474	12727	1.70	Closed[a] + 5 kPa[e]
30 + 30[b]	7176	12181	1.70	Closed[a] + 5 kPa[e]
30 + 10[b]	7668	13303	1.73	Closed[a] + 50 kPa[f]
30 + 20[b]	6756	12016	1.77	Closed[a] + 50 kPa[f]
30 + 30[b]	6399	11505	1.80	Closed[a] + 50 kPa[f]
20	8163	14896	2.85	ε-Caprolactam[g]
30 + 40	65336	179288	2.74	Closed[a] + 50 kPa argon[h]

[a] Closed vessel and T = 230 °C, [b] second time corresponds to treatments listed under the remarks column, [c] Reflux condenser and T = 230 °C, [d] T = 230 °C with Dean-Stark apparatus for the removal of water, [e] Reduced pressure (5 kPa with airflow) 230 °C, [f] Reduced pressure (50 kPa with air-flow) T = 230 °C with Dean-Stark apparatus for the removal of water, [g] ε-Caprolactam and $Zr(OH)_4$ at 230 °C with Dean-Stark apparatus for the removal of water, [h] Reduced pressure (50 kPa with argon-flow) T = 230 °C with Dean-Stark apparatus for the removal of water.

Additionally, the polymerization reaction was performed applying microwave heating in a closed system. In the equilibrium situation the molecular weights were determined for both the conventionally heated experiments and the microwave-heated experiments, see Table 5.4.

A molecular weight of 15000 g/mol, required for commercial nylon-6, could be reached in a closed system with neither of both heating techniques. Therefore, a post-polymerization treatment under reflux was performed. The selective heating of the catalyst by microwave irradiation facilitated rapid heating of the reaction mixture. Also the heat transfer limitations, caused by the high viscosity of the reaction mixtures with high molecular weight, did not play a role with microwave heating. The post-polymerization under reflux increased M_n to 6000-6500 g/mol. The active removal of water by a Dean-Stark setup shifted this molecular weight to even higher values. After 40 min M_n of 10000 g/mol was obtained. This is relatively close to the desired commercial M_n. The polydispersity index of the polymer produced under atmospheric pressure was around 2, which is the equilibrium state at high conversion. The low molecular-weight fraction is small in these polymers, limiting the influence of the work-up procedure on the polydispersity index. To further improve the molecular weight, the reaction was performed under reduced pressure (5 kPa). An air-inlet capillary tube ensured a constant air-flow over the sample. This setup guaranteed a constant removal of generated moisture and ammonia from the upper layer of the sample. The active removal of the water and ammonia shifted the equilibrium to higher molecular weight. Unfortunately, the small quantity of ϵ-caprolactam, which is thermally generated from the polymer chain, was also removed under these conditions. ϵ-Caprolactam is mainly generated by "end-biting" of the polymer chain, see Scheme 5.7.[29,30] This end-biting step is normally in equilibrium, but the removal of the ϵ-caprolactam (bp = 160 °C at 5 kPa) shifts this equilibrium to the degraded side. This limited the molecular weight of the produced polymer and led to a sharp decrease in yield.

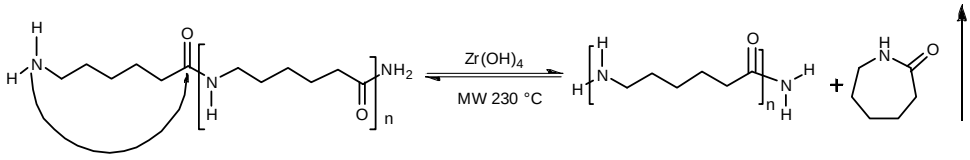

Scheme 5.7: *Degradation of nylon-6 by "end-biting" and subsequent removal of ϵ-caprolactam.*

To circumvent the removal of ϵ-caprolactam from the reaction mixture, a reduced pressure of 50 kPa was employed. At this pressure the reaction temperature was well below the boiling point of ϵ-caprolactam. A molecular

weight of 7600 g/mol was obtained in 10 min and this molecular weight steadily decreased in time. The air-flow over the sample removed the generated water but also introduced oxygen in the system. Oxygen led to degradation and discoloration of the molten polymer, limiting its molecular weight. Substituting the air-flow with an argon-flow at a reduced pressure of 50 kPa prevented oxidation. After 40 min of microwave treatment a molecular weight of 65000 g/mol was obtained. It was reported that this system gave a molecular weight of 10000 g/mol after 24 h at 250 °C under conventional heating.[18,26] The polydispersity index of the microwave-assisted polymer as well as of the reported polymer were in the range of 2.7 indicating a deviation from the normal reaction pathway of the polycondensation.

The microwave-assisted ring opening polymerization of caprolactone[31] and ϵ-caprolactam[32] without heterogeneous catalyst has been reported. The ring opening polymerization of caprolactam at 220 °C was reported not to proceed and an increase of process temperature to 250 °C with a nitrogen flow for more than 2 hours was necessary to yield a polymer with sufficient molecular weight (24 kg / mol).[32] Therefore, the polymerization of ϵ-caprolactam with $Zr(OH)_4$ as catalyst was studied. This resulted in a number-averaged molecular weight of 8160 in only 20 min, stressing the high catalytic activity of the zirconia-based catalyst.

5.4 Conclusion

Microwave irradiation selectively heated the zirconia-based catalyst. This selective heating caused a shift in the hydrolysis equilibrium of the catalyst governed by three equilibrated Zr-species, *i.e.* ZrO_2, $ZrO(OH)_2$ and $Zr(OH)_4$. The catalyst proved to be suitable for the amidation from valeronitrile and *n*-hexylamine, making it a promising catalyst for the polymerization of 6-aminocapronitrile into nylon-6.

The polymerization of 6-aminocapronitrile in a sealed vessel yielded limited molecular weight polymer with conventional heating as well as microwave heating. A post-polymerization step increased the molecular weight by the active removal of water. Microwave irradiation facilitated the active removal of water, increasing the molecular weight. The combination of the $Zr(OH)_4$ catalyst with microwave irradiation gave a very high molecular weight nylon-6 from 6-aminocapronitrile, or ϵ-caprolactam, in short reaction times and relatively mild conditions, making this a promising application.

5.5 Experimental section

General:

See experimental section of Chapter 2. High purity 6-aminocapronitrile was kindly supplied by BASF.

Microwave heating:
See experimental section of Chapter 2.

Thermographic imaging:
See experimental section of Chapter 2.

BET-analysis[33]:
The specific surface area (BET) and average pore size of the oxides were determined on a Micromeritics ASAP 2020 instrument. To desorb contaminating molecules (mainly water) from the catalyst surface, the catalyst was first pretreated at 200 °C under vacuum for over 2 h. For the determination of the BET-surface area, the value of p/p_0 in the range $0 < p/p_0 \leq 0.3$ was used. For the pore size measurements, the value of p/p_0 was further increased to 1 and subsequently reduced to 0.14.

Size-exclusion chromatography (SEC):
Size-exclusion chromatography (SEC) was measured on a system equipped with a Waters 1515 isocratic HPLC pump, a Waters 2414 refractive index detector (40 °C), a Waters 2707 autosampler, a PSS PFG guardcolumn followed by 2 PFG-linear-XL (7 μm, 8 x 300 mm) columns in series at 40 °C. Hexafluoroisopropanol (HFIP, Apollo Scientific Limited) with potassium trifluoroacetate (3 g/l) was used as eluent at a flow rate of 0.8 $mL.min^{-1}$. The molecular weights were calculated against polymethyl methacrylate standards (Polymer Laboratories, M_P = 580 Da up to $M_P = 7.1*10^6$ Da).

Calcination of $Zr(OH)_4$: Zirconia was prepared from a commercially available precursor (MEL XZ01247 / 01) donated by Mel Chemicals (Manchester, UK). Dynamic calcination: to guarantee a uniform air-flow through the packed bed of catalyst during calcination, needed for an uniform calcination process, $Zr(OH)_4$ was compressed in tablets, crushed in a mortar and sieved on a 125-250 mesh sieve stack. The sieved $Zr(OH)_4$ was calcinated in a synthetic air stream (80 % N_2 and 20 % O_2) for 6 hours at 300 °C. Static calcination: $Zr(OH)_4$ was placed in an oven of 300 °C for 6 hours.

Amidation from valeronitrile and *n*-hexylamine with conventional heating: Valeronitrile (0.87 g, 8.6 mmol), *n*-hexylamine (0.71 g, 8.6 mmol), water (0.31 g, 17.2 mmol) and $Zr(OH)_4$ (0.4 g, 2.5 mmol) were introduced in a stainless-steel reactor that contained a glass insert (these autoclaves were home made at the Eindhoven University of Technology). The vessel was purged with argon for 10 min before

sealing. The reaction mixtures were stirred with a magnetic stirring bar. The vessel was heated with a heating mantle to 230 °C for the mentioned time. The whole reaction mixture was cooled down and the autoclave was opened. A small aliquot was dissolved in $CDCl_3$ and filtered. The conversion was determined by ^{1}H-NMR and GC / MS. *N*-hexylpentanamide**:** ^{1}H-NMR (400 MHz, $CDCl_3$) δ: 5.68 (br s, 1H), 3.20 (q, 2H), 2.21 (t, 2H), 1.58 (m, 2H), 1.46 (m, 2H); 1.26 (m, 8H), 0.86 (m, 6H); GC / MS: r.t. 7.0 min., m/z: 185.2. Maximum yield = 1.51 g (95 %).

Amidation from valeronitrile and *n*-hexylamine with microwave irradiation: Valeronitrile (8.7 g, 86 mmol), *n*-hexylamine (7.1 g, 86 mmol), water (3.1 g, 172 mmol) and $Zr(OH)_4$ (4 g, 25 mmol) were introduced in a modified PTFE / PEEK microwave reactor (Milestone s.r.l., MedCHEM Kit, Reactor 45111T). The vessel was purged with argon for 10 min before sealing. The reaction mixtures were stirred with a magnetic stirring bar. The vessel was heated by microwave irradiation (maximum power = 300 W) to 230 °C for the time mentioned. The reaction mixture was cooled down to room temperature and the autoclave was opened. A small aliquot was dissolved in $CDCl_3$ and filtered. The conversion was determined by ^{1}H-NMR and GC / MS. *N*-hexylpentanamide**:** ^{1}H-NMR (400 MHz, $CDCl_3$) δ: 5.68 (br s, 1H), 3.20 (q, 2H), 2.21 (t, 2H), 1.58 (m, 2H), 1.46 (m, 2H); 1.26 (m, 8H), 0.86 (m, 6H); GC/MS: r.t. 7.0 min., m/z: 185.2. Maximum yield = 15.2 g (97 %).

Polymerization of 6-aminocapronitrile with microwave irradiation: 6-Amino-capronitrile (9.0 g, 80 mmol), water (2.9 g, 160 mmol) and $Zr(OH)_4$ (4.0 g, 25.3 mmol) were introduced in a modified PTFE / PEEK microwave reactor (Milestone s.r.l., MedCHEM Kit, Reactor 45111T). The vessel was purged with argon for 10 min before sealing. The reaction mixtures were stirred with a magnetic stirring bar. The vessel was heated by microwave irradiation (maximum power = 300 W) to 230 °C for the mentioned time. The complete reaction mixture was cooled down to room temperature and the autoclave was opened. Either a small aliquot was taken and the vessel was resealed or the complete reaction mixture was subjected to the work-up procedure. As the reactor setup did not allow the polymer-catalyst separation in the melt, the separation was achieved by first dissolving the polymeric product in formic acid. After removal of the zirconia catalyst by centrifugation for 30 min at 4000 rpm and subsequent decantation, the polymer was precipitated by pouring into water and separated from the liquid phase by centrifugation for 30 min at 4000 rpm and subsequent decantation. The polymer was redispersed in ethanol and separated from the liquid phase by centrifugation for 30 min at 4000 rpm and subsequent decantation. The polymer was dried in a

vacuum-oven at 50 °C for 24 h. This method resulted in the loss of the low molecular weight fraction of the product (mainly ϵ-caprolactam: ^{1}H-NMR (400 MHz, $CDCl_3$) δ: 6.71 (br s, 1H), 3.71 (q, 2H), 2.43 (t, 2H), 1.65 (m, 6H), mp = 64-66 °C, literature 66-68 °C. The molecular weight distribution of the polymer was analyzed with size-exclusion chromatography. Yield: 80 %.

Post-polymerization treatment: A three-neck 50 mL flask was charged with 10 g of crude product of the sealed-vessel polymerization (*i.e.* not subjected to the precipitation procedure). A temperature probe was inserted and an air-inlet (or argon-inlet) tube was connected to the neck of the flask. The air-inlet (or argon-inlet) tube was connected to a capillary tube. The capillary tube ensured a constant air-flow (or argon-flow). The flask was held at a constant pressure of 5 kPa (or 50 kPa) by an oil pump connected to the other neck**.** A Dean-Stark apparatus was connected to the flask and the reaction mixture was heated to 230 °C by temperature-controlled microwave irradiation (P_{max}= 350 W). The temperature was maintained for the described times by microwave irradiation (P_{max} = 200 W). The complete reaction mixture was subjected to the work-up procedure. The separation was achieved by first dissolving the polymeric product in formic acid. After removal of the zirconia-catalyst by centrifugation for 30 min at 4000 rpm and subsequent decantation, the polymer was precipitated by pouring into water and separated from the liquid phase by centrifugation for 30 min at 4000 rpm and subsequent decantation. The polymer was redispersed in ethanol and separated from the liquid phase by centrifugation for 30 min at 4000 rpm and subsequent decantation. The polymer was dried in a vacuum-oven at 50 °C for 24 h. This method resulted in the loss of the low molecular-weight fraction of the product (mainly ϵ-caprolactam: ^{1}H-NMR (400 MHz, $CDCl_3$) δ: 6.71 (br s, 1H), 3.71 (q, 2H), 2.43 (t, 2H), 1.65 (m, 6H), mp = 64-66 °C, literature 66-68 °C). The molecular-weight distribution of the polymer was analyzed with size-exclusion chromatography. Yield: 85 % (100 kPa), 87 % (50 kPa, argon), 50 % (50 kPa, air), 32 % (5kPa, air).

Polymerization of 6-aminocapronitrile with conventional heating: 6-Amino-capronitrile (0.90 g, 8.0 mmol), water (0.29 g, 16.0 mmol) and $Zr(OH)_4$ (0.40 g, 2.53 mmol) were introduced in a stainless-steel reactor that contained a glass insert (these autoclaves were home-made at the Eindhoven University of Technology). The same procedure was used as described above, substituting microwave heating by a heating mantle. The molecular weight distribution of the polymer was analyzed using size-exclusion chromatography.

5.6 References

(1) Tada, M.; Iwasawa, Y. *Chem. Commun.* **2006**, 2833-2844.

(2) Lambert, J. F.; Che, M. *J. Mol. Catal. A: Chem.* **2000**, *162*, 5-18.

(3) Shiju, N. R.; Guliants, V. V. *Appl. Catal., A* **2009**, *356*, 1-17.

(4) Zabeti, M.; Daud, W.; Aroua, M. K. *Fuel Process. Technol.* **2009**, *90*, 770-777.

(5) Helwani, Z.; Othman, M. R.; Aziz, N.; Kim, J.; Fernando, W. J. N. *Appl. Catal., A* **2009**, *363*, 1-10.

(6) Reddy, B. M.; Khan, A. *Catal. Rev. Sci. Eng.* **2005**, *47*, 257-296.

(7) Cowley, M.; de Klerk, A.; Nel, R. J. J. *Ind. Eng. Chem.* **2005**, *44*, 5535-5541.

(8) Aranda, D. A. G.; Goncalves, J. D.; Peres, J. S.; Ramos, A. L. D.; de Melo, C. A. R.; Antunes, O. A. C.; Furtado, N. C.; Taft, C. A. *J. Phys. Org. Chem.* **2009**, *22*, 709-716.

(9) Jasik, A.; Wojcieszak, R.; Monteverdi, S.; Ziolek, M.; Bettahar, M. M. *J. Mol. Catal. A: Chem.* **2005**, *242*, 81-90.

(10) Han, C.; Lee, J. P.; Lobkovsky, E.; Porco, J. A. *JACS* **2005**, *127*, 10039-10044.

(11) Zhou, X.; Zhang, C.; Li, Y.; Zhao, Q.; Jiang, T.; Yin, H. *J. Chin. Ceram. Soc.* **2009**, *37*, 1032-1037.

(12) Yang, Z. Q.; Mao, D. S.; Zhu, H. L.; Lu, G. Z. *Chin. J. Inorg. Chem.* **2009**, *25*, 812-817.

(13) Hembram, K. P. S. S.; Rao, G. M. *J. Nanosci. Nanotechnol.* **2008**, *8*, 4159-4162.

(14) Strizhak, P. E.; Tripol'Skii, A. I.; Gurnik, T. N.; Tuzikov, F. V.; Moroz, E. M.; Konstantinova, T. E.; Tuzikova, N. A.; Kol'Ko, V. P.; Danilenko, I. A.; Gorban, O. A. *Theor. Exp. Chem.* **2008**, *44*, 144-149.

(15) Bora, U.; Saikia, A.; Boruah, R. C. *Indian J. Chem., Sect B* **2005**, *44*, 2523-2526.

(16) Gajare, A. S.; Sabde, D. P.; Shingare, M. S.; Wakharkar, R. D. *Synth. Commun.* **2002**, *32*, 1549-1555.

(17) Gronnow, M. J.; Macquarrie, D. J.; Clark, J. H.; Ravenscroft, P. *J. Mol. Catal. A: Chem.* **2005**, *231*, 47-51.

(18) Van Dijk, A. J. M.; Duchateau, R.; Hensen, E. J. M.; Meuldijk, J.; Koning, C. E. *Chem.-Eur. J.* **2007**, *13*, 7673-7681.

(19) Van Dijk, A. J. M.; Heyligen, T.; Duchateau, R.; Meuldijk, J.; Koning, C. E. *Chem.-Eur. J.* **2007**, *13*, 7664-7672.

(20) Schlack, P., patent number CA 414365, **1942.**

(21) Kohan, M. I.; Mestemacher, S. A.; Pagilagan, R. U.; Redmond, K. *Ullmann's Encyclopedia of Industrial Chemistry: Polyamides*, **2003**.

(22) Achhammer, G.; Bassler, P.; Fischer, R.; Fuchs, E.; Luyken, H.; Schnurr, W.; Voit, G.; Hilprecht, L.; Scnurr, W.; Aharmay, G.; Basler, P.; Phischer, R., patent number WO9723454-A, **1997**.

(23) Mohrschladt, R.; Winterling, H.; Krauss, D. patent number WO200148053-A, **2001**.
(24) Bogdal, D.; Penczek, P.; Pielichowski, J.; Prociak, A. *Adv. Polym. Sci.* **2003**, *163*, 193-263.
(25) Zhang, C.; Liao, L. Q.; Gong, S. Q. S. *Green Chem.* **2007**, *9*, 303-314.
(26) Van Dijk, A. J. M., Thesis, Eindhoven University of Technology, **2006**.
(27) Meuldijk, J.; Van Dijk, A. J. M.; Duchateau, R.; Koning, C. E. *Macromol. Symp.* **2007**, 164-173.
(28) Flory, P. J. *Principles of polymer chemistry*; Cornell University Press, Ithaca, NY **1953**.
(29) Davis, R. D.; Gilman, J. W.; VanderHart, D. L. *Polym. Degrad. Stab.* **2003**, *79*, 111-121.
(30) Levchik, S. V.; Weil, E. D.; Lewin, M. *Polym. Int.* **1999**, *48*, 532-557.
(31) Liao, L. Q.; Liu, L. J.; Zhang, C.; He, F.; Zhuo, R. X. *J. Appl. Polym. Sci.* **2003**, *90*, 2657-2664.
(32) Fang, X. M.; Simone, C. D.; Vaccaro, E.; Huang, S. J.; Scola, D. A. *J. Polym. Sci., Part A: Polym. Chem.* **2002**, *40*, 2264-2275.
(33) Brunner, S.; Emmet, P. H.; Teller, E. *J. Am. Chem. Soc.* **1938**, *60*, 309.

Chapter 6

Comparison of conventionally and microwave-heated drying of non-natural amino acids

Abstract

The drying behavior of (S)-N-acetylindoline-2-carboxylic acid, precipitated and non-precipitated, and N-acetyl-(S)-phenylalanine, has been determined in a straightforward drying setup. The method of supplying energy to the system has a profound influence on the drying rate and on the internal temperature of the samples during drying. The drying time of (S)-N-acetylindoline-2-carboxylic acid with the low moisture content (5 wt%) can be reduced from 40 min to 10 min using microwave irradiation instead of conventional heating, while keeping the sample temperature under 35 °C. N-Acetyl-(S)-phenylalanine with a higher moisture content (22 wt%) demonstrated a decrease in drying time from 100 min to 40 min upon applying microwave irradiation, while the sample temperature remained below 45 °C. At higher microwave powers, 150 W instead of 100 W, the temperature of the sample increased to 60 °C, presumably due to a higher loss tangent, and a drying time of 25 min was achieved. A reduction in drying time of the precipitated (S)-N-acetylindoline-2-carboxylic acid (17 wt% moisture) from 70 min to 35 min was demonstrated for drying at 150 W of microwave irradiation instead of using a water bath of 70 °C. The sample temperature increased to 60 °C under microwave irradiation compared to 48 °C with conventional heating. To achieve similar drying times as under microwave irradiation for the three examples, extremely high energy inputs should be applied with conventional heating, resulting in extremely high temperature differences between the heating source and the sample. The results indicate that microwave irradiation is particularly useful for drying of thermally unstable materials in short periods of time.

6.1 Introduction

In Chapter 5 it was shown that microwave irradiation, in combination with a zirconia-based catalyst, has a profound influence on the production of nylon-6 from 6-aminocapronitrile. In particular, the active removal of water, which shifts the molecular weight of this polycondensation to higher values, was influenced beneficially by microwave irradiation. Another process where the active removal of water plays a vital role is drying.

Thermal drying converts a solid, semisolid, or liquid feedstock into a solid product by evaporation of the liquid into the vapor phase via application of heat.[1] Drying is one of the oldest and most common unit operations in chemical engineering and is an essential procedure for purifying and isolating products.[2] Drying is one of the highest energy consuming and most expensive processes in the pharmaceutical industry.

Microwave irradiation is an established heating technique in the drying of food,[3-7,] chemicals,[8,9] agricultural products,[10] polymers,[11] ceramics,[12] pulp and paper,[13] textiles,[14] in mineral processing[15] as well as in wood processing industries.[16] The application in the pharmaceutical industry is still limited. Drying of pharmaceutical powders with microwave heating (MW) has been shown to increase drying rates and product stabilities during the drying process.[17] Field inhomogeneity of domestic microwave ovens culminating in uneven heating rates, dictate the use of dedicated equipment for microwave processing.[18]

The drying curve

Drying can be accomplished in numerous ways which can be divided according to several criteria[1], see Table 6.1. One method is batch-wise vacuum drying, with a stationary sample heated by conduction. During this drying process three distinct drying stages can be distinguished, see Figure 6.1.[19]

At the start of the drying process the sample is at room temperature. The energy that is supplied to the sample leads to an increase of the temperature while no moisture is evaporated. This period is named the transient period. At a certain temperature the partial pressure of the volatiles (solvent, water, etc) becomes high enough to allow a significant rate of evaporation at the process pressure. The free moisture, *i.e.* surface moisture, starts to evaporate. The evaporation of the moisture utilizes all of the energy supplied to the sample, causing a constant temperature. This constant temperature depends on the equilibrium partial pressure of the volatiles, which in turn depends on a balance between the air-flux and the evaporation rate. The constant temperature leads to a constant temperature difference between the sample and the surrounding medium. Consequently, the rate of heat transfer from the surrounding medium to the sample is dictated by this

Table 6.1: *Division criteria for the classification of a drying process.*

Criteria	
Mode of operation:	batch, continuous, or semicontinuous.
Heat input mechanism:	convection, conduction, radiation, electromagnetic fields, combination of heat transfer modes) or adiabatic / non-adiabatic.
Drying temperature:	below boiling point, above boiling point, below freezing point.
State of material in the dryer:	stationary, moving, agitated, dispersed.
Relative motion between drying medium and the solids to be dried:	cocurrent, countercurrent, mixed flow.
Operating pressure:	vacuum, atmospheric.
Drying medium:	air, superheated steam, flue gases.
Number of stages:	single, multistage.

temperature difference and is also constant. During this stage the steady power input leads to a constant evaporation rate and, therefore, this stage is called the constant drying rate period.

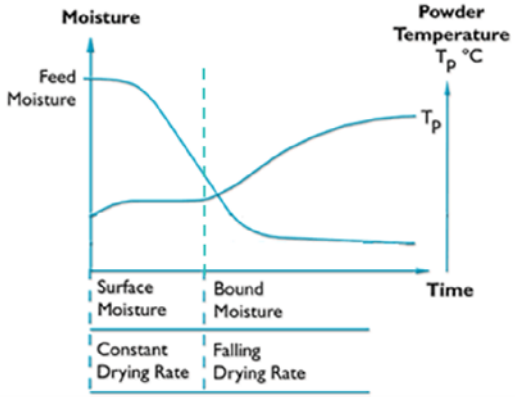

Figure 6.1: *Theoretical drying curve showing typical time-mass and time-temperature histories.* [19]

When most of the surface moisture has been removed, the evaporation of moisture starts to consume less energy. The energy - supplied to the sample - leads to an increase of the temperature. The moisture still present at the surface of the particles has to diffuse through the channels between the particles with a smaller difference in partial pressure, which is the driving force, and is removed much more slowly than the major part of the volatiles during the constant drying rate

period. The moisture that is bound to the sample, *i.e.* A_w* < 1, requires a higher temperature to evaporate, while less energy is supplied by the heating source, due to the smaller temperature difference between the heating source and the sample. The diffusion rate of the bound moisture is also much lower than that of "free" moisture. Therefore, this moisture is removed at a lower rate and at a higher temperature.

All of these factors determine the drying rate at the later stages of the drying process. These complex phenomena lead to a decreasing drying rate during the so-called falling rate period, and make it hard to predict the drying rate based on simple models. The falling rate period is dominant in time consumption. The exact behavior of a drying material during the falling rate period is strongly dependent on the specific material and the drying procedure.

The whole drying process can be considered as highly energy consuming. The largest part of this energy consumption is utilized for the evaporation of the volatiles. The way this energy is transferred, either through dielectric heating or by normal conduction / convection, can have a profound influence on the evaporation rate and, therefore, the drying rate.

6.2 Drying behavior and heating method

Previously reported results demonstrated that microwaves interact with heterogeneous systems in a beneficial manner.[20,21] These beneficial effects are thought to originate from the heating mechanism of microwave irradiation. In particular, selective heating can positively influence certain processes, such as regenerating catalysts[22], sintering ceramics[23,24] and extractions[25,26]. To determine the influence of microwave irradiation on the drying of pharmaceutical intermediates and to clarify whether its application beneficially influences the drying process, a comparison of conventional heating with microwave heating was made. To simplify this comparison between the performance of both heating methods a straightforward drying procedure was selected, see Figure 6.2.

The three-necked flask, containing the static sample held at a pressure of 5 kPa, was heated by either a water bath or by a multi-mode microwave apparatus, while an air-inlet capillary tube ensured a constant air-flow over the sample. This setup guaranteed a constant removal of evaporating moisture from the upper layer of the

* Water activity A_w, is the ratio of the vapor pressure of water in the product (P) to saturation pressure of water vapour (P_0) at the same temperature.

sample and excluded mass transport limitations in the gas phase. In this way, the diffusion rate of the moisture in the sample and the evaporation rate of the moisture govern the rate of the drying process.

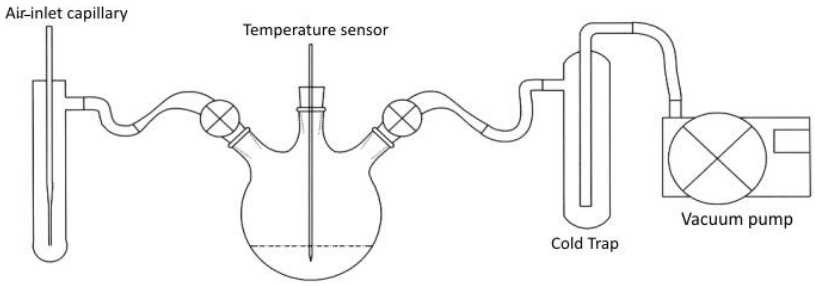

Figure 6.2: *The setup for the drying experiments.*

To compare the different heating methods, the power supplied by the water bath to the flask at t=0 was estimated for the applied temperatures, see experimental section. The actual power input of the water-bath is lower than these values. Due to the complexity of the heat- and mass transfer processes during the drying process a more precise calculation of the power input during conventional heating would yield inaccurate results without an elaborate characterization of these processes. The used water-bath temperature and the microwave power inputs are collected in Table 6.2.

Table 6.2: *Temperatures, corresponding theoretical power inputs and actual power inputs used in the microwave-assisted experiments.*

T (°C)	45	60	75
$Q_{CH,\ estimated,\ t=0}$ (W)	13	42	71
$Q_{MW,used}$ (W)	50	100	150
$Q_{MW,used\ effectively}$ (W)	~5	~10	~15

The energy efficiency of the microwave irradiation in the used setup is variable during the drying process. Also the efficiency of a microwave is usually proportional to the degree of charging the cavity which makes a direct comparison of the heating techniques cumbersome.[27]

The larger the sample is with respect to the cavity used, the higher the microwave energy efficiency becomes, see Figure 6.3. The results of preliminary experiments showed that, although the energy efficiency was assumed to be 10 %,

a power input of 420 W[†] (corresponding to the energy input at t=0 of a water-bath with a temperature of 60 °C) strongly outperformed the conventionally heated (CH) experiments.

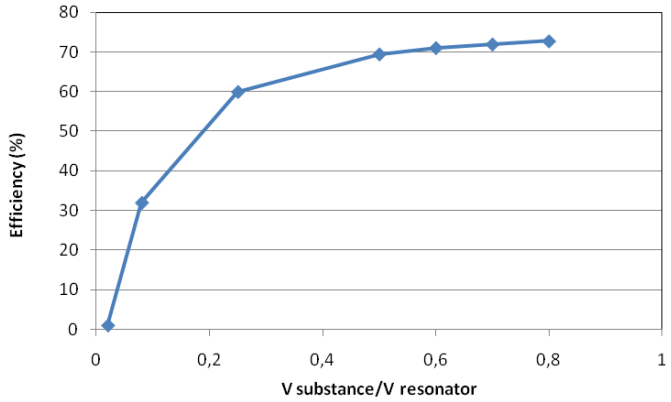

Figure 6.3: *MW energy efficiency as a function of the occupancy of the MW resonator; $V_{substance}$ – the volume of the substance loaded in the MW resonator; $V_{resonator}$ – the volume of the MW resonator.*

Therefore, the used microwave power inputs were determined empirically. The microwave equipment used in the experiments was inaccurate with power settings below 40 W. The selected power inputs of 50, 100 and 150 W were adequate to get comparable drying rates for microwave and conventional heating.

For the drying experiments two substances were selected based on earlier work,[20] (*S*)-*N*-acetylindoline-2-carboxylic acid and *N*-acetyl-(*S*)-phenylalanine, see Figure 6.4.

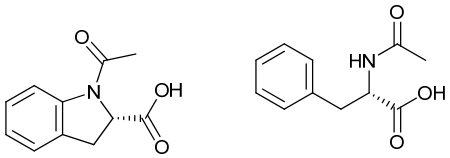

Figure 6.4: *(S)-N-acetylindoline-2-carboxylic acid (left) and N-acetyl-(S)-phenylalanine (right).*

[†] The filling level of the microwave was in the range of 5 %. Figure 2.3 shows an efficiency of 10 % for this situation. The theoretical power input with a water-bath at 60 °C was calculated at 42 W. Therefore, the preliminary experiments were performed with a microwave setting of 420 W.

The moisture content of (*S*)-*N*-acetylindoline-2-carboxylic acid, provided by DSM, was 5 wt%. To study the effect of higher moisture contents, and in particular the influence of microwave irradiation on the constant drying interval, *i.e.* the removal of surface moisture, and on the most crucial falling rate period usually determining the overall drying time, *i.e.* the removal of moisture in the inner pores, the sample of (*S*)-*N*-acetylindoline-2-carboxylic acid was subjected to an acid / base precipitation procedure. This resulted in an initial moisture content of 17 wt%.

The sodium salt of (*S*)-phenylalanine was acetylated with acetic anhydride under Schotten-Baumann conditions. Acetylation of (*S*)-phenylalanine resulted in a product with a moisture content of 22 wt%, which was immediately suitable for the drying experiments.

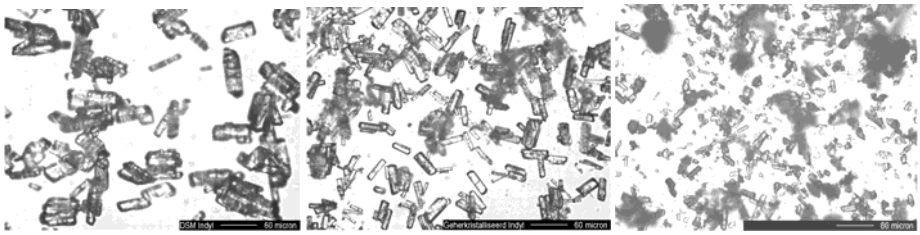

Figure 6.5: *Microscopic images. Left: original grade of (S)-N-acetylindoline-2-carboxylic acid. Middle: precipitated (S)-N-acetylindoline-2-carboxylic acid. Right: N-acetyl-(S)-phenylalanine.*

The particle sizes of the precipitated (*S*)-*N*-acetylindoline-2-carboxylic acid and *N*-acetyl-(*S*)-phenylalanine are approximately 3 times and 5 times smaller than that of the original grade of (*S*)-*N*-acetylindoline-2-carboxylic acid, respectively, see Figure 6.5.

The similarity in chemical structure between (*S*)-*N*-acetylindoline-2-carboxylic acid and *N*-acetyl-(*S*)-phenylalanine cannot be directly translated to a similar drying behavior. Also the particle size may be of influence on the drying behavior. A smaller particle size corresponds with a higher specific surface and a smaller channel or pore size. The higher surface area could increase the drying rate, particularly for the unbound water. A smaller pore size may decrease the amount of pore moisture but could inhibit the removal of the moisture from these pores. The packing of the particles of various sizes is also different, leading to a smaller pore size and a difference in diffusion rate of the moisture through the sample. All of these factors make it hard to predict the effect of a smaller particle size on the drying behavior.

Drying behavior of (*S*)-*N*-acetylindoline-2-carboxylic acid

To investigate microwave irradiation as an alternative way for drying of an industrially relevant material,[28] *(S)-N*-acetylindoline-2-carboxylic acid was selected as a test material. This pharmaceutical intermediate investigated in the drying experiments was supplied by DSM and had a moisture content of 5 wt%. The results of the drying experiments using conventional and microwave heating are shown in Figure 6.6.

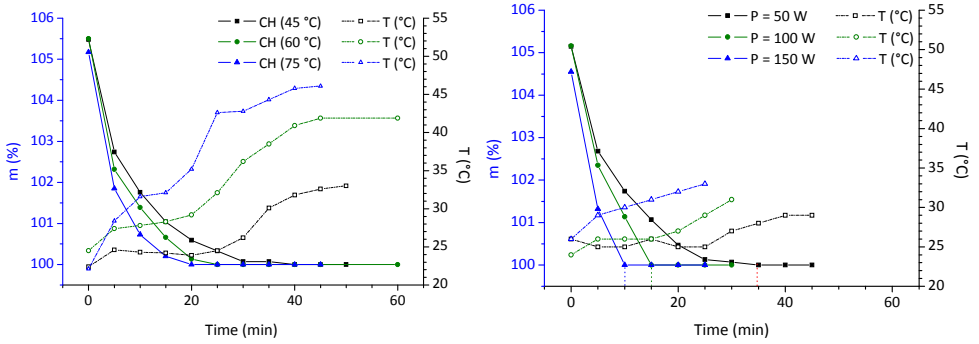

Figure 6.6: *Drying and temperature profiles for drying of (S)-N-acetylindoline-2-carboxylic acid (obtained from DSM Pharmaceuticals) at 5 kPa, at different temperatures and with different microwave powers. Left: conventional heating (CH). Right: microwave heating (MW).*

Application of microwaves reduced the drying time significantly. The experiments with conventional heating showed a drying time of 35 min at 45 °C which was also obtained with a microwave power of 50 W (corresponding to an actual power input of 5 W). The seemingly very short constant drying rate period could indicate that (*S*)-*N*-acetylindoline-2-carboxylic acid mostly contained moisture in the interstitial space. Also in this case removal of pore moisture was dominant in time and in energy consumption during the drying process. The drying time could be reduced drastically by increasing the microwave power input to 100 W (15 min drying time) and 150 W (10 min drying time). Increasing the temperature of the water, and thus increasing the power input supplied by the water-bath to the flask, also decreased the drying time.

Temperatures of 60 °C and 75 °C corresponded to a 25 and 20 min drying time for conventional heating, see Figure 6.6 (left). A striking difference between both heating methods is the temperature of the sample. Higher water-bath temperatures also increase the sample temperature, shown most pronouncedly for the final equilibrium temperature at the end of the drying

process. To gain a similar drying rate as for the 150 W microwave drying experiments, a temperature exceeding 200 °C should be applied for conventional drying. This would lead to a sample temperature of more than 150 °C, which is impractical and could be detrimental for the stability of the sample.

The temperature measurements were performed at the center of the sample for both heating methods. When applying a conventional heat source, the sample will be heated from the outside which creates a temperature profile and a drying front. The temperature will have the lowest value at the center of the sample. Therefore, the recorded temperatures of the sample with conventional heating are *lower* than the average temperature, see Figure 6.7. This is in sharp contrast with drying using microwave irradiation. The volumetric heating distributes the energy relatively evenly over the sample, especially with low loss tangent materials which have a large penetration depth. The insulation of the central point of the sample by the surrounding material causes a minimal heat loss in the center and, therefore, the temperature in the center of the sample in the microwave experiments has the *highest* value. The dielectric properties of the sample also determine the energy distribution in the sample, see Figure 6.8.[29] The dielectric loss factor (ε'') of a substance strongly depends on the moisture content of the sample. The dielectric loss factor only increases slightly with a moisture content below the critical moisture content (m_c).

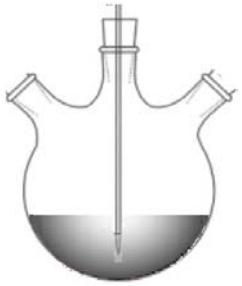

Figure 6.7: *For conventional drying the sample temperature is higher at the exterior zones of the sample.*

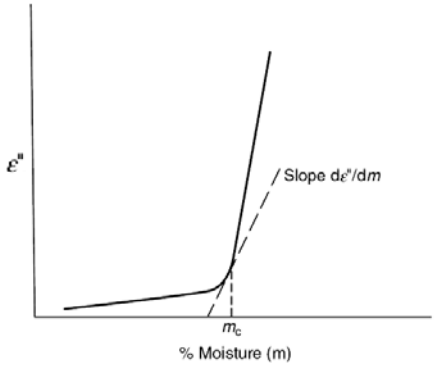

Figure 6.8: *Dielectric loss factor (ε'') as function of the moisture content, with m_c as the critical moisture content.*

For moisture contents above m_c, ε'' steeply increases with increasing moisture content. As a consequence, a higher moisture content results in a higher loss tangent. So, the higher moisture content regions of the sample are heated more efficiently causing higher evaporation rates than in the regions where the moisture content is relatively low. Finally, as compared to conventional heating the moisture distribution will be more homogeneous when using microwave heating. As a consequence, the energy uptake will be relatively even.[30] The even temperature distribution (*i.e.* no hotspots) and the relatively high drying rate make microwaves of great interest for drying of thermally unstable compounds.

The drying behavior of the 5 wt% and the 17 wt% samples has been studied for conventional heating (75 °C) and microwave heating (150 W). The results are collected in Figure 6.9. The precipitated (*S*)-*N*-acetylindoline-2-carboxylic acid with 17 wt% water displayed drying times of 70 and 35 min for conventional (75 °C) and microwave heating (150 W), respectively. The original (*S*)-*N*-acetylindoline-2-carboxylic acid grade (5 wt% water) required a drying time of 20 min for conventional heating (75 °C) and 10 min for microwave heating (150 W).

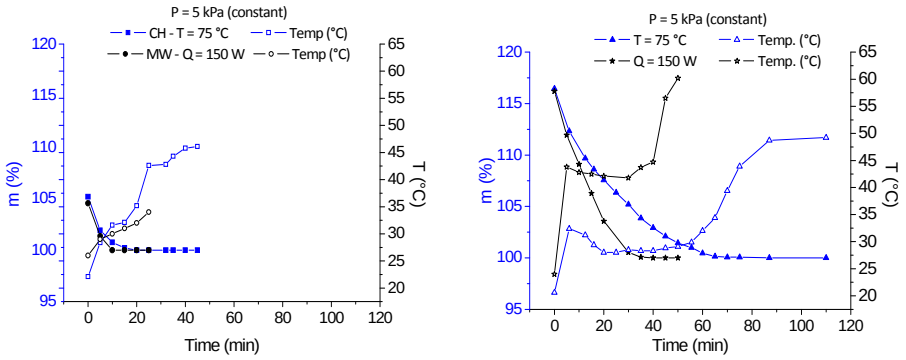

Figure 6.9: *Weight loss- and temperature curves for conventional and microwave heating. Left: non-precipitated (S)-N-acetylindoline-2-carboxylic acid. Right: precipitated (S)-N-acetylindoline-2-carboxylic acid.*

The measured bulk temperature during the drying experiments with the precipitated (*S*)-*N*-acetylindoline-2-carboxylic acid was higher with microwave heating than with conventional heating. This result is in contrast with the observations for the original (*S*)-*N*-acetylindoline-2-carboxylic acid grade containing 5 wt% water. The higher moisture content of the precipitated grade caused a higher loss tangent of the sample. Consequently, the microwave energy

was converted more readily into heat, resulting in an imbalance in the heat supplied by the microwave irradiation and the heat consumed by evaporation of the moisture. The microwave energy, converted into heat in the sample, at 150 W was too high to be compensated by the heat consumption due to evaporation, leading to higher temperatures. When the air-flow over the sample is insufficient to remove all of the evaporating moisture, then the air is saturated leading to a higher equilibrium temperature. The higher loss tangent is beneficial for the drying rate of (*S*)-*N*-acetylindoline-2-carboxylic acid, which has relatively good thermal stability. Although the higher energy absorption initially caused faster heating and drying rates, as compared to the original (*S*)-*N*-acetylindoline-2-carboxylic acid grade, the higher bulk temperature indicates that microwave irradiation should be applied with due caution for thermally unstable materials.

Drying behavior of *N*-acetyl-(*S*)-phenylalanine

To gain more insight into the drying behavior of other solid organic substances using microwave irradiation, the drying behavior of *N*-acetyl-*(S)*-phenylalanine was studied. The drying behavior of *N*-acetyl-(*S)*-phenylalanine with microwave and conventional heating is depicted in Figure 6.10.

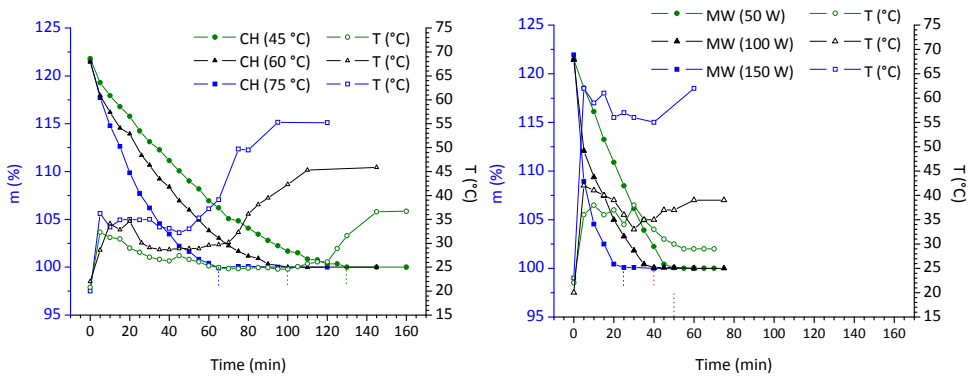

Figure 6.10: *Drying- and temperature profiles of N-acetyl-(S)-phenylalanine at various temperatures and powers at 5 kPa. Left: conventional heating (CH). Right: microwave heating (MW).*

The moisture content of *N*-acetyl-(*S)*-phenylalanine was even higher than that of the precipitated (*S*)-*N*-acetylindoline-2-carboxylic acid. This high water content could also lead to superheating of the sample, as described in the previous section. This is indeed observed for the microwave drying experiment at 150 W, leading to a sample temperature of 60 °C. The drying time for this high energy input was 25

min. This is extremely short compared to the drying times with conventional heating, for which drying times of 130, 100 and 65 min, at 45, 60 and 75 °C respectively, were registered. At a high bulk temperature of 63 °C *N*-acetyl-(*S*)-phenylalanine remained stable and hence microwave irradiation is a very suitable heating technique for drying this substance. The advantage of lower bulk temperatures combined with a high drying rate under *mild* microwave irradiation was demonstrated by the drying experiments with a lower microwave power input. The drying times were 40 and 50 min for 100 and 50 W, respectively. Thes were shorter drying times than observed for the conventionally heated samples using a water bath of 75 °C, where the sample temperature increased to 55 °C, while the sample temperature under these low microwave power inputs remained below 45 °C. This indicates that even at high moisture contents microwave irradiation can lead to higher drying rates with lower bulk temperatures, as long as the microwave power is applied mildly.

Probing drying without mass determination

Because the temperature of the substance is an indication of the drying rate and of the different drying stages, temperature is a suitable parameter to characterize the drying behavior of the sample. Intermittent weighing of the sample needed for determining the drying curve caused a temperature drop. Detachment and reconnection of the system to the vacuum pump resulted in minor pressure variations in the flask, which both could influence the drying rate. To exclude these disturbances (*S*)-*N*-acetylindoline-2-carboxylic acid (17 wt% and 5 wt% water) and *N*-acetyl-(*S*)-phenylalanine (22 wt% water) were dried under microwave irradiation without weighing. In this way, little or no influence of pressure or temperature drops was observed.

For the drying of the (*S*)-*N*-acetylindoline-2-carboxylic acid (Figure 6.11) the temperature profile indicates that the drying process is complete after 10 min, which is in accordance with the experiments monitored by mass determination. After an equilibrium temperature of 68 °C was reached, the microwave oven was shut down and the sample was left to cool. Subsequently, the dry sample was irradiated again. The temperature rose to the same equilibrium temperature. From the initial heating rate of the higher moisture containing precipitated (*S*)-*N*-acetylindoline-2-carboxylic acid (Figure 6.12) it can be derived that the microwave heat absorption of the wet sample corresponds to 3.8 W.‡

‡ The initial microwave absorption was calculated by determining the slope at t = 0 in the temperature curve.

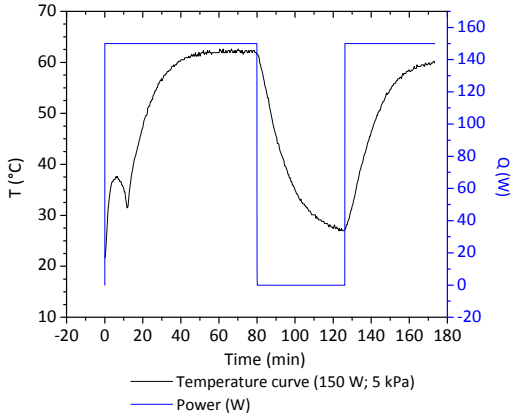

Figure 6.11: *The temperature-time history for microwave-assisted drying (150 W) of the original (S)-N-acetylindoline-2-carboxylic acid grade. Initial moisture content 5 wt%.*

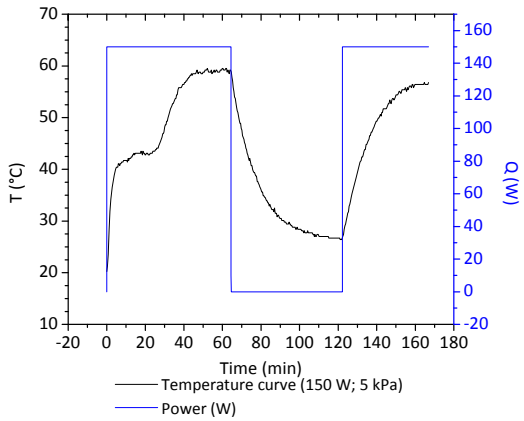

Figure 6.12: *The temperature-time history (left) for microwave-assisted drying of the precipitated (S)-N-acetylindoline-2-carboxylic acid. Initial moisture content 17 wt%.*

The temperature increase was observed after 30 min, indicating the end of the drying process. During this time the sample has absorbed 6 kJ of heat which corresponds to the heat of evaporation of 17 % x 15 g water. Almost the same equilibrium temperature was reached for the precipitated and the original (*S*)-*N*-acetylindoline-2-carboxylic acid grades.

This indicates that the dry substance was heated during microwave irradiation. When the steady state temperature is reached, the microwave absorption is equal to the heat loss to the surroundings. This heat loss can be estimated by the initial cooling rate, at the moment that the power source was turned off. For (*S*)-*N*-acetylindoline-2-carboxylic the initial cooling rate corresponds to a heat loss of 1.2 W. From this value it can be concluded that the microwave absorption of the dry (*S*)-*N*-acetylindoline-2-carboxylic is a factor of 3 times smaller than that of the wet grade.

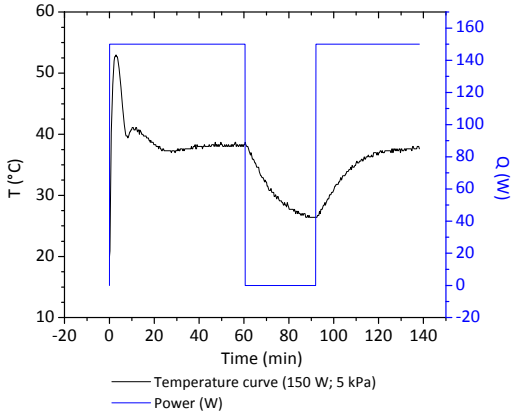

Figure 6.13: *The temperature-time history for microwave-assisted drying (150 W) of N-acetyl-(S)-phenylalanine. Initial moisture content 22 wt%.*

The temperature profile of the *N*-acetyl-(*S*)-phenylalanine (Figure 6.13) differs from the profile of (*S*)-*N*-acetylindoline-2-carboxylic acid. The initial heating rate corresponds to a microwave adsorption of 18 W, which is much higher than the 3.8 W observed for the precipitated (*S*)-*N*-acetylindoline-2-carboxylic acid. The energy input of 18 W would indicate a time of approximately 7 min to absorb the 8 kJ necessary to evaporate the 22 % x 15 g water. This is in accordance with the measured time-temperature histories. After a sharp increase in temperature to 55 °C a lower equilibrium temperature was reached than with (*S*)-*N*-acetylindoline-2-carboxylic acid. For *N*-acetyl-(*S*)-phenylalanine the initial cooling rate corresponds to a heat loss of 0.5 W. From this low value it can be concluded that the microwave absorption of the dry *N*-acetyl-(*S*)-phenylalanine is 40 times smaller than that of the wet grade. This demonstrates that *N*-acetyl-(*S*)-phenylalanine is more transparent for microwaves than (*S*)-*N*-acetylindoline-2-carboxylic acid. The difference in microwave adsorption of the dry substances is in contrast with their similarity in chemical structure. Also the particle sizes, shown in Figure 6.5, have no direct correlation with the drying behavior, indicating that each substance has

to be characterized in terms of dielectric properties, both wet and dry, before a suitable microwave-assisted drying procedure can be developed.

6.3 Conclusion

From the results described for the drying of (*S*)-*N*-acetylindoline-2-carboxylic acid, both original and precipitated grades, and of *N*-acetyl-(*S*)-phenylalanine under conventional and microwave heating, it can be concluded that microwave irradiation leads to considerably higher drying rates. The power input when using microwave irradiation should be chosen carefully. A high power input enables a dramatic decrease of the drying time of the sample but can also lead to overheating and thermal product decomposition. A balance between overheating and fast drying should be sought. However, even for mild conditions the drying rate is much higher than for similar heat-flow rates with conventional heating. To obtain similar drying rates, conventional heating demands for much higher heat-flow rates than microwave heating. Higher heat-flow rates lead to rather high temperature differences between the heating element and the sample and to very high temperatures inside the sample, which may be detrimental for thermally unstable materials. Lower temperatures during drying by microwave irradiation make this heating technique extremely useful for drying of these materials in short periods of time. Although microwave heating is a very promising technique it should be mentioned that each substance has to be characterized in terms of dielectric properties first, both in the wet and dry state.

6.4 Experimental section

General:
See experimental section of Chapter 2. (*S*)-*N*-acetylindoline-2-carboxylic acid was kindly supplied by DSM.

Microwave heating:
See experimental section of Chapter 2.

Thermographic imaging:
See experimental section of Chapter 2.

Acid-base precipitation procedure of (*S*)-*N*-acetylindoline-2-carboxylic acid: A 2500 mL three-neck round-bottomed flask was charged with (*S*)-*N*-acetylindoline-2-carboxylic acid (300 g, 1.47 mol) and was dissolved in 770 mL NaOH-solution (2.0 M). Using a dropping-funnel this mixture was brought at a pH of 3 with 4 M

HCl (approximately 385 mL) under stirring. The precipitated product was then filtered under vacuum and washed with saturated brine (200 mL) and demineralised water (100 mL). The filtrate was dried in air for two days, yielding 95 % (*S*)-*N*-acetylindoline-2-carboxylic acid. After drying in air for two days the moisture content was 17 wt%.

Synthesis of *N*-acetyl-(*S*)-phenylalanine*:* A 2500 mL three-neck round-bottomed flask was charged with (*S*)-phenylalanine (198 g, 1.2 mol). The (*S*)-phenylalanine was dissolved in 300 mL NaOH-solution (4.0 M). Under vigorous stirring and ice-bath cooling, acetic anhydride (122.4 g; 1.2 mol) was added drop-wise with simultaneous addition of 300 mL NaOH-solution (4.0 M). The pH was maintained at 10. After 2 h additional acetic anhydride (122.4 g; 1.2 mol) was added drop-wise with simultaneous addition of 300 mL NaOH-solution (4 M). Using a dropping-funnel this mixture was brought to a pH of 3 with 6 M HCl. The precipitated product was then filtered under vacuum and washed with brine (200 mL) and demineralised water (100 mL). The filtrate was dried in air for two days, yielding 295 g, with a moisture content of 22 wt%, which corresponded to a yield of 93 % (230 g dry product). ^{1}H-NMR (400 MHz, CD_3OD) δ: 7.51 (m, 5H) 4.92 (m, 1H), 3.45 (dd, 2H), 3.20 (dd, 2H), 2.15 (s, 3H) confirmed that all (*S*)-phenylalanine was acetylated. The specific rotation of the dry product was $[\alpha]^{23}_D$ = +28° (c = 1.0, MeOH). Literature: $[\alpha]^{23}_D$ = +33° (c = 1.0, MeOH).[31]

Drying experiments: For the experiments, a three-neck 250 mL flask was charged with 15 g of either *N*-acetyl-(*S*)-phenylalanine or (*S*)-*N*-acetylindoline-2-carboxylic acid. A temperature probe was inserted in the central neck and placed at a constant height in the exact center of the sample. An air-inlet tube was connected to the neck of the flask. The air-inlet tube was connected to a capillary tube. The capillary tube ensured a constant air-flow. The flask was held at a constant pressure of 50 mbar by an oil pump connected to the other neck. The flask was heated by either a magnetically stirred (750 rpm) water-bath of the indicated temperature for the conventionally heated experiments or the power-controlled microwave oven with the indicated power settings. The weight was measured at constant time intervals and the temperature of the sample was recorded at constant time intervals by either a fiber-optic sensor in the microwave oven or by a thermocouple for the experiments with conventional heating. The dry substances showed no traces of degradation after the drying procedure.

Calculation of power input

$$Q = U \cdot A \cdot \Delta T \quad (1)$$

$$A = 2\pi r \partial h \quad (2)$$

Q = power supplied to the flask (W)
U = overall heat transfer coefficient (W/K.m²)
A = heat transfer area (m²)
ΔT = temperature difference (K)
*d*h = submerged depth of the flask in the water bath (m)

$$\frac{1}{U} = \frac{1}{h_{water}} + \frac{l}{k} \qquad h_{water} = \frac{Nu \cdot k_{water}}{D} \quad (3)$$

Nu = Nusselt number
k = thermal conductivity coefficient (W/m K)
D = diameter (m) *(0,085 m)*

$$Nu = 2.0 + 0.66\,\mathrm{Re}^{\frac{1}{2}} \cdot \mathrm{Pr}^{\frac{1}{3}} \quad (4)$$

$$\mathrm{Re} = \left(\frac{\rho \cdot \upsilon \cdot D}{\mu} \right)_{H_2O} \Rightarrow \frac{998 \cdot 3.34 \cdot 0.085}{0.000894} \approx 3.2 \times 10^5 \quad (5)$$

$$\mathrm{Pr} = \left(\frac{c_p \cdot \mu}{k} \right)_{H_2O} \Rightarrow \frac{4200 \cdot 0.000894}{0.58} \approx 6.47 \quad (6)$$

$$v = 2\pi r \cdot \left(\frac{n}{60} \right) \Rightarrow 2\pi \cdot 0,0425 \cdot \left(\frac{750}{60} \right) \approx 3.34\ m/s \quad (7)$$

Re = Reynolds number
Pr = Prandtl number
ϱ = density (kg/m³) *(998 kg/m³)*
ν = velocity (m/s)
r = radius flask (m) *(0,0425 m)*
n = rotational speed stirrer *(750 rpm)*
D = diameter (m) *(0,085 m)*
μ = viscosity (Pa/s) *(8,94 x 10⁻⁴ Pa/s)*
c_P = heat capacity (J/kg K) *(4200 J/kg K)*

6.5 References

(1) McCormick, P. Y.; Mujumdar, A. S. *Drying, Kirk-Othmer Encyclopedia of Chemical Technology*, 2004.

(2) Mujumdar, A. S.; Devahastin, S. *Fundamental Principles of Drying*; Exergex Corp, Brossard, 2002.

(3) Zhang, M.; Tang, J.; Mujumdar, A. S.; Wang, S. *Trends Food Sci. Technol.* **2006**, *17*, 524-534.

(4) Torringa, E.; Esveld, E.; Scheewe, I.; Van den Berg, R.; Bartels, P. *J. Food Eng.* **2001**, *49*, 185-191.
(5) Regier, M.; Knorzer, K.; Erle, U. *Chem. Ing. Tech.* **2004**, *76*, 424-432.
(6) Hamer, A.; Puschner, H. A. *Chem. Ing. Tech.* **1997**, *69*, 480-483.
(7) Puschner, H. A. *Elektrotech. Z. B* **1968**, *20*, 278-279.
(8) Esveld, E.; Chemat, F.; Van Haveren, J. *Chem. Eng. Technol.* **2000**, *23*, 279-283.
(9) Esveld, E.; Chemat, F.; Van Haveren, J. *Chem. Eng. Technol.* **2000**, *23*, 429-435.
(10) Askari, G. R.; Emam-Djomeh, Z.; Mousavi, S. M. *Drying Technol.* **2009**, *27*, 831-841.
(11) Bakass, M.; Mokhlisse, A.; Lallemant, M. *Thermochim. Acta* **2000**, *356*, 159-171.
(12) Clark, D. E.; Sutton, W. H. *Annu. Rev. Mater. Sci.* **1996**, *26*, 299-331.
(13) Kumar, P.; Mujumdar, A. S.; Koran, Z. *Drying Technol.* **1990**, *8*, 1061-1087.
(14) Haghi, A. K. *Asian J. Chem.* **2005**, *17*, 639-654.
(15) Haque, K. E. *Int. J. Miner. Process.* **1999**, *57*, 1-24.
(16) Vongpradubchai, S.; Rattanadecho, P. *Chem. Eng. Process.* **2009**, *48*, 997-1003.
(17) Chee, S. N.; Johansen, A. L.; Gu, L.; Karlsen, J.; Heng, P. W. S. *Chem. Pharm. Bull.* **2005**, *53*, 770-775.
(18) Kelen, A.; Pallai-Varsanyi, E.; Ress, S.; Nagy, T.; Pintye-Hodi, K. *Eur. J. Pharm. Biopharm.* **2006**, *62*, 101-109.
(19) Pakowski, Z.; Mujumdar, A. S. *Basic Process Calculations and Simulations in Drying*; Roca Baton : CRC Press, 2006.
(20) Dressen, M. H. C. L. PhD-thesis, Eindhoven University of Technology, **2009**.
(21) Dressen, M. H. C. L.; Van de Kruijs, B. H. P.; Meuldijk, J.; Vekemans, J. A. J. M.; Hulshof, L. A. *Org. Process Res. Dev.* **2007**, *11*, 865-869.
(22) Kirkbride, C. G. Regenerating coke-contaminated fluidised cracking catalysts by treating with microwave energy US4144189-A, **1979**.
(23) Das, S.; Mukhopadhyay, A. K.; Datta, S.; Basu, D. *Bull. Mater. Sci.* **2009**, *32*, 1-13.
(24) Das, S.; Mukhopadhyay, A. K.; Datta, S.; Basu, D. *Bull. Mater. Sci.* **2008**, *31*, 943-956.
(25) Pickles, C. A. *Miner. Eng.* **2009**, *22*, 1112-1118.
(26) Mandal, V.; Mohan, Y.; Hemalatha, S. *J. Pharm. Biomed. Anal.* **2008**, *46*, 322-327.

(27) Hoogenboom, R.; Wilms, T. F. A.; Erdmenger, T.; Schubert, U. S. *Aust. J. Chem.* **2009**, *62*, 236-243.
(28) Gruenfeld, N.; Stanton, J. L.; Yuan, A. M.; Ebetino, F. H.; Browne, L. J.; Gude, C.; Huebner, C. F. *J. Med. Chem.* **1983**, *26*, 1277-1282.
(29) Perkin, R. M. *Int. J. Heat Mass Transfer* **1980**, *23*, 687-695.
(30) Monzó-Cabrera, J.; Díaz-Morcillo, A.; Catalá-Civera, J. M.; Reyes, E. D. l. *Microwave Opt. Technol. Lett.* **2001**, *30*, 166-168.
(31) Smith, H. E.; Neergaard, J. R. *J. Am. Chem. Soc.* **1997**, *119*, 116-124.

Summary

Microwave-matter effects in metal(oxide)-mediated chemistry and in drying

Microwave irradiation is a well-accepted heating technique for lab-scale organic synthesis but its application for large-scale operation is still limited. To determine the potential of microwave heating in producing fine chemicals beyond the kg-scale, the added value of this heating technique, compared to conventional heating, has been evaluated at accurately controlled conditions on lab-scale. The research described in this thesis focuses on comparing microwave heating with conventional heating for a series of heterogeneous reactions and for purification, *i.e.* drying. This enabled to elucidate factors determining the benefits of microwave-mediated technology. In Chapter 1 the state of the art in the application of microwave technology is discussed and the outline of the thesis is presented.

In Chapter 2 the Grignard reagent formation, involving a heterogeneous metal, *i.e.* magnesium, is discussed. Microwave irradiation of magnesium turnings led to electrical discharges, which modify the surface and, therefore, the reactivity of magnesium. The influence of modifying the magnesium surface on the reactivity of the metal in the Grignard reagent synthesis was determined for a series of halo-compounds. The initiation time significantly shortened upon irradiating the reaction mixtures of relatively reactive (2-bromothiophene, 2-bromopyridine, bromobenzene, iodobenzene and *n*-octyl bromide) and moderately reactive (2-chlorothiophene and 2-chloropyridine) halo-substrates. In contrast, irradiating the reaction mixtures of non-reactive halogenated compounds (3-bromopyridine and *n*-octyl chloride) led to major magnesium carbide formation causing a reduced reactivity of the metal and prolonged initiation times.

In Chapter 3 the influence of microwave heating on another heterogeneous organometallic reaction, the Reformatsky reaction, involving metallic zinc, is discussed. In this system microwave-induced electrical discharges caused major zinc carbide formation, irrespective of the presence of a species reactive towards zinc. The zinc carbide formation coated the zinc surface, which was responsible for inhibition of zinc insertion in acetate, propionate and isobutyrate esters. This zinc carbide formation limited the beneficial use of microwave heating in the Reformatsky reaction to such an extent that conventional heating has to be preferred.

Information on the influence of microwave energy on a heterogeneous organometallic reaction involving metallic copper, the Ullmann coupling of 2-chloro-3-nitropyridine, is given in Chapter 4. In this case, microwaves did not seem to interact with the copper directly, limiting the impact of this heating mode. The reaction was optimized in terms of temperature, copper source, stoichiometry and solvent. Surprisingly, fine copper powder (45 μm) is a better metal source than

traditional copper-bronze (74 μm) for this Ullmann carbon-carbon coupling. A ratio of 1:1 of copper to 2-chloro-3-nitropyridine resulted in reaction profiles similar to those resulting from an excess of copper. Switching solvent from *N*,*N*-dimethylformamide (DMF) to *N*,*N*-dimethylacetamide (DMA) or *N*-methyl-2-pyrrolidone (NMP) diminished reaction rates, prolonged initiation times, lowered yields and gave rise to the formation of 2,2'-oxybis(3-nitropyridine) as byproduct. Therefore, DMF is the preferred solvent for this Ullmann coupling. Comparison of microwave heating with conventional heating for the reactions performed at optimized conditions (in DMF at 110 °C), as well as under less ideal conditions (in DMA and NMP at various temperatures) revealed identical time-conversion histories, yields and selectivities.

The results with magnesium, zinc and copper reveal that, although, the Grignard reagent formation, the Reformatsky reaction and the Ullmann coupling are very similar processes, the influence of microwave irradiation on the outcome of the process is not.

In Chapter 5 the influence of microwave irradiation on a freshly prepared zirconium-based heterogeneous catalyst for the amide formation from a nitrile and an amine is presented. The ZrO_2-based catalyst not only efficiently catalyzes the formation of *N*-hexylpentamide from valeronitrile and *n*-hexylamine but also the polymerization of 6-aminocapronitrile and ϵ-caprolactam and does so with conventional as well as microwave heating. Microwave energy, however, heats the catalyst substantially, inducing selective heating that enhances the catalytic activity, compared to conventional heating.

The drying behavior of (*S*)-*N*-acetylindoline-2-carboxylic acid with various moisture contents and of *N*-acetyl-(*S*)-phenylalanine, in a straightforward microwave-mediated drying setup, is presented in Chapter 6. The way energy is supplied to the system has a profound influence on the drying rate and on the internal temperature of the samples during drying. To achieve similar drying times with conventional heating as reached under microwave irradiation, extremely high energy inputs are required, causing extremely large temperature differences between the heating source and the sample. These results demonstrate that microwave energy is particularly useful for drying thermally unstable materials in short periods of time.

Microwave heating is not a universally beneficial technique applicable to all reactions. The results we gathered suggest that every reaction has to be evaluated separately to judge whether microwave heating is a suitable scaling-up tool and whether microwave heating is to be preferred over conventional heating.

Samenvatting

Ook al is microgolfstraling een veel gebruikte techniek voor syntheses van organische moleculen op labschaal, het gebruik in een productieomgeving is nog steeds beperkt. Om de bruikbaarheid van microgolfstraling voor het produceren van chemicaliën in grote hoeveelheden te toetsen, moet eerst de toegevoegde waarde van het verwarmen met microgolfstraling - vergeleken met conventionele verwarmingsmethoden - worden vastgesteld op labschaal. Vooral het effect op de omzetsnelheid en de selectiviteit is hierbij van belang. De vergelijking van microgolfverwarming en conventionele verwarming moet onder zo vergelijkbaar mogelijke omstandigheden plaatsvinden om zo een goed onderbouwd besluit te kunnen nemen over het al dan niet toepassen van microgolfstraling in een productieomgeving. In dit proefschrift is de vergelijking tussen microgolf-verwarming en conventionele verwarming doorgevoerd voor een aantal heterogene reactiesystemen en voor droogprocessen van enkele farmaceutische tussenproducten.

In hoofdstuk 1 wordt de theoretische achtergrond van het verwarmingsprincipe van microgolfstraling en de tot nu toe veronderstelde invloed op het verloop van chemische reacties besproken.

De Grignard-reagens vorming, waarin het metaal magnesium gebruikt wordt, staat beschreven in hoofdstuk 2. Het bestralen van magnesium krullen met microgolfstraling leidt tot elektrische ontladingen. Deze ontladingen beïnvloeden het magnesiumoppervlak en daardoor ook de reactiviteit van het magnesium. De invloed van microgolfstraling op de reactiviteit van magnesium is bepaald voor een aantal gehalogeneerde substraten. De initiatietijd werd beduidend korter voor reactieve substraten (2-broomthiofeen, 2-broompyridine, broombenzeen, joodbenzeen en *n*-octylbromide) en voor enigszins reactieve substraten (2-chloorthiofeen en 2-chloorpyridine). Daarentegen werd de initiatietijd verlengd door competitieve magnesiumcarbide vorming bij relatief inerte substraten (3-broomthiofeen en *n*-octylchloride).

De Reformatsky-reactie, waarbij gebruik wordt gemaakt van het metaal zink, is beschreven in hoofdstuk 3. Bij bestraling van zinkkrullen treden, net als bij bestraling van magnesiumkrullen, elektrische ontladingen op. De invloed van deze ontladingen op de reactiviteit van zink is echter anders dan met magnesium. Door de elektrische ontladingen werden relatief grote hoeveelheden zinkcarbide gevormd. Ongeacht de reactiviteit van het toegepaste substraat, werd de reactie vertraagd door de zinkcarbide laag. Deze laag bleek verantwoordelijk voor een verlenging van de initiatietijd, of zelfs voor totale inhibitie van de zinkinsertie in acetaat, propionaat en isobutyraat esters. Hierdoor zijn conventionele verwarmingsmethoden geschikter voor het uitvoeren van de Reformatsky-reactie dan microgolfverwarming.

De invloed van microgolfbestraling op de reactiviteit van koper wordt behandeld in hoofdstuk 4. Bij het bestralen van koper, gebruikt in de Ullmann-koppeling van 2-chloor-3-nitropyridine, vinden geen elektrische ontladingen

plaats. De reactie werd geoptimaliseerd met betrekking tot de temperatuur, de koperbron, de verhouding koper en substraat en het oplosmiddel. Koper-poeder (45 μm) bleek een verassend betere koperbron te zijn dan het traditionele koper-brons (74 μm). Een molaire verhouding van 1:1 van koper en substraat leidde tot reactieprofielen die gewoonlijk waargenomen worden bij het gebruik van een overmaat koper. Het oplosmiddel had een zwaarwegend effect op het verloop en de selectiviteit van de reactie. Bij gebruik van dimethylacetamide (DMA) en *N*-methyl-2-pyrrolidone (NMP) i.p.v. dimethylformamide (DMF) werd de reactie vertraagd, werden de initiatietijden langer, verminderden de opbrengsten en werd er een bijproduct, 2,2'-oxybis(3-nitropyridine), gevormd. Daardoor werd geconcludeerd dat DMF een geschikter oplosmiddel voor deze Ullmann koppeling is. De vergelijking tussen verwarming door microgolfstraling en conventionele verwarming onder geoptimaliseerde condities (in DMF bij 110 °C) evenals bij minder ideale omstandigheden (in DMA and NMP bij verschillende temperaturen) toonden aan dat het conversieverloop met de tijd, opbrengsten en selectiviteiten vergelijkbaar waren.

Hoewel de Grignard-reagens vorming, de Reformatsky-reactie en de Ullmann-koppeling vergelijkbare processen zijn, alle betreffen een insertie van een metaal in een koolstof-halide binding, is duidelijk geworden dat de invloed van microgolfstraling op deze processen zeer verschillend is.

In Hoofdstuk 5 wordt de invloed van microgolfstraling op de door een zirkonium-oxide gekatalyseerde amidering van een nitril met een amine beschreven. De zirconia katalysator is niet alleen geschikt voor de amidering van valeronitril en *n*-hexylamine maar ook voor de polymerisatie van 6-aminocapronitril en de polymerisatie van ϵ-caprolactam. Microgolfstraling zorgt voor selectieve opwarming van de katalysator, waardoor de katalytische activiteit van het zirkonia significant toeneemt. Microgolfstraling in combinatie met de zirkonia katalysator leidt tot nylon-6 met een hoog molgewicht in een relatief korte tijd en onder relatief milde omstandigheden.

Het drooggedrag van (*S*)-*N*-acetylindoline-2-carbonzuur en *N*-acetyl-(*S*)-phenylalanine onder invloed van microgolfstraling is beschreven in Hoofdstuk 6. Deze verwarmingsmethode heeft een grote invloed op de droogsnelheid en de interne temperatuur van deze processen. Om soortgelijke droogsnelheden te realiseren onder conventionele verwarming zijn er extreme verschillen in temperatuur tussen het monster en het verwarmingselement nodig. Uit de resultaten blijkt dat microgolfstraling uitermate geschikt is om thermisch instabiele stoffen in korte tijd te drogen.

De resultaten die beschreven staan in dit proefschrift duiden erop dat microgolfstraling allesbehalve universeel bruikbaar is als warmtebron voor chemische processen en dat de toegevoegde waarde van het gebruik van microgolfstraling voor elke reactie afzonderlijk bepaald moet worden alvorens een weloverwogen beslissing genomen kan worden over toepassing van microgolfstraling bij de opschaling van processen.

Curriculum Vitae

Bastiaan van de Kruijs is geboren op 18 oktober 1978 te Weert. Na het voltooien van zijn VWO-opleiding aan het Bisschoppelijk College Weert begon hij in 1997 met de studie Scheikundige Technologie aan de Technische Universiteit Eindhoven. In 1999 is hij gestart met de studie Chemische Technologie aan de Fontys Hogeschool Eindhoven. Deze opleiding werd afgerond in 2002. Hierna heeft hij zijn studie Scheikundige Technologie aan de Technische Universiteit Eindhoven voortgezet. Deze studie werd in 2005 afgerond met een afstudeerproject bij de vakgroep Polymeertechnologie onder leiding van prof. dr. P.J. Lemstra. Vanaf december 2005 werkte hij aan een promotieonderzoek in de onderzoeksgroep Toegepaste Organische Chemie in de capaciteitsgroep Molecular Science & Technology van de faculteit Scheikundige Technologie van de Technische Universiteit Eindhoven onder leiding van eerste promotor prof. dr. L.A. Hulshof, tweede promotor prof. dr. J. Meuldijk en co-promotor dr. J.A.J.M. Vekemans. De belangrijkste resultaten van dit onderzoek zijn beschreven in dit proefschrift.

Bastiaan van de Kruijs was born on October 18th, 1978 in Weert, the Netherlands. After completing his secondary education at the Bisschoppelijk College in Weert in 1997, he started studying Chemical Engineering at the Eindhoven University of Technology. In 1999 he switched to the study Chemical Engineering at the 'Fontys Hogeschool Eindhoven' where he obtained his bachelor degree in 2002. In the same year he started his masters in Chemical Engineering at the Eindhoven University of Technology. He obtained his master degree in 2005 with a graduation project at the laboratory of Polymer Technology under guidance of prof. dr. P.J. Lemstra. He started his Ph.D. research in December 2005 within the research unit Applied Organic Chemistry as part of the group Molecular Science & Technology at the department of Chemical Engineering & Chemistry at the Eindhoven University of Technology under supervision of prof. dr. L.A. Hulshof, prof. dr. J. Meuldijk and dr. J.A.J.M. Vekemans. The most important results of this research are described in this thesis.

List of publications

Oxo-crown-ethers as comonomers for tuning polyester properties
Van der Mee, L.; Antens, J. B. M.; Van de Kruijs, B. H. P.; Palmans, A. R. A.; Meijer, E. W. *J. Polym. Sci., Part A: Polym. Chem*. **2006**, *44*, 2166-2176.

Vanishing microwave effects: influence of heterogeneity
Dressen, M. H. C. L.; Van de Kruijs, B. H. P.; Meuldijk, J.; Vekemans, J.A.J.M.; Hulshof, L. A. *Org. Process Res. Dev.* **2007**, *11*, 865-869.

The mechanism of the oxidation of benzyl alcohol by iron(III)nitrate: conventional versus microwave heating
Dressen, M. H. C. L.; Stumpel, J. E.; Van de Kruijs, B. H. P.; Meuldijk, J. A. J. M.; Vekemans, J.; Hulshof, L. A. *Green Chem.* **2009**, *11*, 60-64.

From batch to flow processing: racemization of N-acetylamino acids under microwave heating
Dressen, M. H. C. L.; Van de Kruijs, B. H. P.; Meuldijk, J.; Vekemans, J. A. J. M.; Hulshof, L. A. *Org. Process Res. Dev.* **2009**, *13*, 888-895.

Flow processing of microwave-assisted (heterogeneous) organic reactions
Dressen, M. H. C. L.; Van de Kruijs, B. H. P.; Meuldijk, J.; Vekemans, J. A. J. M.; Hulshof, L. A. *Org. Process Res. Dev.* **2010**, *in press*.

Microwave-induced electrostatic etching: generation of highly reactive magnesium for application in Grignard reagent formation
Van de Kruijs, B. H. P.; Dressen, M. H. C. L.; Meuldijk, J.; Vekemans, J.A.J.M.; Hulshof, L. A. *Org. Biomol. Chem.* **2010**, *in press*.

Beneficial microwave effects and scalability of some drying processes
Pinchukova, N. A.; Voloshko, A. Y.; Shyshkin, O. V.; Chebanov, V. A. ; Van de Kruijs, B. H. P.; Arts, J. C. L.; Dressen, M. H. C. L.; Meuldijk, J.; Vekemans, J. A. J. M.; Hulshof, L.A. *Org. Process Res. Dev.* **2010**, *manuscript in preparation.*

Dankwoord

Een promotieonderzoek is een fascinerend leerproces. Er zijn tal van mensen die aan dit leerproces hebben bijgedragen. Daarom wil ik in het laatste gedeelte van mijn proefschrift een aantal van die mensen bedanken.

Allereerst ben ik mijn promotoren Bert Hulshof en Jan Meuldijk en co-promotor Jef Vekemans veel dank verschuldigd. Elke maandagochtend werden vol overgave mijn bevindingen besproken. Ook al bleek magnetronchemie niet altijd superieur aan verwarmen met het vertrouwde oliebad, zoals aanvankelijk werd gedacht, toch hebben we er samen een interessant onderzoek van weten te maken. Bert, bedankt je begeleiding en dat je het mogelijk gemaakt hebt dat ik een promotieonderzoek kon doen met veel onderzoeksvrijheid. Jouw industriële kijk op de vraagstukken heeft erg geholpen in het onderzoek. Ik hoop dat je veel kunt gaan genieten van de aankomende vrije tijd en dat de camper nog veel kilometers gaat maken. Succes met het afronden van je boek. Jan, naast mijn promotor ook mijn dagelijkse begeleider, de variëteit van alle onderzoeken waar je bij betrokken bent maakt je tot een zeer veelzijdige en dus waardevolle begeleider. Bedankt daarvoor en natuurlijk voor het grondig inspecteren van mijn presentaties, publicaties en natuurlijk mijn proefschrift. Je hebt het altijd druk, maar nooit te druk om me te helpen. Jef, het grootste gedeelte van mijn dagelijkse begeleiding is op jouw schouders gevallen. Je stond altijd voor me klaar om uiteenlopende dingen te bespreken; nooit een korte discussie, maar altijd een leerzame. Jouw advies over de organische synthese heeft mijn onderzoek enorm geholpen. Ik heb de voorbesprekingen van de werkcolleges organische chemie als heel leerzaam en prettig ervaren. Jouw inspectie van mijn presentaties, publicaties en natuurlijk mijn proefschrift was volledig complementair aan de suggesties van Jan, al is jouw oog voor detail onnavolgbaar. Zonder jou had mijn proefschrift, en mijn promotie, er heel anders uitgezien, bedankt daarvoor.

De rest van de commissie ben ik zeer erkentelijk voor het lezen van mijn manuscript. I am grateful to Prof. C. Oliver Kappe and Prof. Michael G. Organ for evaluating the manuscript. You are leading scientists in the field of microwave-assisted chemistry. Your participation in the defense committee means a great deal to me. Graag wil ik ook Bert Meijer bedanken voor het vlot kunnen doornemen van mijn manuscript. Ik heb veel respect voor de wijze waarop je leiding geeft aan de capaciteitsgroep en je zo een productief onderzoeksklimaat creëert waar jonge onderzoekers zich uitstekend kunnen ontplooien. Verder gaat mijn dank uit naar Gerard Kwant voor het deelnemen in de commissie.

Ook wens ik Mark te bedanken. In de afgelopen 4 jaar was je naast kamergenoot, labgenoot, ook een goede vriend. We hebben 4 jaar goed samengewerkt, frequent geluncht, labervaringen gedeeld en veel gelachen en soms gevloekt (of was het nu andersom...). Veel succes met Dymph en Lisa in het hoge noorden.

Onderzoek doe je natuurlijk nooit alleen. De resultaten in dit boekje zouden nooit tot stand gekomen zijn zonder de hulp van een groot aantal mensen. Daarom wil ik Joost van Dongen bedanken voor het draaiende houden van de gehele chromatografische analyse afdeling. Ralf Bovee en Lou X. voor het meten van de MALDI-TOF en de ondersteuning bij de GC/MS. Henk Eding voor de elementanalyse en natuurlijk zijn ongeëvenaarde inzet om de koffiekamer te blijven runnen. Hans Damen voor de ondersteuning en de gezelligheid. Daarnaast wil ik Hanneke, Carine, Joke, Angela, Janna, Patricia voor de geweldige ondersteuning. Michel Ligthart voor zijn hulp bij de bereiding van de zirkonium katalysator. Peter Lipman voor het meten van de BET-adsorptieisothermen. Gilbère Mannie voor het meten van de XPS-spectra. Nicole Papen-Botterhuis, en Pauline Schmit voor de mooie SEM plaatjes. Niek Lousberg voor de hulp met de EPMA-metingen. Frans Visscher voor het doneren van 6-aminocapronitril. Jan Diepens van de faculteit bouwkunde voor het beschikbaar stellen van de FLIR-infrarood camera.

Tijdens mijn onderzoek heb ik het voorrecht gehad om ook een aantal studenten te mogen begeleiden. Jelle Stumpel, Mark was je hoofd-begeleider, maar toch... Je was altijd enthousiast en je hebt mooi werk geleverd. Alleen heb ik nog nooit iemand zo vreemd een boterham zien eten. Succes met je promotieonderzoek. Jeroen Arts, jouw droog-experimenten waren niet altijd even spannend maar ze vormen wel de basis van hoofdstuk 6. De vele kopjes koffie en sigaretten waren heel gezellig. Veel succes bij Banner Pharmacaps. Ronnie Saris, je werk heeft een deel van hoofdstuk 4 opgeleverd. Ik hoop dat PSV nog vaak landskampioen mag worden en een suggestie: groen is niet per definitie smerig. Veel succes bij TNO. Brigitte Vendel ("de aller-leukste stagiaire"), ook jouw werk heeft een grote bijdrage geleverd aan hoofdstuk 4. Jouw uitbundige persoonlijkheid maakte het nooit saai. Succes met de rest van je studie.

Ook waardeer ik mijn labgenoten van de afgelopen 4 jaar voor een goede werksfeer, Romero, Nicole, Erica, Raymond, Jan v.d. Bos, Henk ("de grote baas") Janssen, Serge, Marieke, Freek, en Mark. Mijn kamer aan de westkant heeft een wisselende bezetting gehad. Maar het was altijd gezellig. Daarvoor wil ik Mark,

Frank, Andrea, Christian, Shahid en Munazza, Veronique en Roxanna bedanken. I will leave the banana plant to Renaud, Benjamin and Michelle (please, take good care of it).

Ook wens ik alle leden van SyMO-Chem, Michel, Gaby, Ron, Joris, Maarten (trek eens jas aan als je naar de kennispoort loopt, straks vat je nog een koudje), Henk K., Serge en Freek bedanken voor de prettige lunches.

Recentelijk zijn Faysal en Narendra begonnen met microgolfonderzoek onder de vleugels van o.a. Bert. Narendra, Faysal, succes met jullie promotieonderzoek. Narendra, you should be able to read these words with your Dutch classes.

Naast het werk is er natuurlijk ook nog een ander leven. Ik wil mijn ouders bedanken voor het feit dat jullie mij op deze aarde gezet hebben. Jullie luisterden altijd heel aandachtig en geboeid als ik dingen van mijn onderzoek probeerde uit te leggen. Ik geloof alleen niet dat jullie er veel van begrepen hebben. Wouter, je bent een goede broer. Ik vind het bijzonder prettig dat je, samen met Mark, mijn paranimf wilt zijn. Veel succes met je studie en natuurlijk veel geluk met Saskia en meer recentelijk Kenzie. Gaby, ik hoop dat we nog lang samen kunnen zijn.

Bastiaan